University of Alberta

The EGFR Within: From Endosomal Signaling to Cbl-Mediated Degradation

by

Steven Pennock

A thesis submitted to the Faculty of Graduate Studies and Research
in partial fulfillment of the requirements for the degree of

Doctor of Philosophy

Department of Cell Biology

Edmonton, Alberta
Spring 2008

Your file Votre référence
ISBN: 978-0-494-45580-7
Our file Notre référence
ISBN: 978-0-494-45580-7

Abstract

Signals transduced from ligand-activated receptor tyrosine kinases (RTKs) lead to a diverse array of biological outcomes, including cell proliferation and survival. Strict regulation of RTK activity is therefore necessary to prevent aberrancies in cell signaling that lead to diseases such as cancer. RTKs are activated at the plasma membrane (PM), but they are not inactivated immediately following endocytosis, and continue to be active while trafficking in endosomes.

The first part of my thesis examined the physiological significance of endosomal RTK signaling. I have focused my research on both epidermal growth factor (EGF) receptor (EGFR) and platelet-derived growth factor (PDGF) receptor (PDGFR). By devising a system whereby RTKs can be specifically activated at endosomes, I was able to show that endosomal RTK signals effect full biological outcomes. Once activated at the endosome, RTKs nucleate signaling complexes capable of transducing downstream signals which lead to cell survival. Next, by revealing the requirement for prolonged ligand exposure to stimulate cell proliferation can be substituted with two short pulses of ligand, I demonstrated that endosome-derived RTK signals cause cell proliferation. The events following each ligand-induced pulse were further characterized: the first pulse arouses cells from quiescence into G1 of the cell cycle, while the second pulse, required several hours later, drives cells through the restriction point and into S-phase. PM-derived and endosome-derived RTK pulses transduced qualitatively similar signals and engaged the cell-cycle machinery in the same manner. These findings reveal the full physiological

relevance of endosomally signaling RTKs.

Last I studied EGFR downregulation by Cbl. Cbl mediates EGFR downregulation through its E3 ubiquitin ligase activity, though whether this occurs at the stage of endocytosis or later during trafficking remains uncertain. I found that Cbl-mediated ubiquitination is neither necessary nor sufficient for EGFR endocytosis. Instead, I showed that two Cbl homologues, c-Cbl and Cbl-b, downregulated EGFR by targeting it for degradation. Either c-Cbl- or Cbl-b-mediated ubiquitination is sufficient for EGFR degradation, and together both are necessary.

The findings of this thesis provide evidence that (1) demonstrates the physiological importance of endosomal RTK signaling, and (2) elucidates the role of Cbl in EGFR downregulation. The findings herein presented represent a significant advance in the current understanding of ligand-mediated RTK endocytosis and signal transduction.

Acknowledgements

Where to start? First, I would like to give my sincerest thanks to my supervisor, Dr. Zhixiang Wang for his mentorship, expertise, and ongoing—nearly relentless—encouragement. His own rapid and successful career has encouraged and inspired me to carry on in this field of study and to pursue a life of scientific research. I would also like to thank my committee members, past and present: Dr. David Brindley, Dr. Manijeh Pasdar, Dr. Thomas Simmen, Dr. Ellen Shibuya, and Dr. Rick Rachubinski for their valuable comments and suggestions. A special thanks goes out to my Ph.D. external examiner, Dr. Alan Wells, for his inspiring presence and extremely helpful insights. And of course, thanks to all my lab members, past and present. Xinmei Chen was my first hands-on mentor in a laboratory research environment, and her technical expertise and relentless attention to detail (reminiscent of her husband) has been instrumental in my training. Thanks especially to Dr. Yi Wang, George Kourouniotis, and Qian Wang—long-term friends and great labmates, who softened my frustrations and made me laugh when times were tough. Also I would like to acknowledge Lisa Dahl, Allison Kraus, and Zhiming Wan, who assisted in my own research projects, and to all the other members of the Wang lab who have made my work experience so much more interesting and colorful: Lisa Li, Justin Pahara, Peng Wu, and Lei Liu. I would like to give heartfelt thanks to my family and friends whose emotional support has been monumental. Lastly, I am grateful to the Department of Cell Biology for providing a stimulating atmosphere in which to conduct this research, and the Canadian Institutes for Health Research (CIHR) for financial support.

Table of Contents

List of Tables

List of Figures

List of Abbreviations

AP-1	activator protein 1
+E / +P	addition of EGF or PDGF
AFX/FXHR	forkhead transcription factors
Akt (PKB)	AK-mouse transforming lymphoma protein
ARFs	adenosine diphosphate (ADP)-ribosylation factors
ATP	adenosine triphosphate
BAD	BCL2-antagonist of cell death
Bcl2	B-cell CLL/lymphoma 2
BrdU	bromodeoxy-uridine
Cbl	casitas B-lineage lymphoma
CCV	clathrin-coated vesicle
cdk	cyclin-dependent kinase
CHX	cycloheximide
c-Myc	myelocytomatosis oncogene cellular homolog
CR	cysteine-rich
C_T	carboxyl-terminus
DAG	diacylglycerol
DMSO	dimethyl sulfoxide
DNA	deoxyribonucleic acid
E2	ubiquitin-conjugating enzyme
E3	ubiquitin ligase
EEA1	early endosomal autoantigen 1
EGF	epidermal growth factor
EGFR (ErbB1)	epidermal growth factor receptor
ER	endoplasmic reticulum
ErbB	erythroblastic leukemia viral oncogene homolog
Erk (MAPK)	extracellular signal-regulated kinase
FBS	fetal bovine serum
G0	quiescence
GAP	GTPase activating protein
GEF	guanine nucleotide exchange factor
GF	growth factor
GFP	green fluorescent protein

GHR	growth hormone receptor
Grb2	growth factor receptor bound protein 2
GSK-3	glycogen synthase kinase-3
GTP	guanine triphosphate
GTPases	guanosine triphosphatases
IB	immunoblot
IF	immunofluorescence
IgG	immunoglobulin
IP	immunoprecipitation
IP_3	inositol 1, 4, 5-triphosphate
IRS-1	insulin receptor substrate-1
JM	juxtamembrane
kD	Kilo Daltons
KD	knockdown
LPA	lysophosphatidic acid
MAPK (Erk)	mitogen-activated protein kinase
MDCK	Madin-Darby Canine Kidney Epithelial
MEK (MAPKK)	MAPK kinase
MVB	multivesicular (sorting) body
NGF	nerve growth factor
NGFR	nerve growth factor receptor
PBS	phosphate buffered saline
PDGFR	platelet-derived growth factor receptor
PDK1	3-phosphoinositide dependent protein kinase 1
PH	pleckstrin homology
PI	phosphoinositide
PI3K	phosphatidyl-inositol 3-kinase
PKA	protein kinase A
PKB (Akt)	protein kinase B
PKC	protein kinase C
PLC-γ1	phospholipase C-γ1
PM	plasma membrane
pRb	retinoblastoma protein
pS / pSer	phosphorylated serine
PTB	phosphotyrosine binding (domain)
PtdIns(3)P	phosphatidylinositol 3-phosphate

$PtdIns(3,4,5)P_3$	phosphatidylinositol 3,4,5-trisphosphate
$PtdIns(4,5)P_2$	phosphatidylinositol 4,5-bisphosphate
pY or pTyr	phosphorylated tyrosine
Rac1	Ras-related C3 botulinum toxin substrate 1
Raf	v-Raf-1 leukemia viral oncogene homolog 1
RF	RING finger (domain)
RNAi	RNA interference
R-point	restriction point
RTKs	receptor tyrosine kinases
s.d.	standard deviation
SF	serum free
SH2	Src homology 2
SH3	Src homology 3
SHC	Src homologous and collagen like protein
siRNA	small interfering RNA
S-phase	DNA synthesis phase
Src	sarcoma oncogene cellular homolog
TM	transmembrane
TR-EGF	Texas red-conjugated EGF
Ub	ubiquitin
UBA	ubiquitin-associated domain
UBPY	ubiquitin-specific protease Y
Wt	wild type
YFP	yellow fluorescent protein

CHAPTER 1:

Introduction

1.1 Characterization of Two RTKs: EGFR and PDGFR

Epidermal growth factor receptor (EGFR) and platelet-derived growth factor receptor (PDGFR) belong to the tyrosine kinase family of transmembrane cell surface receptors, or RTKs. Ligand binding and consequent dimerization of these receptors activates their intrinsic tyrosine kinase activity, leading to the tyrosine phosphorylation of target substrates, recruitment of signaling complexes, and ultimately, downstream transduction of signaling cascades leading to biological outcomes such as cell growth and survival (Jiang and Hunter, 1999; Lemmon and Schlessinger, 1994; Schlessinger, 1988). Indeed, mutations which lead to overexpression and/or unregulated activity of these receptors has been implicated in the tumorigenesis of a wide variety of tissues (Wells et al., 1990; Worthylake et al., 1999).

1.1.1 EGFR

EGF is among the first discovered growth factor, and is found in most body fluids, especially in milk (Cohen, 1962; Carpenter and Cohen, 1990). Its cognate receptor, EGFR, is likewise one of the first RTKs discovered, and is expressed to varying degrees in most tissues (Kondo and Shimizu, 1983; Carpenter et al., 1978; Carpenter et al., 1979; Wells, 1999; Hunter and Cooper, 1981). After identifying EGFR (also called ErbB) as a homologue of the avian erythroblastosis virus oncogene *v-ErbB*, it was quickly implicated in many human cancers, especially breast carcinomas (Frykberg et al., 1983; Wood et al., 2004; Gullick and Srinivasan, 1998; Yarden, 2001). Subsequent characterization of EGFR has shown it plays a major role in the control and regulation of many fundamental cellular processes, among them cell proliferation, differentiation, migration, and survival (Schlessinger and Ullrich, 1992; Yarden and Sliwkowski, 2001).

EGFR is a single-pass transmembrane glycoprotein of 170 kD. Similar to other

RTKs, EGFR consists of an N-terminal ligand-binding ectodomain, a transmembrane domain, a juxtamembrane region, a tyrosine kinase domain, and a loosely structured C-terminal tail (Fig 1.1A). EGFR's ectodomain comprises four domains commonly referred to as L1, CR1, L2, and CR2. Biophysical studies suggest that EGFR dimerization is driven and stabilized with a 2:2 EGF:EGFR stoichiometry, where one EGF molecule interacts with each EGFR monomer via coordination of the L1 and L2 domains (Lemmon et al., 1997; Ferguson et al., 2000). The juxtamembrane region of EGFR appears to have several putative regulatory functions involved in, among others, receptor downregulation, ligand-dependent internalization, and basolateral sorting events (Frykberg et al., 1983; He et al., 2002; Hobert et al., 1997; Kil et al., 1999). EGFR's kinase domain is similar to other tyrosine kinases, wherein the ATP is nestled between a N-terminal β-sheet-containing lobe and a larger C-terminal α-helical lobe (Hunter, 1998; Stamos et al., 2002). Although greatest sequence variation exists among the C-terminal tails of RTKs, all contain tyrosine residues whose phosphorylation modulates RTK-mediated signal transduction. EGFR contains at least eight such tyrosines, each which serve as direct docking sites for signaling enzymes and adaptors (Honegger et al., 1990a; van der Geer et al., 1994; Okutani et al., 1994; McCarty, 1998; Hashimoto et al., 1998; Serth et al., 1992; Milarski et al., 1993; Keilhack et al., 1998; Zhu et al., 1994).

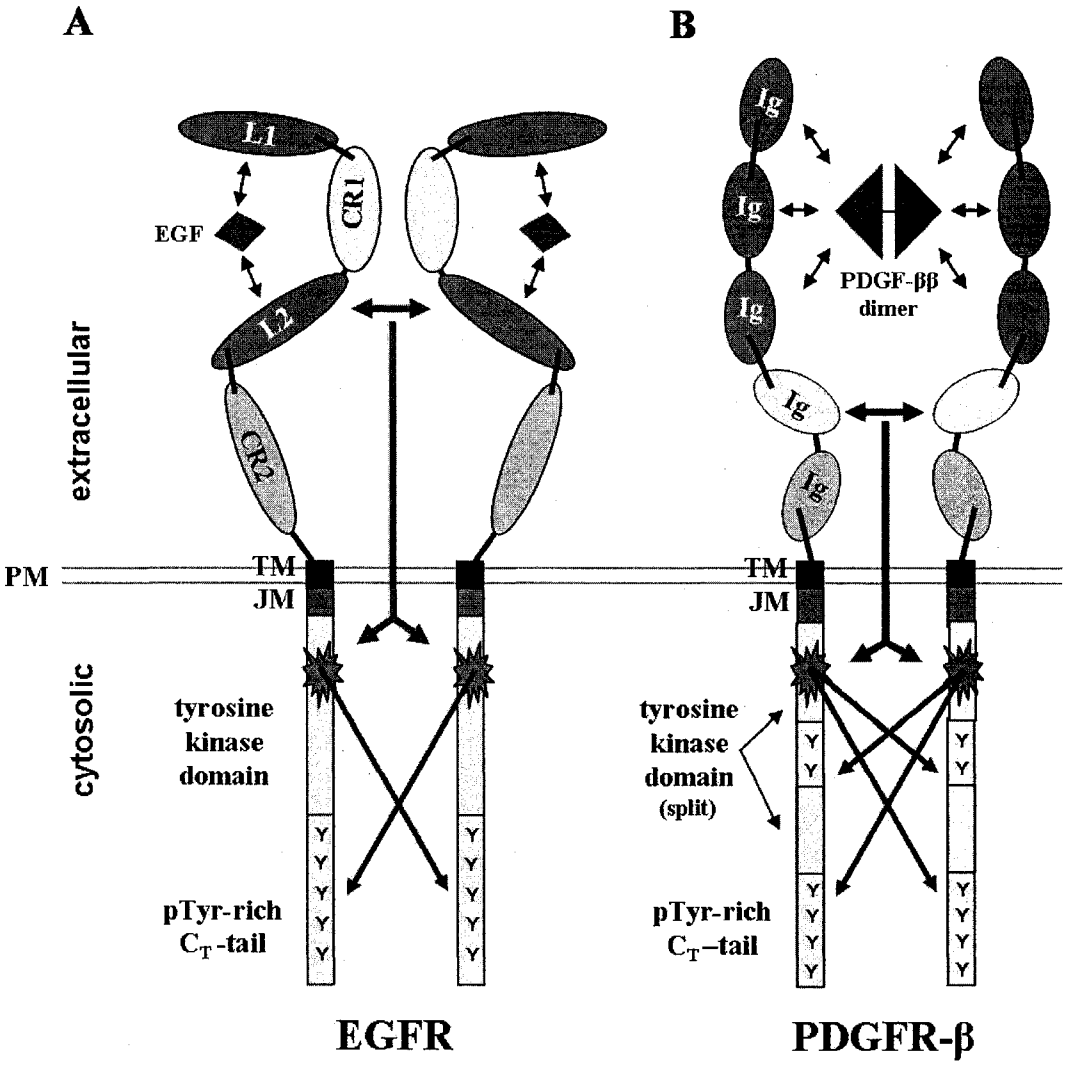

Fig 1.1. Structure and ligand-induced activation of (A) EGFR and (B) PDGFR-β. Both receptors are single-pass transmembrane proteins containing a modularly structured ectodomain and a catalytic intracellular tail. Colored arrows represent the events of receptor activation: ligand-binding (black arrows) induces the structural re-orientation in the extracellular domains of both receptors, leading to dimerization (blue arrows), robust activation of the intracellular kinase (green arrows), and lastly trans-phosphorylation (red arrows) at multiple tyrosines along the C-terminal tail of monomers in each pair. The extracellular region of EGFR consists of alternating ligand-binding (L1 and L2) and cysteine-rich (CR1 and CR2) domains, while PDGFR consists of five immunoglobulin-like (Ig) domains. C-terminal to the transmembrane domain (TM) and juxtamembrane domain (JM), both receptors possess a tyrosine kinase domain, and a C-terminal tail containing the phosphorylated tyrosines (pTyr) required for downstream signal transduction. PM, plasma membrane.

1.1.2 PDGFR

PDGF was originally identified as a component of human platelets, but since then has been found to also be coexpressed with its cognate receptor, PDGFR, in fibroblasts and smooth muscle cells (Hart et al., 1988; Heldin and Westermark, 1999; Kohler and Lipton, 1974; Ross et al., 1974). Like other RTKs PDGF-induced PDGFR signaling is involved in a multitude of cellular processes, including cell division, chemotaxis, differentiation, metabolism, and cytoskeletal arrangements (Betsholtz, 2003; Heldin et al., 1998). As shown in Fig 1.1, PDGFR shares many structural elements with EGFR. It is a single-pass transmembrane glycoprotein consisting of a ligand-binding ectodomain, a transmembrane domain, a juxtamembrane region, a tyrosine kinase domain, and a flexible C-terminal tail. In contrast to EGFR, the ectodomain of PDGFR consists of five Ig-like domains, the first three of which are involved in ligand binding, and its intracellular kinase domain is interrupted by a sequence characteristic of its C-terminal tail (Matsui et al., 1989). The polymorphic nature of PDGF and its receptor is also distinct. Four different PDGF ligands are known, termed A, B, C, and D, which bind their receptor as disulfide bridged homo- or heterodimers. Two homologous receptor isoforms exist: PDGFR-α and PDGFR-β, with molecular sizes of 170 and 180 kD, respectively, and these receptors can form homo- or heterodimers depending on which ligand dimer is bound (Heldin and Westermark, 1989). The C-terminal tail of PDGFR, like EGFR, contains multiple tyrosine sites which, when phosphorylated, serve as tethering sites for a variety of downstream signal transduction proteins (Heldin et al., 1998; Heldin and Westermark, 1999; Kelly et al., 1991).

1.2 RTK Activation and Formation of Signaling Complexes

The intrinsic kinase activity of RTKs is stimulated by their ligand-induced dimerization (Jiang and Hunter, 1999; Lemmon and Schlessinger, 1994). In the absence of ligand binding, many RTKs, including EGFR and PDGFR, actually exist on the plasma membrane as both monomers and dimers, though ligand binding stabilizes the receptor dimers by inducing a conformational change that brings the kinase domains proximal, leading to receptor activation (Sako et al., 2000; Jiang and Hunter, 1999; Lemmon and Schlessinger, 1994; Schlessinger, 1986; Schlessinger, 1988; Hubbard et al., 1998). Once activated, these receptor dimers autophosphorylate multiple tyrosines along their C-terminal tails in a *trans* manner (Kelly et al., 1991; Hubbard et al., 1998; Hubbard and Till, 2000; Margolis et al., 1989). Tyrosine autophosphorylation is vital for the recruitment of signaling proteins, many of which are phosphorylated in turn by the RTK kinase (Hubbard and Till, 2000). Activated receptors thus serve as both kinase enzymes and as platforms for the recognition and recruitment of signaling molecules.

The modular nature of signaling proteins ensures the efficient transduction of signals from RTKs to downstream targets (Kuriyan and Cowburn, 1997; Schlessinger and Ullrich, 1992). The complement of protein modules shared among these signaling mediators includes PTB (phosphotyrosine binding), SH2 (Src homology region 2), SH3 (Src homology region 3), PH (pleckstrin homology), WW, and FYVE domains, among others. Direct tethering of signaling proteins to phosphotyrosines (pTyrs) on RTKs, as well as pTyrs on other signaling molecules, is mediated by PTB and SH2 modules, while SH3 and WW domains, which bind to proline-rich motifs PXXP and PXPX, respectively, mediate another level of direct protein interaction (Kuriyan and Cowburn, 1997; Pawson, 1995; Pawson et al., 2002; Schlessinger, 1994; Schlessinger and Lemmon, 2003). The PH and FYVE domains, which bind respectively to phosphoinositides and PtdIns-3-P,

serve to dock signaling complexes at the cell membrane where they can be proximally accessible to the RTKs and their kinase activity (Ferguson et al., 1995; Lemmon et al., 1995).

Signaling proteins that bind directly to RTKs can serve as adaptors that link downstream proteins to RTK-mediated signals. These adaptor proteins contain only SH2 and SH3 domains and include, among others, Grb2, Shc, Nck, and Crk. Grb2 and Shc, for instance, link a variety of RTKs, including EGFR and PDGFR, with the Ras/MAPK signaling pathway (Pawson, 1995; Schlessinger, 1994; Margolis, 1999; Kouhara et al., 1997). Other RTK-bound signaling proteins possess intrinsic enzymatic activities of their own, leading to signal enrichment and amplification. Non-receptor tyrosine kinases (e.g. Src), phosphatases (e.g. Shp2), phospholipases (e.g. PLC-γ), and ubiquitin ligases (e.g. c-Cbl) all fall into this category. A further category of signaling mediators (e.g. GAB, Dos, IRS) do not bind RTKs directly but are recruited proximally to the membrane (mostly via their PH domains) as a consequence of RTK-mediated catalysis. These juxtamembrane docking proteins are themselves phosphorylated in trans by RTKs, where they act as membrane-bound scaffolds for further recruitment of signaling proteins (Sun et al., 1993).

1.3 RTK Signal Transduction Pathways

Ligand stimulation of RTKs leads to the concurrent activation of multiple signaling cascades, including the PI3K/Akt, PLC-γ, and Ras/MAPK pathways (Fig 1.2). The signaling pathways discussed below will be considered separately for clarity though it is important to note that these pathways are functionally interlinked, often sharing signaling components or relying on each other's catalytic products

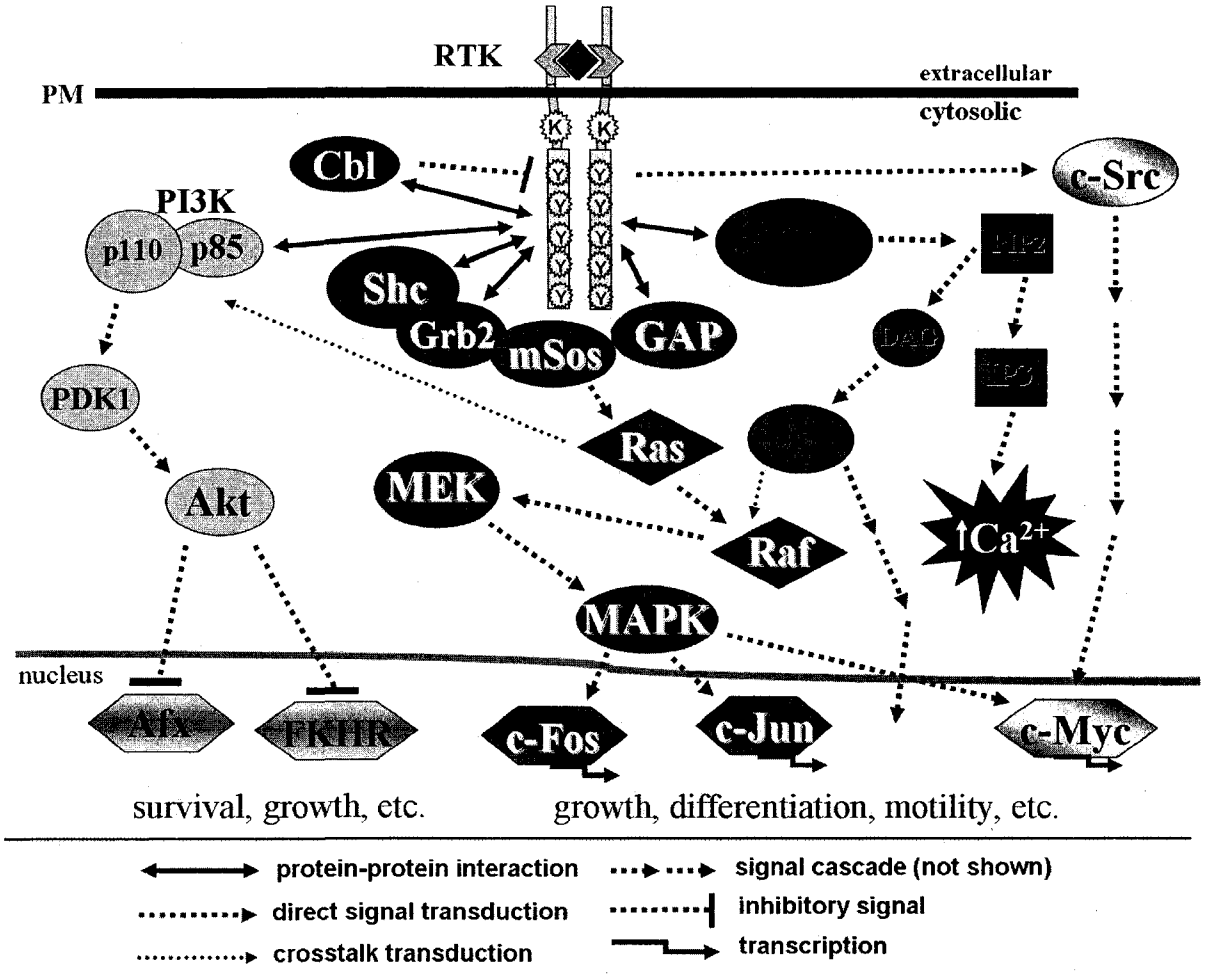

Fig 1.2. Major RTK signaling pathways. The above figure depicts major signaling pathways directly transduced from ligand-activated RTKs. Solid double arrows represent direct interactions between signaling proteins and phosphotyrosine moieties ("Y") on the receptor's carboxyl-terminal tail, while dotted arrows encompass the subsequent downstream signaling events. Signaling components are colored according to their respective pathways: PI3K/Akt pathway components are shown in grey, Ras/MAPK components in green, and PLC-γ pathway components in blue. RTKs can also transduce signals through other tyrosine kinases, such as c-Src (in yellow). Downstream outcomes of RTK signaling can be metabolic (e.g. intracellular influx of Ca2+) and transcriptional (e.g. induction of mitogenic transcription factors). Cbl, depicted in purple, is directly involved in the downregulation of many RTKs, including EGFR and PDGFR.

(Ullrich and Schlessinger, 1990). EGF-stimulation of Ras, for example, can activate PI3K as well as Raf, its cognate substrate (Schlessinger, 2000). Another instance of such crosstalk involves the activation of PLC-γ. This phospholipase is not only dependent upon RTK kinase activity but also ligand-induced generation of PI3K side products, which allows it to efficiently localize at the membrane (Karin and Hunter, 1995; Hunter, 2000).

1.3.1 The PI3K/Akt pathway

The PI3K/Akt pathway is involved in a variety of cellular processes including differentiation, proliferation, adhesion, migration, and is the major mediator of RTK-induced cell survival (anti-apoptosis) (Burgering and Coffer, 1995; Wymann et al., 1999). Three classes of PI3K exist, varying in subunit makeup and preferred lipid substrate, though all of them catalyze the phosphorylation of phosphatidylinositols (PtdIns) at their 3' position . Of the three PI3K classes, only class Ia is directly activated by RTKs. PI3K Ia is a heterodimer consisting of a p85 regulatory subunit and a p110 catalytic subunit. The SH2-domain of its p85 subunit effects PI3K's recruitment to, and phosphorylation by the RTK. This in turn allows its p110 catalytic subunit to phosphorylate PtdIns(4)P and PtdIns(4,5)P2 in order to generate the second messengers PtdIns(3,4)P2 and PtdIns(3,4,5)P3 (PIP3 for short). The PIP3 second messenger mediates the membrane translocation of a number of signaling proteins, among them the Ser/Thr kinases PDK1 and Akt (Downward, 1998; Yoeli-Lerner and Toker, 2006; Toker and Newton, 2000b; Toker and Newton, 2000a). Due to the membrane proximity of these kinases, PDK1 is able to phosphorylate and activate Akt (Toker and Newton, 2000b). The Akt kinase lies at the crux of at least two mechanisms that stimulate the cell survival response. One involves Akt-induced phosphorylation of forkhead transcription factors, which

subsequently leads to the suppression of pro-apoptotic gene expression (Brunet et al., 1999). Another mechanism involves Akt-mediated phosphorylation and inactivation of BAD. Phosphorylation of BAD disrupts its ability to complex with apoptotic proteins Bcl-2 and Bcl-x1, thereby attenuating cell death signals (Datta et al., 1997).

1.3.2 The PLC-γ Pathway

Signals transduced via PLC-γ and its second messengers leads to many important biological outcomes such as cytoskeletal reorganization, cell motility, membrane ruffle formation, branching tubulogenesis, and cell proliferation (Kamat and Carpenter, 1997). Following ligand stimulation of the RTK, PLC-γ1 is rapidly recruited to the receptor via its two SH2 domains, where it is activated by the RTK kinase. Simultaneous activation of PI3K leads to further stabilization of PLC-γ at the membrane, as PIP3, generated by PI3K, serves as a tethering site for PLC-γ's N-terminal PH domain. RTK-mediated phosphorylation of PLC-γ at Tyr771 and Tyr1254 is thought to fully activate the phospholipase, which can then catalyze the hydrolysis of PtdIns(4,5)P2 to yield two important second messengers: 1,2-diacylglycerol (DAG) and inositol 1,3,5-trisphosphate (IP3) (Wahl et al., 1990). Within minutes of EGF, IP3 binds intracellular receptors resulting in release of Ca^{2+} from intracellular stores. Ca^{2+} freed in this manner stimulates a variety of Ca^{2+}-dependent enzymes, including a family of Ca^{2+}/calmodulin-dependent protein kinases (Burgess et al., 1984). The other PLC-γ-generated second messenger DAG acts as cofactor to stimulate Ca^{2+}-dependent PKC Ser/Thr kinases (Nishizuka, 1992). The concerted action of both second messengers therefore leads to stimulation of PKC- and other Ca^{2+}-dependent pathways, including the Ral, NFkB, and JNK pathways, ultimately initiating transcriptional programs required for critical biological outcomes.

1.3.3 The Ras/MAPK Pathway

Every RTK, along with a host of other cell surface receptors, transduce signals through the Ras/MAPK pathway. This pathway regulates multiple processes including cellular metabolism, cell migration and cell shaping, and ultimately leads to transcriptional initiation of genes required for proliferation and differentiation (Marshall, 1994; Marshall, 1996; Madhani and Fink, 1998). Consequently, the core components of this pathway are highly conserved in evolution, from yeast to vertebrates (Waskiewicz and Cooper, 1995). The key initiator of this pathway is the Grb2 adaptor protein. Grb2 constitutively complexes with mSos (a Ras GEF) in the cytosol via its SH3 domains (Bar-Sagi et al., 1993; Pawson, 1995). Upon ligand-stimulation of the RTK, this complex is recruited to the receptor through Grb2's SH2 domains. Grb2-mSos association with the activated RTK can occur in two modes: Grb2's SH2 domain can either bind pTyr residues on the receptor directly, or bind indirectly through SH2-mediated association with Shc, another adaptor protein whose PTB domain interacts with the RTK (Rozakis-Adcock et al., 1992; Schlessinger and Lemmon, 2003). Once tethered to the RTK, mSos effects the exchange of GTP for GDP on the small G protein Ras. This GTP-loaded Ras, itself tethered to the membrane, then initiates a downstream kinase cascade by first activating the Ser/Thr kinase Raf-1. Activated Raf-1 phosphorylates a key Ser residue on MEK (MAPKK), leading to its activation and subsequent phosphorylation of key Thr and Tyr residues on MAPK (also called Erk1/2). A pool of activated MAPK is then rapidly translocated to the nucleus where it phosphorylates and activates transcription factors leading to mitogenic and other important outcomes (Karin and Hunter, 1995). Activated MAPK is also able to phosphorylate a variety of

cytoplasmic and membrane-bound substrates, include its own activating RTK and mSos. Phosphorylation of mSos leads to dissociation of the Grb2-Sos complex from the RTK, thus establishing a negative feedback loop in MAPK activation (Hunter, 2000).

1.4 RTK-Induced Cell Proliferation

1.4.1 RTK-Mediated Engagement of the G1 Cell Cycle Machinery

Proliferating cells move readily through the four cell cycle phases (G1, S, G2, and M), though only the G1 phase is regulated by growth factors (Fig 1.3A) (Pardee, 1989). It is well established that the mitogenic potential of growth factors such as EGF and PDGF is invested in their ability to transduce signals sufficient to engage the cell cycle machinery and surpass the G1 restriction point (R-point) (Pardee, 1974). When cultured cells are deprived of mitogenic stimulus (e.g. serum or purified growth factor), they continue to cycle until after mitosis, whereupon they cease to cycle and enter a quiescent state referred to as G0 (Pardee, 1974; Pardee, 1989). Cells can long endure in this resting state, and may re-enter G1 of the cell cycle during this time if re-introduced to serum or growth factor. In order to effect DNA synthesis however, this mitogenic stimulus must be present until cells reach the R-point, a duration of roughly 6-10 hours (varying with cell type and potency of mitogen) (Planas-Silva and Weinberg, 1997). Although the G1-S phase transition does not occur until several hours after R-point, no further stimulus is required for cells to commit to DNA synthesis and mitosis once R-point is reached. Thus, all growth factor induced events sufficient to engage a full cycle of cell division in serum starved cells occurs within the G0 to R-point interval of G1.

The major events of the mitogenic G1 cell cycle program are outlined in Fig 1.3B [reviewed in (Jones and Kazlauskas, 2001a; Kerkhoff and Rapp, 1998; Sherr, 1994)].

Fig 1.3. Growth factor-dependent engagement of the cell cycle. **(A)** Growth factor (GF)-dependent portion of the cell cycle. Upon stimulation with serum or purified growth factor, quiescent (G0) cells enter into G1 and will only proceed through an entire cell cycle if stimulus is maintained up to the restriction (R)-point. Further mitogenic stimulus is not required after this point. **(B)** The major events of the mitogenic G1 cell cycle program induced by RTK signaling. Activation of Ras/MAPK and PI3K/Akt pathways lead to upregulation and stability of cyclin-D1. PI3K/Akt signaling can also repress the downregulation of cyclin-D1 by glycogen synthase kinase 3 (GSK3), as well as stabilize cyclin-D/cdk complexes by inhibition of forkhead transcription factors (AFX/FXHR), which normally function to upregulate cdk inhibitors such as p27. **(C)** The proposed biphasic paradigm of mitogenic RTK signaling, based on studies of the PDGFR system. Initiating signals transduced by RTKs arouse cells from G0 and render them competent to subsequent mitogenic stimulus, which is required 7-9 hours later. Acute extracellular stimulus appears dispensable for a full mitogenic signal. Although the intracellular events interceding the two RTK-mediated signaling bursts are unknown, it is likely to involve induction of transcription factors (e.g. c-Myc, Elk-1). The second wave of mitogenic signaling, which occurs shortly before R-point, requires the PI3K/Akt pathway and is thought to engage the cell cycle machinery [depicted in (B)]. Dotted arrows indicate points of transcriptional regulation.

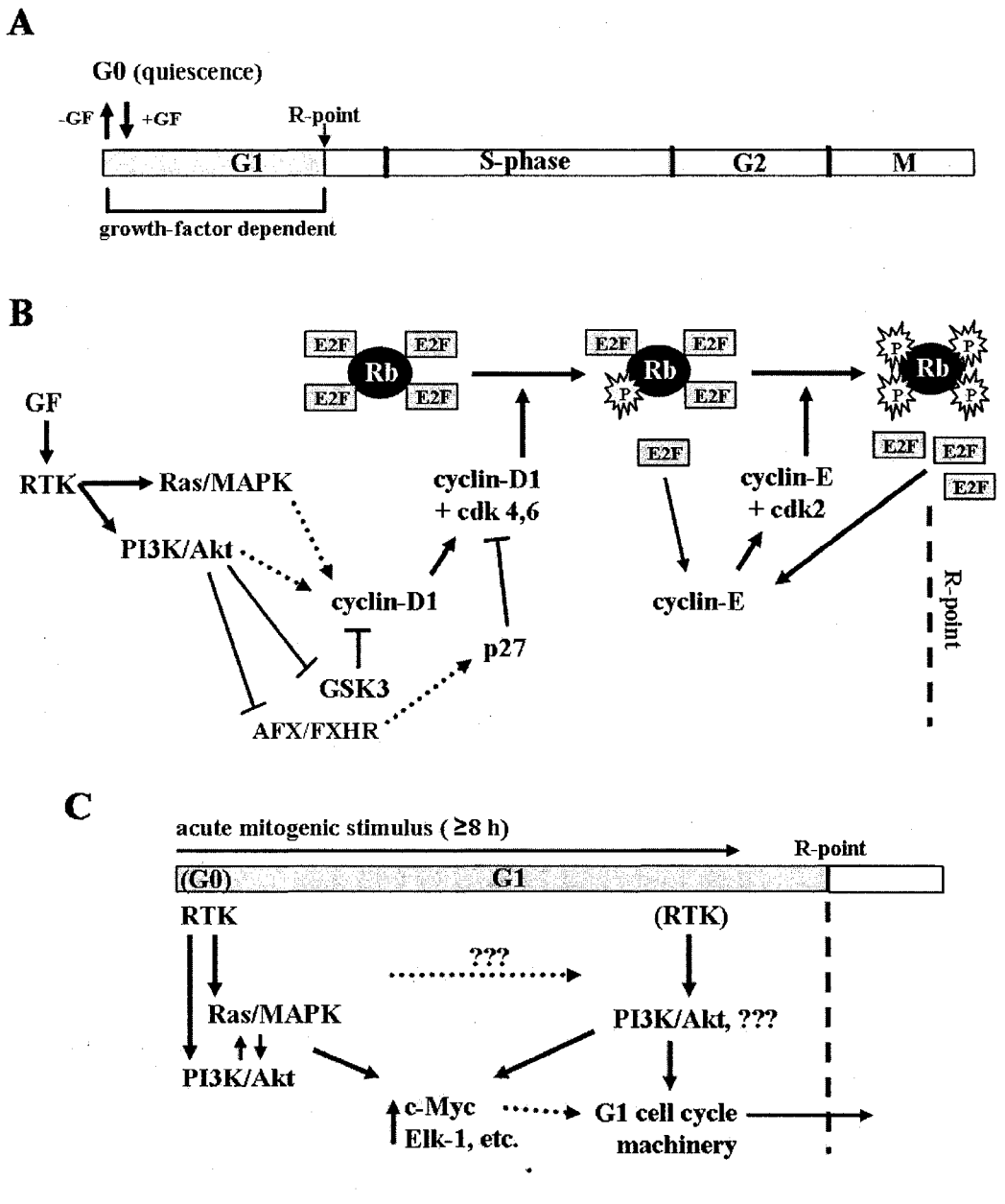
A
G0 (quiescence)
-GF
+GF
R-point
G1
S-phase
G2
M
growth-factor dependent
B
GF
RTK
Ras/MAPK
PI3K/Akt
cyclin-D1
+ cdk 4,6
cyclin-D1
GSK3
AFX/FXHR
p27
E2F
Rb
P
cyclin-E
+ cdk2
cyclin-E
R-point
C
acute mitogenic stimulus (≥8 h)
R-point
(G0)
G1
RTK
(RTK)
???
Ras/MAPK
PI3K/Akt
PI3K/Akt, ???
c-Myc
Elk-1, etc.
G1 cell cycle
machinery

Growth factor-induced RTK signaling promotes accumulation and stability of the cyclin-D1 protein (Aktas et al., 1997; Cheng et al., 1998; Kerkhoff and Rapp, 1997; Lavoie et al., 1996; Peeper et al., 1997; Winston et al., 1996). When expressed at sufficient levels, cyclin-D1 complexes with either of two cyclin dependent kinases (Cdks): Cdk4 or Cdk6 (Cheng et al., 1998). This cyclinD1/Cdk4,6 complex then effects hypophosphorylation of the E2F-loaded retinoblastoma (Rb) protein, leading to the release of a small portion of E2F. E2F is a mitogenic transcription factor normally inhibited by Rb sequestration, though cyclinD1/Cdk4,6-mediated phosphorylation of Rb catalyzes the release of enough E2F to drive the transcription of the second major G1 cyclin, cyclin-E (Sherr, 1996; Leone et al., 1997). This cyclin in turn complexes with Cdk2 to further phosphorylate Rb. This feed-forward mechanism leads to increasing release of E2F and phosphorylation of Rb, eventually resulting in a pool of E2F-free, fully phosphorylated (hyperphosphorylated) Rb protein, which is the current molecular definition of R-point (Planas-Silva and Weinberg, 1997).

As depicted in Fig 1.3B, many RTK-initiated signaling events converge upon the G1 cell cycle components necessary for engagement of mitogenesis. Both Ras/MAPK and PI3K/Akt signaling pathways regulate the mitogenic program by inducing transcription factors (e.g. c-Myc) involved in promoting the expression and stability of cyclins and by downregulating Cdk inhibitors (e.g. $p27^{Kip1}$, $p21^{Cip1}$) (Amati et al., 1998; Cheng et al., 1998; Gille and Downward, 1999). Several groups have shown that RTK-induced Ras/MAPK and PI3K/Akt signaling increases cyclin-D1 mRNA levels (Sherr, 1996; Lavoie et al., 1996; Leone et al., 1997; Peeper et al., 1997). By driving the expression of the c-Myc transcription factor, Ras/MAPK signaling can induce the accumulation of cyclin-E and E2F, thereby enhancing the positive feedback effected

between cyclin-D1 and cyclin-E (Leone et al., 1997). PI3K/Akt signaling, in addition to inducing the direct transcriptional activation of cyclins, can stabilize the cyclin D1 proteins; the mechanism behind this appears to involve Akt-mediated inhibition of glycogen synthase kinase 3B (GSK3B), a kinase which phosphorylates cyclin-D1 and targets it for proteasomal degradation (Cross et al., 1995; Rimerman et al., 2000). PI3K/Akt signaling is also important for elimination of Cdk inhibitors, namely $p27^{Kip1}$ (Gille and Downward, 1999). Akt-mediates the phosphorylation of forkhead transcription factors (e.g. AFX/FKHR), thereby effecting their transit out of the nucleus. As these transcription factors normally drive the expression of $p27^{Kip1}$ (along with pro-apoptotic genes), their nuclear exit releases the inhibitory effect on Cdk-mediated phosphorylation of the Rb protein.

1.4.2 The Biphasic Nature of Mitogenic RTK Signaling

The classical conception of how growth factors drive cell proliferation has been substantially modified in recent years [reviewed in (Jones and Kazlauskas, 2000; Jones and Kazlauskas, 2001a)]. Quiescent cells acutely stimulated with ligand such as EGF or PDGF undergo a rapid initial burst of signaling activity which endures no longer than 1 or 2 hours and then subsides, despite the continued presence of growth factor. Equally puzzling is that the cascade of G1 cyclin-dependent events immediately preceding the R-point are triggered by this brief burst of growth factor signaling which occurred several hours earlier. Since most cultured cells require at least 8 hours of continuous exposure to mitogen to surpass the R-point (Pardee, 1974; Pardee, 1989; Stiles et al., 1979b; Stiles et al., 1979a), researchers hypothesized that there must be later times at which growth factor input was required.

The first insights to this phenomenon came from microinjection studies in cultured

cells (Mulcahy et al., 1985). Neutralizing antibodies to various signaling proteins were injected into cells following exposure to growth factor. From these and similar experiments investigators found that neutralizing signaling proteins such as Ras, SHP-2, and PI3K hours after the initial burst of ligand-induced signaling abolished S-phase entry (Bennett et al., 1996; Mulcahy et al., 1985; Roche et al., 1994; Roche et al., 1996; Rose et al., 1998). This suggested that signal transduction mediated by the neutralized components re-occurred at one or more points following the initial burst of signaling. The next series of investigations involved monitoring molecular signaling events in cells over long spans of growth factor exposure. Interestingly, some of these investigators observed biphasic activation of several signaling proteins, including Ras, PI3K and PKC (Balciunaite et al., 2000; Gille and Downward, 1999; Jones et al., 1999; Taylor and Shalloway, 1996). With only minor variations in duration and onset, all these proteins displayed an initial peak of activity lasting 10-60 min and a second peak of activity occurring ~5-6 hours later and lasting approximately the same time as the first. These studies therefore suggested that mitogenesis was preceded by two distinct phases of signaling.

A pertinent question arising from these observations was how the two waves of mitogenic signaling compared to each other. Previous experiments, supported by subsequent findings, demonstrated that RTK-induced mediators such as Ras and PI3K were required for the second peak of signaling and thus essential for S-phase entry (Dobrowolski et al., 1994; Takuwa and Takuwa, 1997). The situation was further complicated when it was discovered that certain signaling enzymes made unequal contributions to each wave of growth-factor driven mitogenesis. For instance, inhibitors which blocked PI3K or PKC activity during the second wave of signaling abolished

PDGF-induced DNA synthesis, though the same inhibitors had no effect when applied during the first wave (Balciunaite et al., 2000; Jones et al., 1999). It appeared that although PI3K and PKC signaling were occurring during the first wave, they were dispensable at this point for S-phase entry. The overall picture emerging can be stated as follows: the first observed wave of signaling induced by growth factor appears to render cells capable of receiving subsequent stimulus, characterized by a distinct second wave of signaling which occurs many hours later. This second wave allows cells to respond mitogenically to growth factor. This biphasic signaling paradigm is depicted in Fig 1.3C.

It seemed more than coincidental that the second wave of growth factor-induced signaling was temporally proximal to the molecular events of the G1 cell cycle program (i.e. induction of cyclin-D1 complexes, cyclin-E complexes, and hyperphosphorylation of Rb). Researchers reasoned that perhaps the second signaling wave was directly triggering the G1 cell cycle machinery. Significant elucidation came from the work of Jones *et al.* (Jones et al., 1999; Jones and Kazlauskas, 2001c). In characterizing the signaling events of PDGF-stimulation in fibroblasts, they demonstrated that PDGF need only be administered at times corresponding to the two observed signaling waves during acute stimulation, and thus growth-factor dependent signaling was not required continuously throughout G1. This group also showed that the kinetics of S-phase entry and engagement of G1 cell cycle events occurred comparably in cells treated continuously (acutely) or discontinuously with PDGF, and that the second wave of PDGF-induced signaling, and not the first, rapidly engaged the cell cycle program by leading to the induction of cyclin-D1. Based on these findings, the authors proposed dividing G1 into two subphases: G1E (early) and G1L (late), where G1E begins with arousal of quiescent cells following the first pulse of growth factor and ends with the

engagement of the G1 cell cycle machinery driven by the second pulse of growth factor, while G1L encompasses the R-point and the remaining interval of G1.

By testing different mitogens in fibroblasts, Kazlauskas and colleagues revealed that growth factors differed in their interchangeability and overall mitogenicity in the biphasic paradigm. Interestingly, this reflected the old concept of competence and progression, which proposed that cell cycle progression required the input of two different growth factors (Pledger et al., 1977; Pledger et al., 1978; Stiles et al., 1979a). While many mitogens, including PDGF, FBS, FGF, and lysophosphatidic acid (LPA) were completely interchangeable at either pulse, both EGF and insulin were insufficiently mitogenic when administered during the first pulse, even though these ligands engaged the same signaling pathways as the fully mitogenic growth factors. The apparent deficiency of EGF and insulin to engage the first wave of signaling is possibly cell type-dependent, as both these factors are well established mitogens. Nevertheless, these and related studies reveal a common mitogenic signaling cascade engaged by a wide array of different mitogens.

1.5 Regulation of RTK Signaling by Endocytosis

1.5.1 Endocytosis of RTKs

Regulation of RTK signaling must be tightly monitored in order to maintain cell homeostasis and prevent hyperactivation of cellular processes. Aberrant expression or dysfunction of RTKs and their signaling mediators is responsible for many cancers, developmental disorders, and other diseases (Arteaga, 2001). Consequentially, cells have evolved a variety of mechanisms to attenuate RTK signaling. Among these are mechanisms involving suppression of RTK activity by ligand antagonists, phosphatases,

Ser/Thr kinases, ubiquitin ligases, and other enzymes.

Ligand-induced endocytosis has also been traditionally held as a potent effector of RTK signal attenuation (Wiley and Burke, 2001; Ceresa and Schmid, 2000). Just minutes following growth factor stimulation at the PM, activated RTKs rapidly cluster into clathrin-coated pits, which invaginate further and eventually pinch off in a dynamin and ATP-dependent manner as internalized clathrin coated vesicles (CCVs) (Carpenter, 1987; Schlessinger, 1986). Although a complete mechanistic understanding of clathrin-mediated endocytosis has yet to be obtained, many of its components are well characterized (Robinson, 1994; Ullrich and Schlessinger, 1990). Clathrin itself is a oligomeric complex consisting of three heavy chains and three light chains combined in a characteristic triskelion structure. Adjacent structures of clathrin assemble along the membrane to deform bilayer curvature and effect invagination of the coated pits (Zaremba and Keen, 1983). Other factors such as endophilin, β-arrestin, and AP-2 selectively direct RTKs to clathrin-coated regions of the PM and link them directly to the endocytic machinery, while the activity of the GTPase dynamin is involved in catalyzing the pinching-off of coated pits to form internalized CCVs (Petrelli et al., 2002; Barbieri et al., 2000; Vieira et al., 1996; Wiley and Burke, 2001; Zaremba and Keen, 1983).

Following endocytosis, RTK-containing CCVs shed their clathrin coats and enter the vesicular trafficking route as early endosomes (Barbieri et al., 2000). Endosomal trafficking is indeed a complex process, involving a wide variety of endosome subpopulations, membrane budding and fusion events, routing modes, and trafficking mediators [reviewed in (Goldstein et al., 1985; Robinson, 1994)]. A number of soluble and membrane-bound proteins have been found to regulate endocytic trafficking, including members of the adenosine diphosphate ADP-ribosylation factor (ARF) family

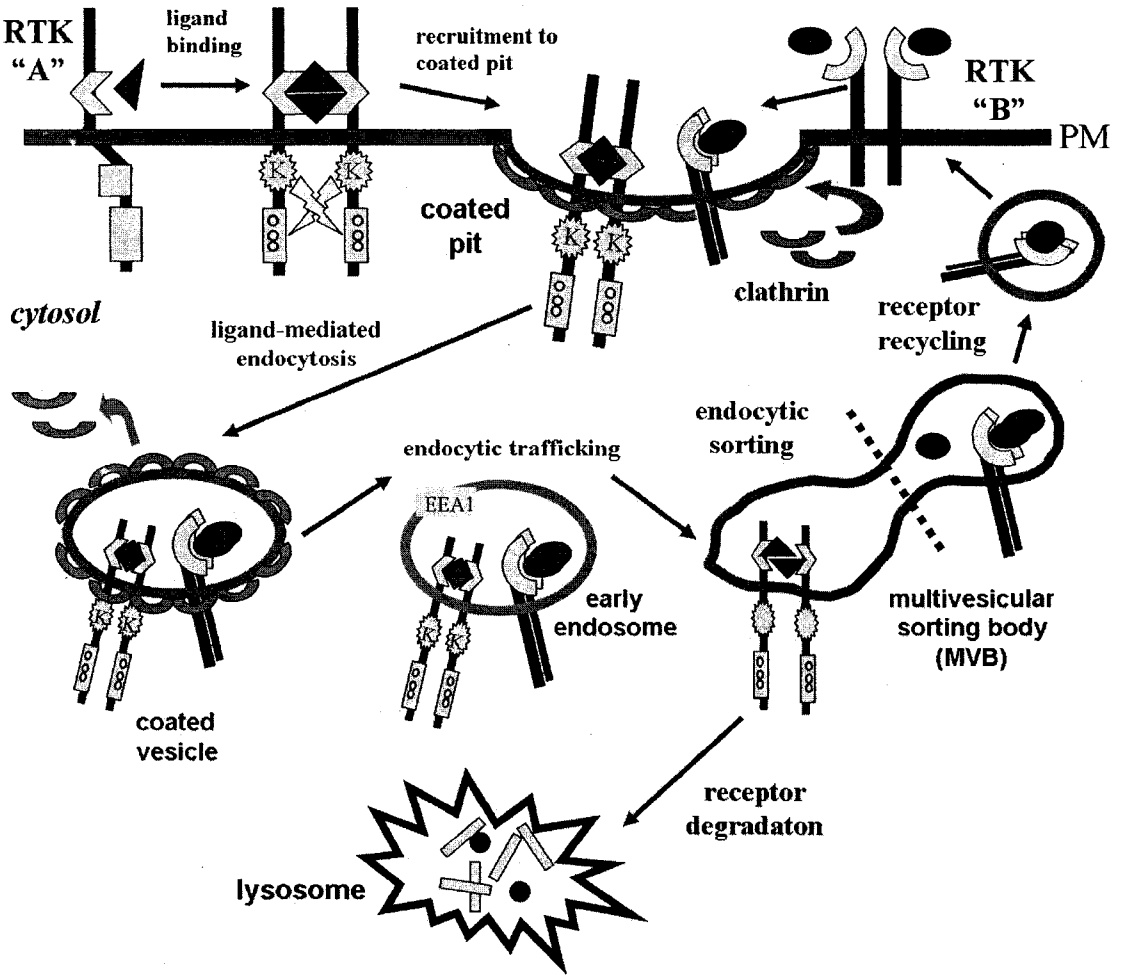

Fig 1.4. Endocytic trafficking of RTKs. RTKs undergo clathrin-mediated endocytosis following their activation by ligand at the plasma membrane (PM). Once routed into early endosomes from clathrin-coated pits and vesicles, internalized receptors are trafficked into sorting endosomes called multivesicular bodies (MVBs) from where they take divergent paths, depending on their nature and activity. Kinase active, ligand-retaining receptors ("A" RTKs) tend to be sorted into late endosomes and on to lysosomes where they are degraded, while kinase inactive receptors ("B" RTKs) tend to return to the PM via recycling endosomes. EEA1: early endosome autoantigen-1, a marker of early endosomes.

and the Ras-like Rab GTPases (Bottger et al., 1996; Valencia et al., 1991). The Rab proteins, for instance, are thought to mediate *trans* coordination of membranes during vesicular fusion and to direct correct membrane transport of endosomal proteins (Valencia et al., 1991). Furthermore, different Rab isoforms mediate these events in specific endosome subpopulations: Rab4 and Rab5, for example, localize to and function on early endosomes, Rab7 regulates trafficking at late endosomes, while Rab9 and Rab11 target to the recycling branch of endosomes (Feng et al., 1995; Bucci et al., 1992; Bottger et al., 1996).

The different endocytic RTK trafficking pathways are schematized in Fig 1.4. The simple view of RTK endosomal trafficking entails movement of the activated receptor in the direction of increasing lumenal acidity of endosomes (i.e. early endosomes → late endosomes / multivesicular bodies (MVBs) → lysosomes) (Clague and Urbe, 2001). Once localized in lysosomes, ligand-RTK complexes are degraded by lysosomal hydrolases (Sorkin and Waters, 1993). The ultimate fate of internally trafficking RTKs thus appears to be proteolytic degradation. It is for this reason that endocytosis has been regarded as strictly a means of RTK attenuation. Internalized RTKs do not traffic along the endosomal route automatically, but are directed via trafficking motifs contained within their sequences that recruit various mediators to sense receptor state (e.g. SNX1, c-Cbl) and cause further modifications (e.g. ubiquitination) that assist sorting mechanisms (Kil et al., 1999; Kurten et al., 1996; Lee et al., 1999; Levkowitz et al., 1998; Opresko et al., 1995). In this way, kinase active ligand-bound RTKs tend to be sorted towards lysosomes whereas transiently active and/or kinase inactive RTKs are preferentially recycled (Fukazawa et al., 1996; Chen et al., 1989; de Melker et al., 2001; Felder et al., 1992; Glenney, Jr. et al., 1988; Honegger et al., 1990b; Sorkin and Waters,

1993). Such sorting mechanisms limit receptor hyperactivity and ensure that non-active receptors are not wasted by degradation (Burke et al., 2001; Ceresa and Schmid, 2000).

1.5.2 Evidence for RTK Signaling from Endosomes

A major question arising over the last decade and a half is the relationship between signal transduction pathways and the endocytic system (Leof, 2000). The traditional view held that endocytosis was simply a means for downregulating RTKs by clearing active receptors from the membrane, thereby preventing excess signaling at the cell surface (Wiley and Burke, 2001; Ceresa and Schmid, 2000). According to this view, endocytosis was considered as a mechanism of tumor suppression. Indeed, experiments in which EGFR endocytosis was inhibited resulted in an increase in receptor signaling, and in some instances enhanced tumorigenesis was demonstrated (Wells et al., 1990; Worthylake et al., 1999). A similar phenomenon was observed for the insulin receptor (Kao et al., 1998). When dominant-negative dynamin was employed to inhibit endocytosis, little effect was seen in insulin receptor autophosphorylation or in its ability to stimulate downstream signaling. It is also known that EGFR-ErbB2 heterodimers generate more potent signals than EGFR homodimers, and ErbB2 has a markedly diminished endocytic capacity (Waterman et al., 1998). Together these results implicate the majority of RTK signaling occurs at the PM, and indirectly infers that endocytosis serves primarily to remove receptors from their signaling contexts.

The paradigm of endocytic receptor clearance strictly as a downregulation mechanism appears unable to withstand several levels of scrutiny. Experiments in which enhanced signaling was observed from PM-localized RTKs does not rule out the possibility of endocytic signaling or its importance (Shen et al., 2001; Vieira et al., 1996). It can not be distinguished, for instance, whether the observed effects arose from lack of

endosomal signaling or prolonged PM signaling. Furthermore, inhibition of endocytosis by employing such means as dominant-negative dynamin or clathrin makes it impossible to discern whether the observed effects are due to inhibition of a specific receptor's internalization or due to the global inhibition of endocytic mechanisms.

There is in fact a significant body of evidence implicating physiological RTK signaling from endosomes. As early as the mid-1980s, researchers found that PM-stabilized EGFR lacks EGF-mediated mitogenicity, while RNA synthesis was not substantially affected (Wakshull and Wharton, 1985). Other findings distinguished two classes of phosphotyrosine substrates for EGF: one immediately accessible to PM-localized EGFR and another accessible only at a later time, corresponding to when receptors had already internalized (McCune and Earp, 1989). Indeed, RTKs are known to remain phosphorylated and kinase-active well after their internalization (Clague and Urbe, 2001; Di Guglielmo et al., 1994; Di Guglielmo et al., 1998; Haugh et al., 1999; Kuruvilla et al., 2000; Levkowitz et al., 1998; Wang et al., 1996b). Given these results, it is even plausible that different signaling pathways utilize distinct membrane locations for initiation. A series of studies investigating EGFR and insulin receptor signaling after blockage of endocytosis revealed a demarcation in the location-dependence necessary for signaling output (Vieira et al., 1996; Chow et al., 1998). It appeared EGF-induced EGFR internalization was required for MAPK activation, despite the fact that Shc phosphorylation proceeded normally. In the case of insulin receptor, internalization was required for both MAPK and Shc activation, although the activation of IRS1—another key substrate of this receptor—occurred regardless of internalization. The work of Bergeron *et al.* further extended these insights, showing that endosomal fractions were major sites of EGF-mediated Shc and Grb2 recruitment, and insulin-mediated IRS1and

PI3K phosphorylation (Di Guglielmo et al., 1994; Di Guglielmo et al., 1998).

Despite the accumulating evidence in support of endosomal RTK signaling, there remains much uncertainty and conflicting findings. A good example is the apparent paradox regarding EGF-mediated Ras/MAPK pathway activation (Leof, 2000). While some findings indicate that blocking endocytosis effectively blocks MAPK activation, others revealed that trapping RTKs at the PM does not lead to an attenuation of mitogenic output—as would be expected when blocking Ras/MAPK transduction—but in fact enhances mitogenesis in many cell types (Ceresa et al., 1998; Kao et al., 1998; Kranenburg et al., 1999). PM-derived RTK signaling is well characterized, and yet efforts to understand the overall spatiotemporal signaling of RTKs fall short of definitively showing endosome-generated RTK signals. Intuitively, the endosome must be an important location for RTK signaling—receptors internalize only minutes after ligand stimulation, and yet, can spend 1 or even 2 hours trafficking along the endosomal route before their degradation. It also remains to be clarified whether the subcellular location of RTKs can account for differential pathway induction or whether signal specificity is predetermined by the events that occur when receptors are first activated on the cell surface.

1.6 Cbl-Mediated RTK Downregulation

1.6.1 Characterization of Cbl

The Cbls are oncoproteins by virtue of their prominent role in regulating signal transduction (Thien and Langdon, 2001). Fig 1.5 depicts the major domains of Cbl and its many interactions with signaling proteins. The mammalian Cbl protein family consists of the c-Cbl, Cbl-b, and Cbl-3 homologues, all of which associate with a wide

variety of signaling proteins, including RTKs and SH2- and SH3-domain-containing proteins [reviewed in (Thien and Langdon, 2001)]. Through these many associations, Cbl is able to regulate diverse signaling networks. One of the most extensively studied roles of Cbl is its function as a negative regulator of receptor tyrosine kinase (RTK) signaling (Levkowitz et al., 1998; Miyake et al., 1998; Ota and Samelson, 1997; Waterman et al., 1999b; Yoon et al., 1995). Although c-Cbl and Cbl-b are roughly twice the size of Cbl-3, all three possess the same N-terminal domains involved in RTK regulation. Two highly conserved amino-terminal domains in particular lend strongly to this regulatory function. First, Cbl's tyrosine-kinase binding (TKB) domain recognizes phosphotyrosine residues and allows it to directly interact with activated RTKs on the plasma membrane (Galisteo et al., 1995; Lupher, Jr. et al., 1996; Wang et al., 1996a). Second, the RING finger domain recruits ubiquitin-loaded enzymes (E2s), allowing Cbl to function as an E3 ubiquitin ligase to direct the ubiquitination, and presumably the degradation, of its associated RTK (Joazeiro et al., 1999; Levkowitz et al., 1999; Yokouchi et al., 1999). The high homology of the N-terminal domains among the Cbls predicts a similar regulatory role, though there is evidence that the Cbls function distinctly as well. Both c-Cbl and Cbl-b possess an extensive proline rich region, which mediates association with SH3-containing proteins, as well as a ubiquitin associated (UBA) domain. These UBA domains, though nearly identical in sequence in both Cbls, appears functional only for Cbl-b. It was shown, for instance, that the UBA domain of Cbl-b, but not that of c-Cbl, can bind ubiquitinated proteins (Davies et al., 2004).

1.6.2 The Role of Cbl in EGFR Downregulation

Dysregulation of EGFR activity is a major factor in cellular transformation and cancer (Peles and Yarden, 1993). Proper downregulation of EGFR and attenuation of

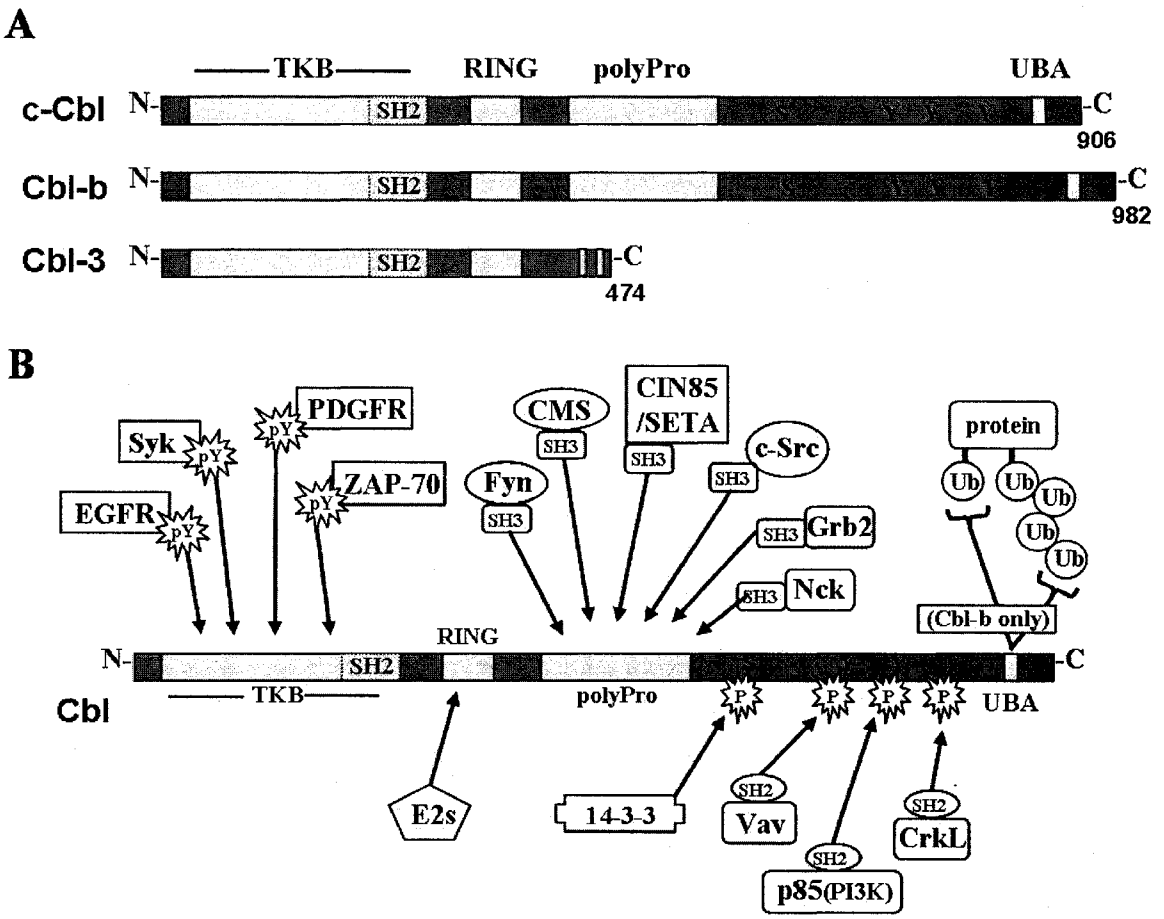

Fig 1.5. Cbl structure and associated signaling proteins. (A) Major domains of the three mammalian Cbl proteins (c-Cbl, Cbl-b, and Cbl-3). All three Cbls have homologous N-terminal regions containing a tyrosine kinase-binding (TKB) domain and a RING finger domain. Both these domains are involved in downregulation of RTKs. c-Cbl and Cbl-b possess additional sites for protein interaction in their C-terminal halves, including poly-proline (polyPro) and ubiquitin-associated (UBA) domains. **(B)** The Cbl "interactome." Cbl proteins associate with multiple signaling proteins via a diverse array of binding motifs. Association with many tyrosine kinases (e.g. EGFR, Syk, PDGFR, ZAP-70) occur in an activation-dependent context, mainly through SH2-phosphotyrosine (pY) interactions in both directions. Some tyrosine kinases (e.g. Fyn, c-Src), as well as a host of signaling adaptors (e.g. Grb2, Nck), can bind Cbl constitutively via their SH3 motifs. The Cbl interactomes, though similar, appear to diverge with regards to their UBA domains: both c-Cbl and Cbl-b possess a UBA domain, though only Cbl-b's is able to bind ubiquitinated proteins.

EGFR signaling are therefore critical in maintaining cell homeostasis. It has become increasingly evident that Cbl plays a prominent role in EGFR downregulation by virtue of its E3 ubiquitin ligase activity (Joazeiro et al., 1999; Levkowitz et al., 1998; Miyake et al., 1998). Fig 1.6 depicts EGF-mediated Cbl recruitment and ubiquitination of EGFR. Upon EGF induction, Cbl is recruited to activated EGFR, associating directly via TKB domain binding with phosphotyrosine 1045 (pY1045) on EGFR (Levkowitz et al., 1999). Cbl can also associate indirectly with activated EGFR through the adaptor protein Grb2, which binds the proline region of Cbl through its SH3 domain, and pY1068 or pY1086 on EGFR through its SH2 domain (Fukazawa et al., 1996). Following binding, Cbl is phosphorylated by EGFR, allowing recruitment of ubiquitin-loaded E2 proteins to its RING finger and subsequent ligation of monomeric ubiquitin at multiple sites along the receptor (Bowtell and Langdon, 1995; Joazeiro et al., 1999). The event of multiple monoubiquitination (often called "multiubiquitination") is thought to be a major determinant in EGFR downregulation, both during the initial sorting of activated EGFR into clathrin-coated pits and later during sorting of the receptor to lysosomes for degradation (de Melker et al., 2004; Haglund et al., 2003a; Longva et al., 2002; Marmor and Yarden, 2004; Ravid et al., 2004; Stang et al., 2000; Stang et al., 2004).

Although it is generally agreed that Cbl acts to negatively regulate EGFR activity, the specific point, or points, at which Cbl acts remains unclear. It is still disputed, for instance, whether Cbl binding or Cbl-mediated ubiquitination is altogether required for ligand-induced EGFR endocytosis. Intuitively, the fact that Cbl binding and receptor ubiquitination occur at the plasma membrane seems to support a role for Cbl in EGFR endocytosis (Longva et al., 2002; Stang et al., 2000). Several studies also support a role

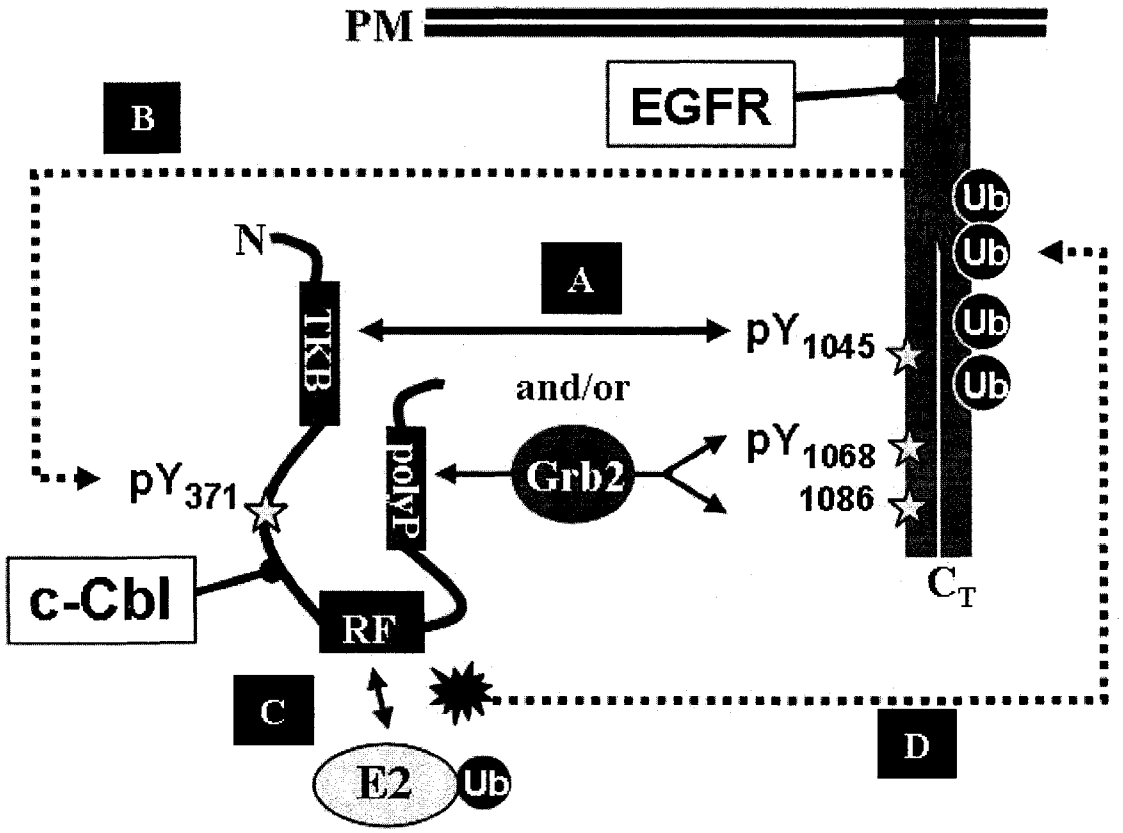

Fig 1.6. EGF-mediated Cbl recruitment and ubiquitination of EGFR. Following EGF-induced activation of EGFR, c-Cbl is recruited to EGFR directly via TKB association with phosphotyrosine (pY) 1045 on EGFR, or indirectly through the Grb2 adaptor protein (A). Once bound, c-Cbl is phosphorylated at pY371by EGFR's kinase (B). An ubiquitin (Ub)-loaded E2 enzyme is then recruited to the activated Cbl (C), allowing Cbl's RING finger (RF) domain to catalyze the monoubiquitination of EGFR at multiple sites along its intracellular region (D). Although the above mechanism pertains to c-Cbl, the function of the other mammalian Cbls (Cbl-b and Cbl-3) are thought to be the same.

for Cbl in EGFR internalization, either through Cbl's E3 ubiquitin ligase activity or by its involvement in endocytic complexes (Haglund et al., 2002; Haglund et al., 2003b; Huang and Sorkin, 2005; Jiang et al., 2003; Petrelli et al., 2002; Yokouchi et al., 1999). Experiments employing various mutants that disrupted Cbl-containing complexes showed impaired rates of receptor internalization, though complete abrogation of internalization was never observed (Haglund et al., 2003b; Huang and Sorkin, 2005; Jiang et al., 2003; Petrelli et al., 2002; Yokouchi et al., 1999). In addition, Cbl was identified as a component of the CIN85/endophilin complex, which is thought to affect the negative membrane curvature required for clathrin-coated pit invagination and endocytosis (Petrelli et al., 2002; Soubeyran et al., 2002; Szymkiewicz et al., 2002). Other findings implicate a role for EGFR multiubiquitination in endocytosis. The modification of certain plasma membrane proteins by multiubiquitination appears sufficient for their internalization (Haglund et al., 2003b; Hicke and Riezman, 1996). Chimeras of EGFR fused to ubiquitin to mimic a Cbl-multiubiquitinated receptor are constitutively internalized (Haglund et al., 2003b; Mosesson et al., 2003).

Alternatively, many studies argue against a role for Cbl in EGFR internalization (de Melker et al., 2001; Duan et al., 2003; Grovdal et al., 2004; Longva et al., 2002; Thien et al., 2001). For example, our group's finding that receptor dimerization rather than kinase activation is sufficient to cause EGFR endocytosis suggests that Cbl tethering to EGFR—an event which requires the receptor to be phosphorylated—is dispensable for internalization (Wang et al., 2005; Wang et al., 2007). It has also been demonstrated that Cbl overexpression does not significantly enhance EGFR internalization (Levkowitz et al., 1998; Thien et al., 2001). In experiments utilizing dominant-negative forms of Cbl, EGFR downregulation was severely inhibited, though the receptor was still observed to

localize to internal vesicles (Lill et al., 2000). Moreover, studies using cells deficient in c-Cbl or conditionally defective in ubiquitination reveal little or no impairment in EGFR internalization, although overall receptor downregulation was reduced (Duan et al., 2003). These studies also suggested that inhibited downregulation was caused by defective sorting of EGFR to lysosomes, and further evidence in support of this was provided by the finding that ubiquitination of EGFR was necessary for its efficient transfer to the inner membrane of multivesicular bodies (Longva et al., 2002). Overall these findings implicate a more downstream role for Cbl in EGFR downregulation, namely, at the level of late endosomal sorting and degradation.

The precise role played by Cbl during intracellular EGFR trafficking also remains to be clarified. While Cbl-mediated ubiquitination is likely a key factor in EGFR degradation, the necessity for continued Cbl-EGFR interaction in this process is uncertain (de Melker et al., 2001; Grovdal et al., 2004; Levkowitz et al., 1998). Many proteins involved in EGFR signaling are also targets of Cbl and/or Cbl-mediated ubiquitination, including Grb2, PI3K, Cdc42, and a wide array of non-receptor tyrosine kinases (e.g. c-Src) (Bao et al., 2003; Buday et al., 1996; Fukazawa et al., 1996; Kassenbrock et al., 2002; Tanaka et al., 1995; Wu et al., 2003). While a number of these proteins are regulated by Cbl concurrently with EGFR (such as those directly in complex with the receptor), others are likely regulated by Cbl following disassociation from EGFR. It was recently demonstrated that EGF-induced activation of Cool-1, while acting as a GEF for Cdc42, is able to sequester Cbl and decrease its association with EGFR, thereby negatively regulating Cbl-mediated EGFR ubiquitination (Feng et al., 2006; Wu et al., 2003). Another significant observation is that Cbl undergoes ligand-induced autoubiquitination during its routing with RTKs (Ettenberg et al., 2001; Wang et al.,

1996a). This leads to the important yet unresolved question whether Cbl is degraded with the EGFR in lysosomes or cytosolically in the proteasome. Cbl-b has been shown to sort with EGFR into later endocytic compartments and to coordinate EGFR degradation. Interestingly, these and related studies reveal both Cbl and EGFR degradation are dependant on a functioning proteasome (Ettenberg et al., 1999b; Ettenberg et al., 2001).

Studies on individual Cbl homologues seems to reveal a basic functional redundancy amongst them, and yet an even more complex picture is emerging (Thien and Langdon, 2001). The possibility that c-Cbl and Cbl-b—both structurally similar and widely coexpressed—may play distinct roles in EGFR regulation is supported by several recent findings (Davies et al., 2004; Ettenberg et al., 1999b; Ettenberg et al., 1999a). For example, overexpressed Cbl-b was more potent than c-Cbl in inhibiting EGF-mediated growth and in decreasing the output of signaling through the PI3K-Akt pathway (Ettenberg et al., 1999b). Another finding showed that the carboxyl-terminal ubiquitin associated (UBA) domain of Cbl-b, but not c-Cbl, can bind ubiquitinated proteins (Ettenberg et al., 1999a). Furthermore, overexpression of Cbl-b's UBA domain blocked EGFR degradation, likely acting in a dominant negative fashion. Differential sorting routes for the Cbls may also exist, as suggested by the involvement of both lysosomal and proteasomal functioning in the degradation of Cbl and its receptor substrate. Together these intriguing differences raise the question as to how the different Cbl's interplay in EGFR downregulation.

1.7 Rationales, Hypotheses, and Objectives

The Physiological Significance of Endosomal RTK Signaling

The endosome must be an important location for RTK signaling. Receptors undergo clathrin-mediated endocytosis only minutes after ligand stimulation, and yet can spend between 1-2 hours trafficking along the endocytic route in a kinase-active, phosphorylated state before being degraded. This would also appear to indicate that RTKs transduce a large proportion of their signals intracellularly. Despite this reasoning, and a body of evidence supporting the endocytic signaling capacity of RTKs, definitive proof of endosome-generated RTK signals has not been forthcoming. This is due in part to the lack of experimental systems that demarcate endosome from PM-generated signal transduction (Wiley and Burke, 2001). Results from endocytosis-blocking experiments used to characterize PM-derived RTK activity seem to preclude the necessity for signaling at another subcellular compartment (Shen et al., 2001; Vieira et al., 1996). By globally inhibiting endocytosis however, these experiments do not truly investigate RTK signal transduction in a spatiotemporal context; nor do they rule out that RTK signaling was occurring elsewhere. For instance, growth factor-induced cell proliferation requires a prolonged mitogenic stimulus that would likely encompass a duration much longer than the physiological occupancy of activated RTKs on the PM. Demonstrating full or even enhanced signaling outputs derived from PM-retained receptors may therefore be misleading. Another related question is whether subcellular location of RTK signaling can dictate the specificity of signaling output. Even in the absence of definitive proof for endosomal RTK signaling, several findings suggest that while some signaling pathways require RTK internalization, others do not.

The hypotheses I propose for the part of my thesis are as follows: **The endosome is**

a physiological location of RTK signal transduction, capable of nucleating RTK signaling complexes which can stimulate downstream signaling pathways and lead to full biological outcomes such as cell survival and proliferation.

To validate this hypothesis, I first assisted in devising a system whereby RTKs can be specifically activated at endosomes. With this system, I aimed to demonstrate that growth factor-induced EGFR and PDGFR signaling occurs from endosomes and that endosome-derived signaling of these receptors is sufficient to effect both anti-apoptotic and mitogenic responses.

The Role of Cbl in EGFR Downregulation

The Cbls are oncoproteins by virtue of their prominent role in regulating signal transduction (Levkowitz et al., 1998; Miyake et al., 1998; Ota and Samelson, 1997; Waterman et al., 1999b; Yoon et al., 1995). Understanding how they regulate upstream receptors such as EGFR is vital to delineating exactly how they contribute to cancer. It is well established that c-Cbl ubiquitinates EGFR and mediates its downregulation in response to EGF (Levkowitz et al., 1998; Levkowitz et al., 1999). However, the controversy endures as to whether c-Cbl functions to regulate the internalization and/or the intracellular trafficking of EGFR. It is also not clear how the other Cbl isoforms, such as Cbl-b, participate with c-Cbl in these processes. Recently, our lab demonstrated that EGFR1044, a mutant truncated from its C-terminus to 1044 and which lacks all known c-Cbl binding sites, is internalized similarly to wild type EGFR (Wang et al., 2005). This suggests that c-Cbl interaction may not be essential for EGFR internalization. In addition, our group has generated an endocytosis-deficient EGFR mutant, EGFR-LL/AA, which replaces two critical leucines at 1010 and 1011 for alanines. As this mutant retains all the known c-Cbl binding sites, it will provide me with

an opportunity to test the sufficiency of c-Cbl interaction in EGF-mediated EGFR internalization.

The hypothesis I propose for this part of my thesis is as follows: **Cbl's role in EGFR downregulation occurs at the level of receptor degradation, not internalization. Neither Cbl interaction nor Cbl-mediated ubiquitination is required for EGF-induced EGFR internalization.**

To validate this hypothesis, I employed various EGFR mutants to test whether Cbl interaction and Cbl-mediated ubiquitination is necessary and/or sufficient in EGF-induced EGFR internalization. Next, I investigated the role of Cbl in EGFR endocytic trafficking and utilized RNA interference (RNAi) to assess the absolute requirement for Cbl in EGFR degradation.

CHAPTER 2:

Materials and Methods

2.1 Materials

Reagents, enzymes, and commercial kits were used according to the respective manufacturers' specifications and in accordance with protocols set out by the Environmental Health and Safety of the University of Alberta and Workplace Hazardous Materials Information System (WHMIS).

2.1.1 Reagents

acetic acid, glacial	BDH
acrylamide/bis	Biorad
AEBSF (4-[2-aminoethyl]-benzenesulfonyl fluoride)	Sigma
AG1296	Calbiochem
AG1478	Calbiochem
agar	Gibco
agarose	Gibco
Alexa-fluor 647-labeled EGF	Mol. Probes
ammonium persulfate	BDH
aprotinin	Sigma
bacto-tryptone	Difco
bromodeoxyuridine (BrdU)	Amersham
bromophenol blue	Biorad
buria-Bertani media, broth base	Gibco
calcium chloride ($CaCl_2$)	Sigma
camptothecin	Calbiochem
coomassie brilliant blue, G250	Biorad
cycloheximide (CHX)	Sigma
dimethyl sulfoxide	Fisher
disulfosuccinimidyl suberate (DSS)	Calbiochem
Dulbecco's modified eagle medium (DMEM)	Gibco
epidermal growth factor (EGF)	Upstate
ethanol, 95%	Fisher
ethidium bromide	OmniPur
ethylene glycol-bis (amino ethyl ether tetra acetic acid) (EGTA)	Sigma
fetal bovine serum (FBS)	Sigma
glucose	EM science
glycerol	BDH

glycine	Biorad
hydrochloric acid	Fisher
isopropanol	Fisher
kanamycin	Sigma
magnesium chloride ($MgCl_2$)	BDH
monensin	Calbiochem
N,N-bis[2hydroxyethyl]-2-aminoethanesulfonic acid (BES)	Sigma
non-essential amino acids	Invitrogen
nonidet P40	BDH
PDGF-β	Upstate
pepstatin a	Sigma
phosphate buffered saline, 10x	OmniPur
potassium chloride	BDH
propidium iodide	Sigma
sodium azide	Sigma
sodium chloride	BDH
sodium dodecyl sulfate (SDS)	Biorad
sodium fluoride (NaF)	Sigma
sodium orthovanadate (Na_3VO_4)	Sigma
sucrose	Biobasic
tetramethylethylenediamine (TEMED)	Gibco
tris (hydroxymethyl) aminomethane	Biorad
Triton X-100	BDH
Tween 20	Fisher
yeast extract, select	Gibco
β-mercaptoethanol	Sigma

2.1.2 Enzymes

DNA ligase, T4	Gibco
dNTPs	Invitrogen
Hot Start Taq, DNA polymerase	Qiagen
Restriction endonucleases	Gibco
RNAase	Sigma

2.1.3 Experimental Kits

QIAprep Spin Miniprep Kit	Qiagen
Apoptosis detection kit	Promega
HiSpeed Plasmid Midi Kit	Qiagen

QIAquick Gel Extraction Kit	Qiagen
QuikChange Site-Directed Mutagenesis Kit	Stratagene
RNAi Max Transfection kit	Invitrogen
Supersignal ECL Western Blotting Detection Reagents	Pierce
Topo-XL PCR cloning kit	Invitrogen

2.1.4 Plasmids

pCR-XL-TOPO	Invitrogen
pEYFP-C1	Clontech

2.1.5 Molecular Size Markers

100bp DNA ladder	Gibco
1kb DNA ladder	Gibco
prestained markers for SDS-PAGE	Sigma

2.1.6 Other Materials

medical X-ray Film	Fuji
glutathione insolubilized on cross-linked 4% agarose	Sigma
goat anti-mouse IgG conjugated with agarose	Sigma
Protein A sepharose 6MB	Pharmacia
Transblot Nitrocellulose	Biorad
Whatman Chromatography Paper	Fisher

2.1.7 Antibodies

All primary and secondary antibodies used in this thesis, as well as their dilutions for immunoblotting, are shown in Table 2.1 below.

Table 2.1 Antibodies and their dilutions used for Immunoblotting

Primary Antibody	Dilution	Provider
Goat anti-phospho-Rb (pRb)	1:500	Santa Cruz
Goat anti-phospho-Y1068-EGFR	1:1000	Santa Cruz
Mouse anti-BrdU	1:200	Amersham
Mouse anti-c-Myc	1:400	Santa Cruz
Mouse anti-Cyclin-D1	1:500	Santa Cruz
Mouse anti-EEA1	1:1000	BD Pharmingen
Mouse anti-EGFR (Ab1)	1:1000	Sigma

Mouse anti-GFP/YFP	1:1000	Clontech
Mouse anti-phopho-ERK1/2	1:1000	Santa Cruz
Mouse anti-phospho-tyrosine (pY99)	1:1000	Santa Cruz
Mouse anti-phospho-Y1045-EGFR	1:500	US Biological
Mouse anti-phospho-Y783-PLC-γ1	1:1000	Medicore
Mouse anti-PLC-γ1	1:500	Upstate
Mouse anti-Ras	1:1000	Upstate
Mouse anti-tubulin	1:1000	Santa Cruz
Rabbit anti-Cbl-b	1:400	Santa Cruz
Rabbit anti-C-Cbl	1:1000	Santa Cruz
Rabbit anti-Cyclin-E	1:400	Santa Cruz
Rabbit anti-EGFR (1005)	1:1000	Santa Cruz
Rabbit anti-ERK/MAPK	1:1000	Santa Cruz
Rabbit anti-GFP/YFP	1:4000	Dr. Luc Berthiaume
Rabbit anti-GFP/YFP	1:1000	Santa Cruz
Rabbit anti-Grb2	1:1000	Santa Cruz
Rabbit anti-p85	1:1000	Upstate
Rabbit anti-PDGFR	1:1000	Santa Cruz
Rabbit anti-phospho-PDGFR	1:1000	Santa Cruz
Rabbit anti-phospho-S473-Akt	1:1000	Cell signaling
Rabbit anti-phospho-Y1086-EGFR	1:1000	Santa Cruz
Rabbit anti-phospho-Y1148-EGFR	1:1000	Santa Cruz
Rabbit anti-phospho-Y1173-EGFR	1:1000	Santa Cruz
Rabbit anti-phospho-Y783-PLC-γ1	1:1000	Santa Cruz
Rabbit anti-phospho-Y992-EGFR	1:500	Santa Cruz
Rabbit anti-PLC-γ1	1:1000	Santa Cruz
Rabbit anti-Raf	1:1000	Santa Cruz
Rabbit anti-SHC	1:2000	BD Transduction

Secondary Antibody	**Dilution**	**Provider**
HRP-conjugated anti-rabbit	1:2000	BioRad
HRP-conjugated anti-mouse	1:2000	BioRad
HRP-conjugated anti-sheep	1:2000	BioRad
HRP-conjugated anti-goat	1:2000	BioRad

2.1.8 Buffers and Other Solutions

Table 2.2 provides a list of all buffers and solutions used in this thesis.

Table 2.2 Buffers and other solutions

Solution	Composition
Acidic Stripping buffer	100 mM acetic acid, 150 mM NaCl, pH 2.7
BES buffer	N,N-bis[2hydroxyethyl]-2-aminoethane sulfonic acid
BOS buffer	50 mM Tris-HCl, pH 7.4, 200 mM NaCl, 1% NP-40, 10% glycerol, 10 mM NaF, 2.5 mM $MgCl_2$, 1mM EDTA
Homogenization buffer	20 mM Tris-Cl, pH7.0, 1mM $MgCl_2$, 4mM NaF
Immunoprecipitation buffer	20 mM Tris-Cl, pH7.5, 150 mM NaCl, 1% NP40, 0.1% sodium deoxycholate
Phosphate-buffered saline (PBS)	137 mM NaCl, 2.7mM KCl, 10 mm phosphate buffer
Protease inhibitor cocktail	0.5mM Na_3VO_4, 0.1mM 4-(2-aminoethyl)-benzenesulfonyl fluoride, 10μg/ml aprotinin and 1μM pepstatin A
SDS-loading buffer	250mM Tris-Cl, 40% glycerol, 8% sodium dodecyl sulfate, 20% b-mercaptoethanol, 2% bromophenol blue
SOC medium	2% bactotyptone, 0.5% yeast extract, 10m $MgCl_2$, 10mM MgSO4, 20 mM glucose
Transfer buffer	48 mM Tris-Cl, 39 mM Glycine, 20% methanol, 0.03% sodium dodecyl sulfate
Transformation buffer	10 mM Pipes, 55mM $MnCl_2$, 15mM $CaCl_2$, 250mM KCl
Triton X-100 lysis buffer	0.4% triton X-100, 140mM NaCl, 50mM Tris-Cl, pH 7.2, 1mM EGTA

2.1.9 Oligonucleotides

Table 2.3 provides a list of all oligonucleotides and their sources used in this thesis.

Table 2.3 Oligonucleotides used in this thesis

Name	Sequence (5'-3')	Provider
c-Cbl stealth siRNA-lead (CBLHSS101416, H08)	CCA GCA GAU UGA UAG CUG UAC GUA U	Invitrogen
c-Cbl stealth siRNA-lag (CBLHSS101416, H09)	AUA CGU ACA GCU AUC AAU CUG CUG G	Invitrogen
Cbl-b stealth siRNA-lead (u26710, H06)	CAA CUC AGU GAG AAU GAG UAG UUU A	Invitrogen
Cbl-b stealth siRNA-lag (u26710, H07)	UAA AGU ACU CAU UCU CAC UGA GUU G	Invitrogen
EGFR-Y1045F-lead (DNA) (*original seq. is A)	GC TTC TTG CAG CGA T(T*)C AGC TCA GAC CCC	Sigma
EGFR-Y1045F-lag (DNA) (*original seq. is T)	GGG GTC TGA GCT G(A*)A TCG CTG CAA GAA GC	Sigma

2.2 Methods

2.2.1 Cell culture

Cell lines were chosen to study either EGFR or PDGFR receptor systems. For the EGFR system, Madin-Darby Canine Kidney Epithelial (MDCK) cells (ATCC CCL-34) and BT-20 cells (ATCC HTB-19) were used, expressing 50-100k or ~150k receptors per cell, respectively. 293T cells (ATCC CRL-11268) transfected with EGFR were comparable to BT20 in receptor number. For the PDGFR system, HepG cells (human hepatocellular carcinoma) stably transfected with PDGF Receptor β, and F442 cells (Obtained from Dr. David Brindley) were used, either of which express between 50-100k receptors per cell. All cells were grown at 37°C in Dulbecco's modified Eagle's medium containing 10% FBS, penicillin, and streptomycin (100U/ml) and were maintained in a 5% CO_2 atmosphere.

2.2.2 Cell treatment

MDCK, BT20, F442, HepG, and transfected 293T cells were grown as described in the previous section. Addition of ligand was performed at 4°C for 15 minutes prior to the onset of stimulation to ensure saturation of cell suface receptors.

Standard treatment. To specifically activate EGFR, MDCK, BT-20, or transfected 293T cells were serum-starved up to 24 h, and EGF was added to a final concentration of 100 ng/ml for indicated pulse times. To specifically activate PDGFR, HepG or F442 cells were serum starved for 24 h, and PDGF was added to a final concentration of 10 ng/ml. To terminate pulse and remove unbound ligand in all cell types, cells were washed five times in PBS and then chased with starvation media.

Endosome activation treatment (i.e. endosomal accumulation of inactive ligand-receptor complexes followed by their activation). This methodology has been previous published by our group (Wang et al., 2002b). (a) *Endosomal EGFR activation:* Quiescent BT20, MDCK, or transfected 293T cells were pre-treated 15 min with 0.5 uM AG1478, and then monensin and EGF were added to final concentrations of 100 uM and 100 ng/ml, respectively. After 30 min incubation (designated as 0 min wash), cells were washed with serum-free medium 3-6 times to activate internalized receptors and then maintained in serum-free medium containing 100 μM monensin for the indicated times. For the monensin-free treatment alternative, cells were pre-treated with 0.5 uM AG1478 for 15 min, and then EGF was added to a final concentrations of 100 ng/ml. After a 30 incubation, cells were cooled down to 4°C and washed with acidic stripping buffer (100 mM acetic acid, 150 mM NaCl pH 2.7) for 1 min (Waterman et al., 1999a). The cells were then washed with PBS four times and chased with starvation media as above. (b) *Endosomal PDGFR activation:* Quiescent HepG or F442 cells were pre-treated 15 min with 0.05 uM AG1296, and then monensin and PDGF were added to final concentrations

of 100 uM and 10 ng/ml, respectively. After 30 min incubation (designated as 0 min wash), cells were washed with serum-free medium 3-6 times to activate internalized receptors and then maintained in serum-free medium containing 100 μM monensin for the indicated times. After a treatment time one 1 h, the cells were washed with phosphate-buffered saline (PBS) five times and chased with starvation medium.

Treatment in conjunction with inhibitors and other chemicals. To inhibit PI3K activation, wortmannin was added to cells at 100nM, 30 min prior to treatment and then maintained in the medium during stimulation pulse times. To inhibit MEK activation (and thus Ras/MAPK pathway transduction) U1026 (dissolved in dimethyl sulphoxide (DMSO) at a stock concentration of 10 mM) was added at 10uM one hour prior to treatment and then maintained in the medium during stimulation pulse times. For discontinuous stimulation experiments testing for recovery of activation after first pulse treatment, cells were washed with PBS two hours after the first pulse, and generally assayed at the 8 h time point (i.e. 6 hours later). To inhibit new protein synthesis when assaying for EGFR degradation, cycloheximide (CHX) was added (final concentration of 0.5uM) 30 min prior to treatment.

2.2.3 Plasmid construction

The pEYFP-N1 expression plasmid containing the wild-type (wt) EGFR sequence was used as template for the construction of all mutants employed in this study. For the creation of EGFR-Y1045F and LL/AA substitution mutations, the QuikChange® XL Site-Directed Mutagenesis Kit from Stratagene was used. Primer pairs were designed which mismatched the wild-type sequence at 2 or 3 central nucleotides to accommodate the required substitution and used to amplify full length plasmids containing the

mutation. For the creation of the EGFR1044 truncation mutant, upstream and downstream primers were designed to be complementary to the starting nucleotide sequence and the nucleotide sequence adjacent to the truncation site, respectively (Wang et al., 2005). Then the various EGFR truncation fragments with XhoI / KpnI restriction sites were amplified from pEYFP/wtEGFR plasmid and subcloned into a new pEYFP vector.

2.2.4 Preparation of total cell lysates

To obtain total lysates, BT20, MDCK , 293T, HepG or F442 cells were lysed and homogenized in ice-cold MPER Mammalian Protein Extraction Reagent (Pierce, Rockford, Illinois) with protease inhibitor cocktail. The lysates were centrifuged at 4^0C for 30 min at 21,000g. Following protein quantification the supernatant was boiled in SDS-loading buffer at 95°C for 5 minutes.

Protein was quantitated using the Bradford protein dye assay, according to the method of Bradford (Bradford, 1976). Absorbance at λ=595nm was measured by a Beckman DU 640 spectrophotometer (Beckman Instrument, Fullerton, CA). Bovine Serum Albumin (BSA) was used as a standard.

2.2.5 Subcellular fractionation of cultured cells

Fractionation method for analysis of cell surface- and endosome-localized receptor. Isolation of plasma membrane (PM), endosomal (EN), and cytosolic (CY) fractions was carried out by a method modified from our previous publication (Wang et al., 1999). For each experimental treatment, four 15-cm-diameter plates of MDCK cells, or eight 15 cm diameter plates of BT-20 cells or F442 cells, or five 15 cm diameter plates of HepG cells

were used. Subconfluent cells were serum starved for 24 h prior to treatment. Followed the specific treatment, all of the following procedures were performed at 4°C. For each treatment, cell monolayers from four plates were scraped into 3-4 ml of homogenization buffer with 0.25M sucrose and protease inhibitor cocktail, and homogenized with a glass Potter-type homogenizer. The homogenates were centrifuged at 200 x g for 5 min to remove cell debris and nuclei (pellet 1 [p1]). The postnuclear supernatant (S1) was then centrifuged at 1500 x g for 10 min to yield a supernatant (S2), which was used to isolate the EN and CY fractions, and a pellet (P2), which was used to isolate the PM fraction. Next, P2 was resuspended in homogenization buffer (0.25 M sucrose), overlaid upon an equal volume of 1.42 M sucrose buffer and centrifuged at 82000 x g for 1 h. The pellicule at the 0.25-1.42 M interface was collected, sucrose concentration adjusted to 0.40 M, and then centrifuged at 20, 000 x g for 30 min to obtain the solid phase PM fraction. The S2 fraction was centrifuged at 200, 000 x g for 30 min to yield the soluble CY fraction and a microsomal pellet. This pellet was resuspended in 0.25 M sucrose buffer and overlaid upon a discontinuous sucrose gradient containing equal volumes of homogenization buffer at 1.00 and 1.15 M sucrose. The resuspension was centrifuged at 200, 000 x g for 1.5 h. To obtain the purified EN fraction, the pellicule at the 0.25-1.00 M interface was collected, sucrose adjusted to 0.25 M, and then centrifuged at 200000 x g for 30 min. Both PM and EN fractions were solubilized overnight using Mammalian Protein Extraction Reagent (MPER, Pierce Chemical Co., IL) prior to electrophoresis. Due to low yields, fractions from multiple experiments were pooled for subsequent analysis on SDS-PAGE.

Fractionation method for analysis of Cbl membrane localization. Following treatment, BT20 or transfected 293T cells were scraped into homogenization buffer

(0.25M sucrose, 20 mM Tris-HCl [pH 7], 1 mM $MgCl_2$, 4 mM NaF, and 0.02% NaN_3) containing 0.5 mM Na_3VO_4, 0.1 mM AEBSF (4-[2-aminoethyl]-benzenesulfonyl fluoride), 10 μg/mL aprotinin, and 1 μM pepstatin A and homogenized by grinding 30x in a glass-walled homogenizer. Homogenates were twice pre-cleared of nuclei by centrifugation (100 x g, 5'), and the resulting post-nuclear supernatant (PNS) was fractionated into total membrane (TM) and cytosolic (CY) fractions by centrifugation at 150 000 x g, 1 h. TM fractions were re-suspended in homogenization buffer and centrifuged again along with CY fractions at the same speed as before. Fractions were then solubilized in 1% NP-40, assayed by the Bradford method for protein concentration (Bradford, 1976), and then separated by SDS-PAGE.

2.2.6 Immunoprecipitation

Immunoprecipitation experiments were carried out as described previously (Wang et al., 1996b). The cells were lysed with immunoprecipitation buffer containing protease inhibitor cocktail for 30 min. Cell lysates were then centrifuged at 21,000 *g* for 30 min to remove insolubilized debris. The supernatants, containing 1 mg of total proteins were first pre-cleared with secondary IP IgG, then nutated overnight at 4°C with 1 μg of primary immunoprecipitating antibody. EGFR or EGFR-YFP precipitates were then incubated with 20 μg secondary IgG (either agarose-conjugated anti-mouse IgG or Protein A Sepharose 6MB-conjugated anti-rabbit IgG) for 3 h, centrifuged (500-1000 x g, 2 min), washed three times with PBS, and the resulting pellet resuspended in sample buffer containing SDS. Protein samples were separated by SDS-PAGE, with equal volumes of IP preparation (20 μL/lane) loaded onto the polyacrylamide gels. For control experiments, normal mouse or rabbit IgG (Sigma) was used. A list of antibodies used for

immunoprecipitation and their concentrations is given in Table 2.4.

Table 2.4 Antibodies and their concentrations used for immunoprecipitation.

Antibody	Concentration (μg/ml)	Provider
Mouse anti-EGFR (Ab1)	1000	Sigma
Rabbit anti-EGFR (1005)	200	Santa Cruz
Rabbit anti-GFP/YFP	(serum)	Dr. Luc Berthiaume
Rabbit anti-GFP/YFP	1000	Clontech
Rabbit anti-PDGFR	200	Santa Cruz

2.2.7 Gel electrophoresis and immunoblotting

Aliquots of protein from each sample were used for SDS-polyacrylamide gel electrophoresis. For the staining of total cell lysates, aliquots containing 20μg of protein from each cell lysate were used. For the detection of immunoprecipitation products, one-tenth of the immunoprecipitate from each lysate was used. To detect each subcellular fraction, aliquots containing one-tenth of the total protein from each fraction were used. Protein samples were separated by electrophoresis through 8%-12% SDS-polyacrylamide gels depending on the size of protein being studied. Prestained protein markers (Sigma) were used for molecular weight standards. Proteins were electrophoretically transferred onto Transblot nitrocellulose membranes (BioRad, Hercules, CA). Transfer was done using a semi-dry blotting apparatus (Model SD transfer cell, BioRad) at 15 mA per minigel for 45 minutes in transfer buffer. Blots were blocked with 3% skim milk in 0.05% Tween-PBS (blocking buffer) for 30 minutes. Membranes were then probed with the respective primary antibody in blocking buffer overnight, washed twice with distilled H_2O, incubated with HRP-conjugated IgG secondary antibody for 1 hour, washed twice with distilled H_2O, washed with 0.05% Tween-PBS for 5 minutes, rinsed twice with distilled H_2O and washed with TBS buffer. Secondary antibodies were detected by

enhanced chemiluminescence, with SuperSignal ECL Western Blotting Detection Reagents (Pierce Chemical) and exposure to X-ray film (Fuji Photo Film Co., Tokyo, Japan). For graphical analysis of immunoblots, exposed film of sub-saturated bands were scanned using a GS-800 calibrated densitometer and quantified using Quantity One software (Bio-Rad). All primary and secondary immunoblotting antibodies used are listed in Table 2.1 with their respective dilutions.

2.2.8 Fluorescence microscopy

Indirect immunofluorescence was carried out as described previously (Wang et al., 1996b). Briefly, cells were grown on glass coverslips and serum starved for 24 h. After treatment, the cells were fixed by methanol and permeabilized with 0.2% Triton X-100. Next, the cells were incubated with indicated primary antibodies at room temperature for 1 h followed by fluorescence-labeled secondary antibodies for 1 h. The stained cells were analyzed and photographed with a Zeiss Axiovert 200 microscope (Thornwood, NY) and an AttoArc2 HBO 100W light source (Atto Instruments, Rockville, MD). Color photographs were taken with a digital camera by superimposing the monochrome graphs of two channels. A list of antibodies used for immunofluorescence and the concentrations at which they were used is given in Table 2.5.

Observation on living cells transfected with YFP fusion constructs were done by using an inverted Zeiss microscope with standard YFP filter. For that purpose, 22 mm cover slips were used and placed upside down in a temperature stable cell chamber. The images were recorded in 1 min intervals. The Video was made using Adobe Premiere 6.0 software (San Jose, CA)

Table 2.5 Antibodies and their dilutions used for immunofluorescence

Primary Antibody	Dilution	Provider
Mouse anti-EEA1	1:100	BD Pharmingen
Mouse anti-phospho-EGFR	1:100	Upstate
Mouse anti-phospho-Tyrosine (py99)	1:100	Santa Cruz
Rabbit anti-EGFR(1005)	1:100	Santa Cruz
Rabbit anti-GFP	1:100	Clontech
Rabbit anti-PDGFR	1:100	Santa Cruz
Rabbit anti-phospho-PDGFR	1:100	Santa Cruz
Sheep anti-EGFR	1:100	Upstate
Secondary Antibody	**Dilution**	**Provider**
Rhodamine-conjugated anti-goat	1:200	Jackson ImmunoResearch
Rhodamine-conjugated anti-mouse	1:200	Jackson ImmunoResearch
Rhodamine-conjugated anti-rabbit	1:200	Jackson ImmunoResearch
Rhodamine-conjugated anti-sheep	1:200	Jackson ImmunoResearch

2.2.9 TUNEL assay

Cells (10,000 per coverslip) were serum starved for three days to initiate a significant level of apoptosis. Cells were then treated (or not) as necessary and incubated 20 h with medium alone or medium containing growth factor (EGF or PDGF) before fixation. As a background control, untreated cells growing in 10% FBS were assayed to determine basal apoptotic level. As a positive control, cells were induced into apoptosis by pre-treating 2 h with 50nM of camptothecin, an inhibitor of DNA topoisomerase I (Calbiochem). Apoptosis was assayed by TdT-mediated dUTP Nick-End Labeling (TUNEL) assay, using an apoptosis detection system kit (Promega) according to the manufacturer's instructions. Briefly, cells were washed, fixed in -20°C methanol for 5 min and then permeabilized with 0.5% Triton X-100 for 10 min. Coverslips were set upon TdT incubation buffer at 37°C for 1 h, and then counter stained with 0.5μg/ml propidium iodide. Cells were visualized in the green channel to morphologically

quantitate apoptotic nuclei, and in the red channel to quantitate all nuclei. The percentage of apoptotic cells was calculated as the number of apoptotic nuclei/total nuclei analyzed x 100. For each experimental treatment, a minimum of 250x3 cells were counted.

2.2.10 DNA synthesis assay

DNA synthesis was assayed by bromodeoxyuridine (BrdU) incorporation. Cells (BT20, MDCK, HepG and F442) were plated at 10,000 cells per glass coverslip and serum starved by incubation in serum free medium for 24 h. DNA synthesis was assayed by bromodeoxyuridine (BrdU) incorporation in the presence of 25 μM BrdU. For discontinuous treatment, BrdU was added back after each subsequent pulse or chase. After 16-18 hours, cells were washed with PBS and fixed with methanol (-20°C) for 5 minutes. Following the denaturation of DNA with 2 M HCl for 30 min at room temperature, cells were incubated with mouse anti-BrdU antibody for one hour before addition of FITC-conjugated anti-mouse IgG for (for detection of BrdU) and 50 μg/ml propidium iodide (to stain for total DNA). The stained cells were analyzed and photographed with a Zeiss Axiovert 200 microscope (Thornwood, NY) and an AttoArc2 HBO 100 W light source (Atto Instruments, Rockville, MD). Cell nuclei were visualized in the red and green channels and digital images quantitated for BrdU incorporation. Percent DNA synthesis was calculated as the number of BrdU positive cells/total number of cells analyzed x 100. For each experimental treatment, a minimum of 500x3 cells were counted.

2.2.11 Flow Cytometry

EGFR internalization was assayed by flow cytometry modified from a method previously described by Duan *et al.*, 2003 (Duan et al., 2003). Cells at ~75% confluency were serum-starved overnight, incubated with cold Alexa Fluor 647-labeled EGF at 4°C for 30 min. Excess ligand was removed by PBS wash and cells were incubated at 37°C for indicated times to allow internalization. Following each time point, cells were acid washed (0.2 M acetic acid, 0.5 M NaCl, PH 2.8) for 1 min to remove non-internalized EGF, and then the fluorescence emission of internalized EGF was detected by flow cytometry.

2.2.12 RNAi

Strong candidate sequences for the coding regions of both c-Cbl and Cbl-b were chosen by algorithms provided by Invitrogen and used to design small interfering RNA duplexes (siRNAs) for use in all RNAi experiments performed (see Table 2.3). Candidate c-Cbl and Cbl-b siRNAs were tested in 293T cells, along with a non-specific control siRNA, to assess optimal times of knockdown and concentrations of dsRNA. RNAi Max transfection kit was employed for cotransfection of dsRNA with EGFR constructs (Invitrogen, CA). Significant (>90%) knockdown was obtained following 48 h transfection using 100 pmol of c-Cbl dsRNA and 200 pmol of Cbl-b dsRNA. Neither Cbl siRNA duplex, nor the negative siRNA duplex, showed non-specific interference effects.

CHAPTER 3:

The Physiological Significance of Endosomal Receptor Tyrosine Kinase Signaling

The majority of data presented in this chapter has been published among three refereed papers (Pennock and Wang, 2003; Wang et al., 2002a; Wang et al., 2004), and has been adapted into this thesis with permission.

3.1 Overview

Traditionally, ligand-induced RTK endocytosis was held as a mechanism for receptor downregulation and signal attenuation (Wiley and Burke, 2001; Ceresa and Schmid, 2000). Indeed, the elimination of endosomal RTK trafficking by inhibiting receptor endocytosis does not attenuate ligand-induced physiological outcomes and in some cases even leads to cell transformation (Wells et al., 1990). Even though this seems to argue against the physiological relevance of endosomal signaling, a growing body of evidence implicates the endocytic signaling capacity of RTKs. It is well established that receptors undergo clathrin-mediated endocytosis only minutes after ligand stimulation, and yet can spend between 1-2 hours trafficking along the endocytic route before being degraded. Studies have shown that these internally trafficking RTKs remain in a kinase-active, autophosphorylated state (Fukazawa et al., 1996; Chen et al., 1989; de Melker et al., 2001; Felder et al., 1992; Glenney, Jr. et al., 1988; Honegger et al., 1990b; Sorkin and Waters, 1993). In addition, several findings suggest that some signaling pathways require RTK internalization and others do not. Inhibition of EGFR internalization, for instance, has been shown to decrease MAPK activation even though cell proliferation is enhanced (Fukazawa et al., 1996; Chen et al., 1989; de Melker et al., 2001; Felder et al., 1992; Glenney, Jr. et al., 1988; Honegger et al., 1990b; Sorkin and Waters, 1993). By globally inhibiting endocytosis however, these experiments do not truly investigate RTK signal transduction in a physiological context, and it is difficult to deduce whether the observed results come from a lack of endosomal signaling or from broad inhibition of endocytosis.

Nor do these experiments rule out that RTK signaling is occurring elsewhere than at the PM. Ligand-induced cell proliferation, for instance, requires a prolonged mitogenic stimulus that would likely encompass an amount of time much longer than the physiological occupancy of activated RTKs at the cell surface. It is therefore misleading to conclude that signaling outputs derived from PM-retained receptors are due to the signaling exclusivity of this location.

There remains considerable controversy over the physiological relevance of endosomal RTK signaling. In short, definitive proof that RTKs can initiate, generate, and/or propagate signal transduction from endosomal compartments does not exist. The inability to demonstrate endosomal RTK signaling is due in large part to the lack of methods allowing exclusive separation and characterization of endosome-generated signaling without contribution from PM-generated signaling.

In this chapter, I investigate the physiological significance of endosomal signaling from two endogenously-expressed receptor types in cell culture: (1) EGFR is studied in BT20 and MDCK cells, and (2) PDGFR is studied in F442 and HepG cells. Both receptors are well characterized RTKs, and share many similarities in signaling function (Schlessinger, 2000). First, I report the development of a system whereby RTK signaling can be studied from the endosomes without contribution from PM signaling. By using this system, I then investigate the ability of endosome-activated RTKs to recruit signaling molecules and stimulate signaling pathways. Most importantly, I then determine whether endosomal RTK signaling can lead to two major biological outcomes: cell survival and cell proliferation. Investigating RTK-induced cell proliferation involves a specific focus due to the requirements of its induction, and consequently encompasses the latter half of this chapter.

3.2 Development of a system to specifically activate EGFR and PDGFR at endosomes

Studies have shown that kinase-inactive EGFR mutants internalize into endosomes in response to EGF, and the same phenomenon has been observed for kinase inactive PDGFR following PDGF stimulation (Felder et al., 1990; Glenney, Jr. et al., 1988; Heldin and Westermark, 1999). Unlike wild-type receptors however, these kinase deficient mutants preferentially recycle to the plasma membrane instead of trafficking to lysosomes for degradation. In addition, treatment of cells with the cationic ionophore monensin inhibits RTK recycling, resulting in the retention of these kinase dead mutants in endosomes (Felder et al., 1990). Based on these findings, I examined whether pre-treating cells with a membrane-permeable kinase inhibitor—specific to either EGFR or PDGFR—in the presence of monensin would lead to internalization of inactive ligand-receptor complexes following EGF or PDGF stimulation.

This approach was first tested for the EGFR system in BT20 cells. AG1478 is a soluble tyrosine kinase inhibitor which competes with ATP for binding to EGFR, thereby antagonizing the receptor's autophosphorylation activity (Arteaga, 2001; Haugh et al., 1999). AG1478 was added to BT20 cells 15 min prior to incubation with EGF in the presence of monensin. After 30 min incubation with this cocktail, immunofluorescence showed complete internalization of EGFR (Fig 3.1A). This endosome-associated EGFR remained inactive, as EGFR and pTyr immunofluorescent signals did not overlap (Fig 3.1A). In control cells treated with EGF alone (referred to as "standard" EGF treatment), EGFR was both phosphorylated and internalized following 15 and 30 min stimulation (Fig 3.1A). To determine if inactive endosome-localized EGFR was still bound to EGF,

Texas-red (TR)-labeled EGF was used in place of unlabeled ligand. In the presence of AG1478 and monensin, triple immunofluorescence staining revealed that TR-EGF colocalized with non-phosphorylated EGFR in endosomes, while in control cells

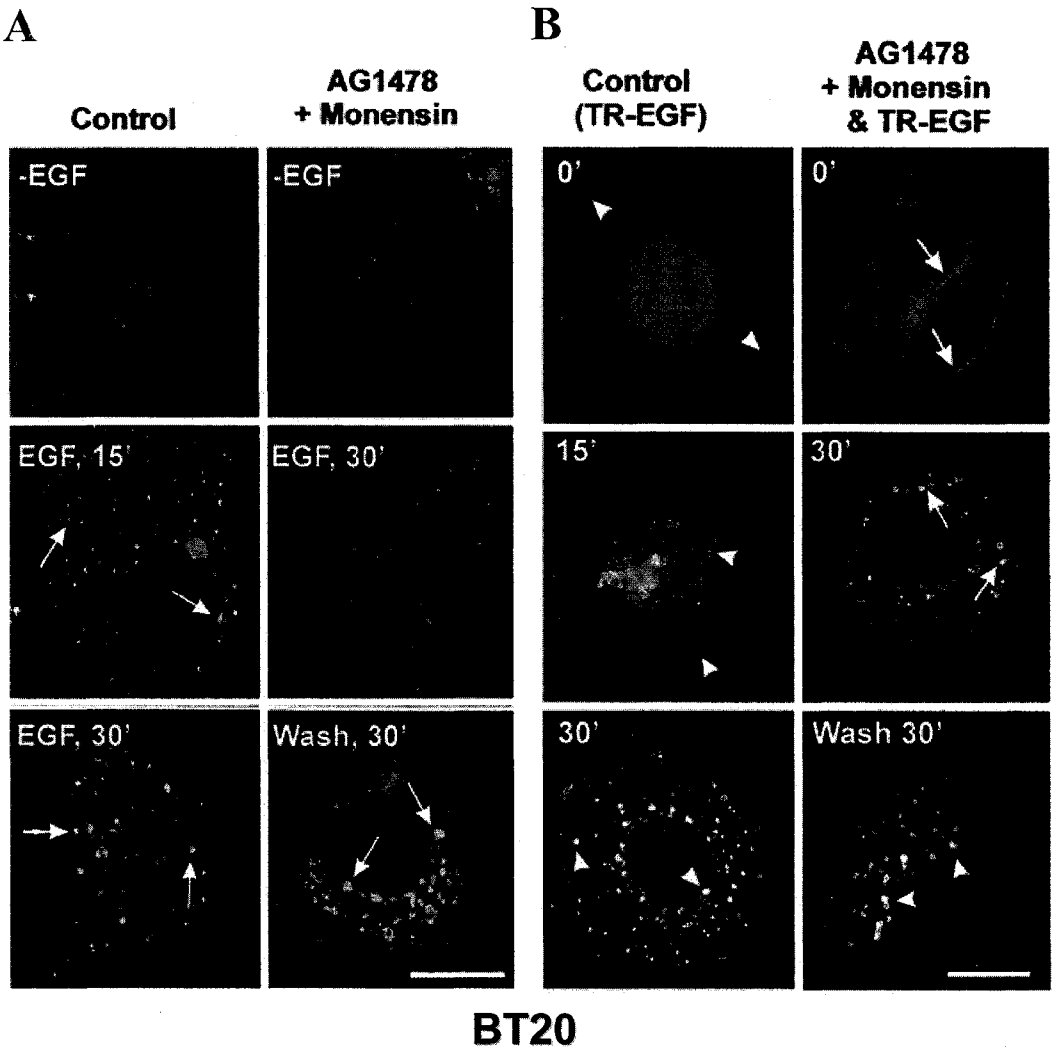

Fig 3.1. Immunofluorescent analysis of selective activation of EGFR after its endocytosis into endosomes. (A) BT20 cells were treated with AG1478 for 15 min and then EGF was added in the presence of monensin at 37°C for 30 min. Some of the cells were then washed with PBS and incubated with serum-free medium for 30 min (right panels). BT20 cells that were serum-starved or treated only with EGF for 15 and 30 min were used as controls (left panels). EGFR (red) and pTyr (green) localization was determined by indirect immunofluorescence, where yellow corresponds to co-localization of EGFR and pTyr. **(B)** BT20 cells were treated and the same controls used as in (A), though TR-EGF was employed in place of EGF. TR-EGF (red), EGFR (green) and phosphotyrosine (blue) localization was determined by triple indirect immunofluorescence. Co-localization of TR-EGF and EGFR (yellow) is indicated by

arrows, while co-localization of TR-EGF, EGFR and pTyr (violet) is indicated by arrowheads. Size bar = 20 μm. Figure reproduced for this thesis with permission.

lacking AG1478 and monensin TR-EGF colocalized with phosphorylated endosome-associated EGFR (Fig 3.1B).

As AG1478 belongs to a tyrphostin family of soluble and reversible kinase inhibitors, it was next determined whether endosome-localized non-phosphorylated EGFR could be activated by washing out AG1478 with excess medium. After incubating cells with AG1478, EGF/TR-EGF, and monensin for 30 min to allow internalization of inactive EGF-EGFR complexes, cells were washed multiple times with medium. Endosomal EGFR was significantly phosphorylated 30 min following medium wash and remained colocalized with TR-EGF (Fig 3.1A and 3.1B). To determine whether this endosomal activation method could apply to other RTK systems, the PDGF receptor was tested in F442 and HepG cells. AG1296 is a PDGFR-specific kinase inhibitor whose mechanism of inhibition is similar to AG1478. F442 and HepG cells were pre-incubated with AG1296 for 15 min and then stimulated with PDGF in the presence of monensin. Following 30 min incubation with PDGF and monensin, PDGFR was internalized into endosomes in a non-phosphorylated state, as indicated by the lack of overlap between PDGFR and pTyr immunofluorescent signals (Fig 3.2A and 3.2B). Endosomal PDGFR activation was then tested by washing cells multiple times with medium to dislodge and dilute AG1296. Following 30 min medium wash, endosomal PDGFR was significantly activated (Fig 3.2A and 3.2B). Thus, treatment of F442 or HepG cells with AG1296, PDGF, and monensin allowed exclusive activation of PDGFR in a manner similar to endosomal EGFR activation in BT20 and MDCK cells. It should also be noted that in

both EGFR and PDGFR systems, no PM-associated receptor or receptor phosphorylation was observed following either standard activation (i.e. receptor activation following addition of ligand alone) or endosomal activation (i.e. activation of receptor following

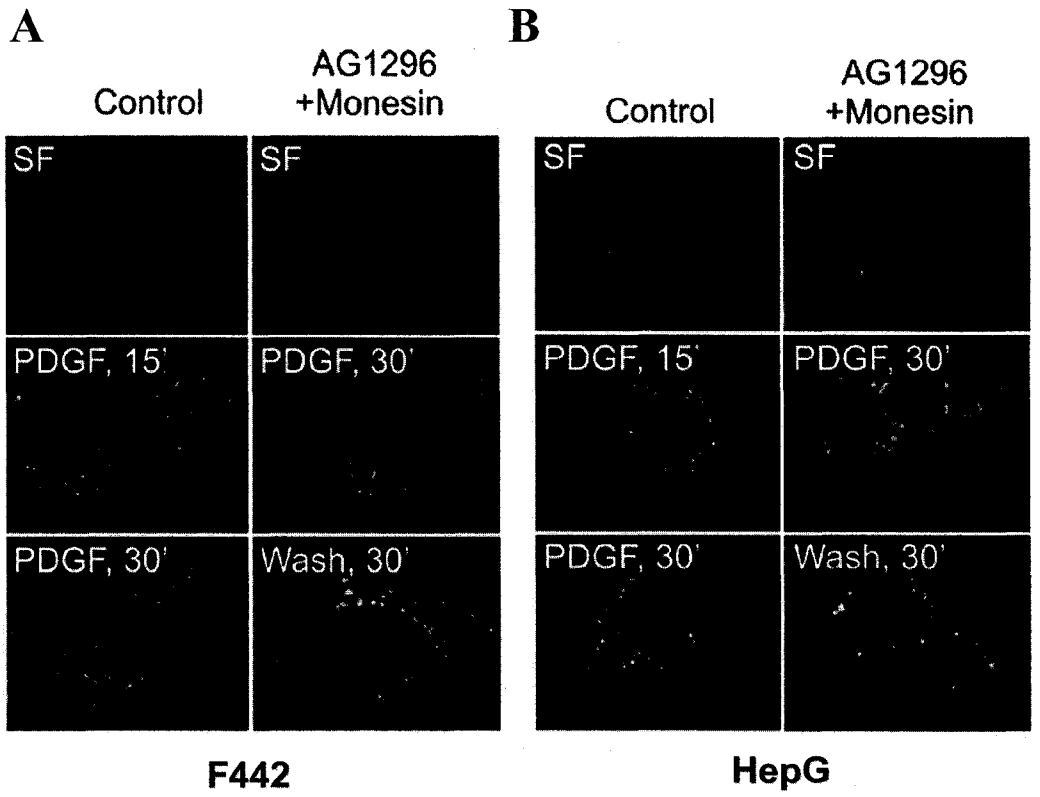

Fig 3.2. Immunofluorescent analysis of selective activation of PDGFR after its endocytosis into endosomes. F442 **(A)** or HepG **(B)** cells were treated with AG1296 for 15 min and then PDGF was added in the presence of monensin at 37°C for 30 min. Some of the cells were then washed with PBS and incubated with serum-free medium for 30 min (right panels). Cells that were serum-starved or treated only with PDGF for 15 and 30 min were used as controls (left panels). PDGFR (green) and pTyr (red) localization was determined by indirect immunofluorescence, where yellow corresponds to co-localization of PDGFR and pTyr. In addition to PDGFR- and pTyr-positive vesicles (yellow), F442 and HepG typically show PDGFR-negative vesicles containing other pTyr-positive proteins (green vesicles). Size bar = 20 μm. Figure reproduced for this thesis with permission.

endosomal accumulation of inactive ligand-receptor complexes) (Fig 3.1 and 3.2). Thus, ligand-induced endocytosis and receptor activation occurred in the absence of receptor recycling.

Subcellular fractionation was employed to biochemically assess the subcellular location and phosphorylation of receptors (EGFR or PDGFR) following standard or endosomal activation (Fig 3.3A & 3.3C). BT20 and MDCK cells (for EGFR characterization), and F442 and HepG cells (for PDGFR characterization) were treated under standard or endosomal activation conditions, homogenized, and separated into cytosol (CY), plasma membrane (PM), and endosome (EN) fractions (fractionation methods are described in detail in Chapter 2.2.5). It is well accepted that RTKs remain PM-localized and non-phosphorylated in the absence of stimulation though become phosphorylated and primarily endosomal in a matter of minutes following ligand-mediated activation. Therefore, the RTK itself can be used as a biochemical marker for PM and endosome fractions. Both EGFR and PDGFR demonstrate this localization pattern. In the absence of ligand-mediated activation, receptors were found primarily in the PM fraction in a non-phosphorylated state (Fig 3.3A & 3.3C lanes 2-4), while they were found primarily in the EN fraction after 30 min of standard ligand-mediated activation (Fig 3.3A & 3.3C lanes 5-7). In addition, the endosome marker protein, early endosome autoantigen 1 (EEA1), is highly enriched in EN fractions from all four cell types. Incubation with kinase inhibitor (AG1478 or AG1296) for 15 min, followed by treatment with EGF/PDGF and monensin for 30 min, resulted in the accumulation of

non-phosphorylated receptor in EN fractions (Fig 3.3, quantitated for EGFR in Table 3.1). Following inhibitor washout and 30 min incubation in medium, EN-localized receptors became phosphorylated (Fig 3.3 & Table 3.1). No increase in PM-associated

Fig 3.3. Biochemical analysis of selective activation of endosome-associated RTKs by subcellular fractionation. **(A)** Selective activation of endosome-associated EGFR. Serum-starved BT20 and MDCK cells were left untreated (-EGF), treated 30 min with EGF (+EGF), or conditioned with AG1478 (15 min) then AG1478+EGF+monensin (30 min) and either left unwashed (-Wash) or washed to remove AG1478 and incubated 30 min in serum-free medium (+Wash). Following treatment, cell homogenates were fractionated into plasma membrane (PM), endosome (EN) and cytosol (CY) fractions. These subcellular fractions were subjected to immunoblotting with anti-EGFR, anti-pTyr and anti-EEA1 antibodies. TL, total lysate. **(B)** Selective activation of endosome-associated EGFR without using monensin. BT20 and MDCK cells were treated with AG1478 for 15 min and then EGF added for 30 min followed by wash with acidic stripping buffer at 4°C for 1 min. Acid buffer and remaining AG1478 was then washed out with PBS and cells returned to 37°C and incubated in serum-free medium for 30 min. Cell homogenates were fractionated into PM, EN and CY fractions as in (A). **(C)** Selective activation of endosome-associated PDGFR. Serum-starved F442 and HepG cells were left untreated (-PDGF), treated 30 min with PDGF (+PDGF), or conditioned with AG1296 (15 min) then AG1296+PDGF+monensin (30 min) and either left unwashed (-Wash) or washed to remove AG1296 and incubated 30 min in serum-free medium (+Wash). Following treatment, cell homogenates were fractionated into PM, EN, and CY fractions as in (A) and (B). Subcellular fractions were subjected to immunoblotting with anti-PDGFR, anti-pPDGFR, and anti-EEA1 antibodies. TL, total lysate. The immunoblots shown are representative of at least three independent experiments.

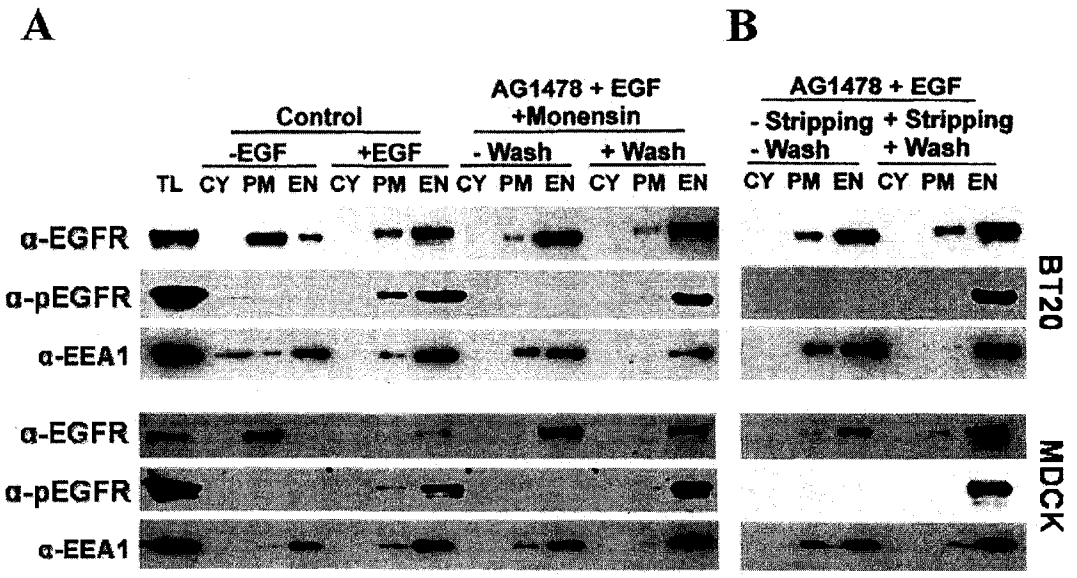
A
B
Control
AG1478 + EGF
+Monensin
-EGF
+EGF
- Wash
+ Wash
TL CY PM EN CY PM EN CY PM EN CY PM EN
α-EGFR
α-pEGFR
α-EEA1
AG1478 + EGF
- Stripping
+ Stripping
- Wash
+ Wash
CY PM EN CY PM EN
BT20
MDCK

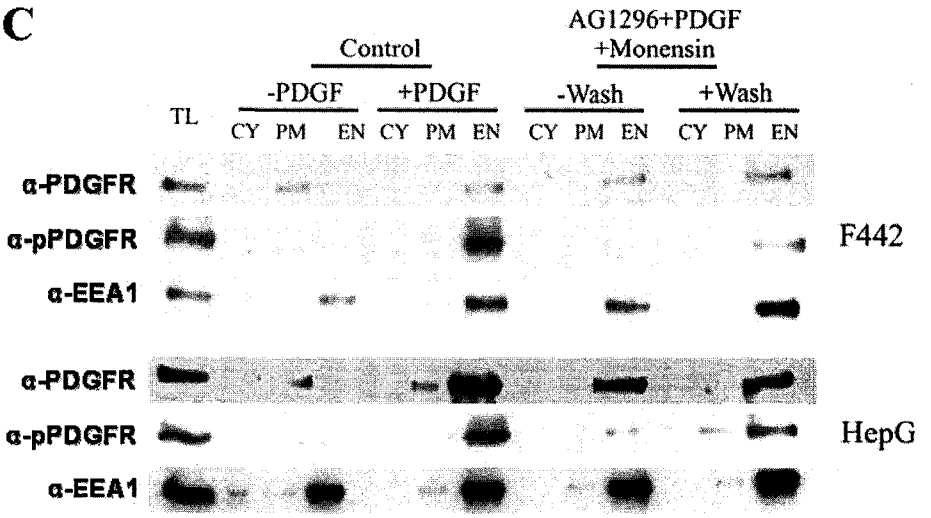
C
Control
AG1296+PDGF
+Monensin
-PDGF
+PDGF
-Wash
+Wash
TL
CY PM EN CY PM EN CY PM EN CY PM EN
α-PDGFR
α-pPDGFR
α-EEA1
F442
HepG

receptor or receptor phosphorylation was observed following washout of kinase inhibitor and monensin, suggesting there was no detectable recycling of receptors from endosomes to the plasma membrane following the removal of monensin. Data from triplicate experiments representative of Fig 3.3A were quantitated by densitometry of band intensities and presented for analysis in Table 3.1. Together these results validate a system to specifically activate RTKs in endosomes without any detectable activation at the plasma membrane.

Monensin is a cationic Na+/H+ ionophore that inhibits the endosomal acidification process necessary for endosomal receptor trafficking (Doebler, 2000; Tartakoff, 1983). Consequently, this chemical has been widely employed to block both receptor recycling and lysosomal sorting (Basu et al., 1981; Wileman et al., 1984; Stein et al., 1984; Pippig et al., 1995). Although the physiological side-effects of monensin were likely minimized by washing it away with the kinase inhibitor prior to endosomal activation, I wanted to validate an alternative endosomal activation system that did not require monensin. This alternative system was tested for EGFR using subcellular fractionation (Fig 3.3B). BT20 and MDCK cells were pre-treated 15 min with AG1478 and then EGF was added for 30 min. At this point most EGFR was localized to EN-fractions while a small amount localized to PM-fractions (Fig 3.3B). Both receptor populations were non-phosphorylated, as indicated by the absence of phosphotyrosine bands. To eliminate any contribution from PM-associated EGF-EGFR complexes, cells were cooled down to 4°C and washed with acidic stripping buffer for 1 min. AG1478 was then washed out with excess medium and cells returned to 37°C. After 30 min incubation, EN-associated EGFR was significantly activated and no activation from the PM-fraction was observed, suggesting that all the recycled EGFR had been successfully stripped of EGF. These

Table 3.1. Quantitative analysis by subcellular fractionation of the selective activation of endosome-associated EGFR.

Cell type and marker	Yield (%) of indicated fraction[a] for:											
	Control cells						Cells treated with AG1478 + EGF + monensin					
	Without EGF			With EGF			Without wash			With wash		
	CY	PM	EN	CY	PM	EN	CY	PM	EN	CY	PM	EN
BT20												
EGFR	0	78	22	0	28	72	0	9	91	0	10	90
p-EGFR	0	0	0	0	27	73	0	0	0	0	2	98
EEA1	29	8	63	3	17	80	2	35	63	4	2	94
MDCK												
EGFR	0	94	5	5	15	80	0	4	95	2	2	96
p-EGFR	0	0	0	0	9	91	0	0	0	0	3	97
EEA1	12	7	81	5	14	81	3	19	78	3	6	91

[a]Data presented as a densitometric quantitation of the results from Fig 3.3A normalized against the total yield of the three subcellular fractions (CY, PM, and EN). Each value is the percentage of the total of each set of three fractions following normalization.

results indicate that even without monensin, endosome-associated receptor can be activated without detectable activation from PM-associated receptors.

Another pertinent question regarding the endosomal activation system is whether the inactive ligand-receptor complexes internalize into the same pool of endosomes as those following standard ligand stimulation. It is well established that RTKs stimulated at the PM internalize into EEA1-positive early endosomes. The results from Fig 3.3 show that following incubation with ligand and kinase inhibitor (with or without monensin), both EGF-EGFR and PDGF-PDGFR complexes colocalized with EEA1-positive EN-fractions to a similar extent as that following 30 min standard stimulation. Thus, active and inactive RTKs can internalize into the same population of endosomes.

Overall, the data provided in this section provide validation for two techniques whereby RTKs can be specifically activated at endosomes.

3.3 Endosomal RTK Activation and Signal Transduction

If the endosome is a physiological location of RTK-mediated signal transduction, then endosome-localized RTKs should be sufficiently active to serve as scaffolds for signaling complexes that can stimulate signaling pathways leading to biological outcomes. The nature of endosomal RTK activity and signal transduction is far from clear. Although it is reasonable to consider receptor activity along the endosomal route as an extension of events initiated at the PM, it remains uncertain whether RTK signaling complexes require initial establishment at the PM or whether the same (or perhaps different) signaling complexes can be nucleated at the endosome. Using the system established in the previous section, these issues can be addressed. This section investigates the ability of endosomally-activated EGFR and PDGFR to initiate signal

transduction.

The level and duration of RTK phosphorylation following activation at endosomes was investigated first. For EGFR, BT20 and MDCK cells were treated with AG1478 and EGF with or without monensin as described in the previous section. Anti-EGFR, anti-pTyr and anti-pEGFR immunoblots together demonstrate that before washout no EGFR was phosphorylated (Fig 3.4A). Incubating with medium following washout led to a gradual increase in EGFR phosphorylation which peaked around 30 min incubation at levels approximately 50% of the level reached with 30 min standard EGF stimulation. By 2 hours, endosomally-activated EGFR phosphorylation was almost undetectable. Moreover, the pattern of endosomally-activated EGFR dephosphorylation was comparable to EGFR dephosphorylation following standard EGF stimulation (Fig 3.4B). The earlier peak of endosomal EGFR phosphorylation observed in this experiment is likely due to differences in the efficiency of kinase inhibitor washout.

To determine the level and duration of PDGFR phosphorylation following activation at endosomes, F442 and HepG cells were treated with AG1296 and PDGF with or without monensin as described in the previous section. Immunoblotting with anti-PDGFR and anti-pPDGFR antibodies showed that before washing, no PDGFR was phosphorylated (Fig 3.4C). After washout of AG1296, incubation in medium gradually induced the phosphorylation of PDGFR, reaching a maximum at 30 min post-washout that is approximately 50% the level following 30 min of standard PDGF stimulation. At 2 hours post-washout, the level of phosphorylated PDGFR was undetectable. Overall, the pattern of endosomally-activated PDGFR dephosphorylation was similar to that of EGFR following both endosomal and standard receptor activation.

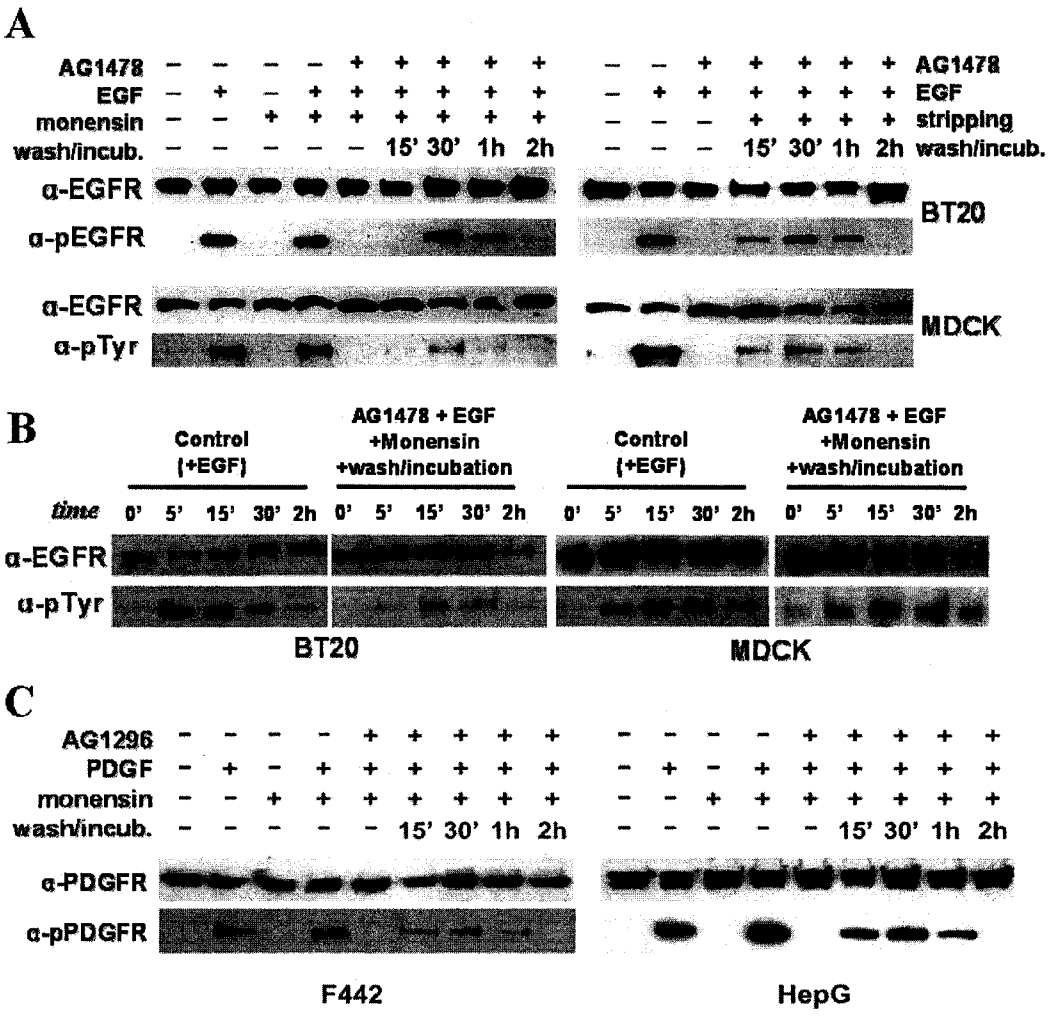

Fig 3.4. Strength and duration of RTK phosphorylation following selective activation in endosomes. (A) Immunoblot analysis of EGFR phosphorylation following its selective activation in endosomes. BT20 and MDCK cells were left untreated, treated 30 min with EGF with or without monensin, or conditioned with AG1478 and EGF with or without monensin. Conditioned cells were either washed to remove AG1478 and incubated for the indicated times in serum-free medium (left panels), or first washed with acidic stripping buffer at 4°C for 1 min, followed by washout of AG1478, and incubation at 37°C in serum-free medium for the indicated times (right panels). Cell lysates were analyzed via immunoblot with rabbit anti-EGFR and mouse anti-pTyr/anti-pEGFR antibodies. **(B)** Comparison in BT20 and MDCK cells of EGFR phosphorylation over 2 h time course following either standard EGF activation (Control) or endosomal EGF activation (AG1478+EGF+monensin). **(C)** Immunoblot analysis of PDGFR phosphorylation following its selective activation in endosomes. F442 cells (left panels) and HepG cells (right panels) were left untreated, treated 30 min with PDGF with or without monensin, or conditioned with AG1296, PDGF, and monensin. After conditioning, cells were either left unwashed or washed to remove AG1296 and incubated for the indicated times in serum-free medium. Cell lysates were analyzed via immunoblot with rabbit anti-PDGFR and pPDGFR antibodies. Figure reproduced with permission. Immunoblots shown are representative of three independent experiments.

It was next determined whether endosome-localized EGFR and PDGFR could recruit signaling complexes and stimulate major signaling pathways following activation at the endosome. Various signaling proteins, including Grb2, Shc, and the p85α subunit of PI3K are known to be recruited via their SH2 or PTB domains to pTyr sites on EGFR and PDGFR following ligand stimulation (Pawson, 1995; Yarden and Sliwkowski, 2001). It has been shown for EGFR that some of these proteins, among them Grb2 and Shc, are co-internalized following EGF-mediated endocytosis and remain associated with the receptor (Clague and Urbe, 2001; Di Guglielmo et al., 1994; Fukazawa et al., 1996; Wang et al., 1996b). However, it is unclear whether the endosome can serve as a direct recruitment site for these signaling proteins or whether signaling complexes require the PM for initiation. Furthermore, little is known regarding the nature of internalized PDGFR signaling complexes. To address these questions, EGFR-expressing BT20 and MDCK cells, or PDGFR-expressing F442 and HepG cells, were treated with the appropriate kinase inhibitor and ligand in the presence or absence of monensin, as described above. Cells were lysed and immunoprecipitated with anti-EGFR or anti-PDGFR antibody. Immunoblotting of the immunoprecipitates revealed both EGFR and PDGFR associated with Grb2 and p85 following receptor activation at endosomes (Fig 3.5A and 3.5C). Endosomal activation of EGFR also leads to recruitment of Shc (Fig 3.5A), and our group has shown this for endosomal PDGFR as well (data not shown). Together these results indicate that activation of both EGFR and PDGFR at endosomes leads to the recruitment of major signaling proteins.

To determine if EGFR and PDGFR could stimulate downstream signaling events following activation at the endosome, cells were treated as above, and lysates probed with antibodies to activated components of major signaling pathways. It is well established

Fig 3.5. Activation of EGFR and PDGFR at endosomes initiates and propagates signal transduction. **(A)** Recruitment of signaling proteins to endosomally activated EGFR. BT20 cells were treated 15 min with AG1478 followed by addition of EGF with monensin (left panel) or without monensin (right panel). After 30 min incubation, cells were washed with PBS to remove AG1478 (left panel) or first washed with acidic stripping buffer at 4°C, returned to 37°C, and washed with PBS. Following wash, cells were incubated with serum-free medium for indicated times. Cell lysates were immunoprecipitated with rabbit anti-EGFR antibody and then subjected to immunoblot analysis using mouse anti-EGFR, anti-Grb2, anti-SHC and anti-p85α antibodies. Controls include BT20 cells serum-starved alone or treated with EGF, monensin, or EGF plus monensin. **(B)** Stimulation of downstream signaling pathway proteins by activation of endosome-associated EGFR. BT20 and MDCK cells were treated as in (A), and cell lysates subjected to immunoblot analysis using anti-pMAPK/Erk and anti-pAkt antibodies. Anti-MAPK and anti-Akt antibodies were used to assess total for protein levels. **(C)** Recruitment of signaling proteins to endosomally activated PDGFR. F442 and HepG cells were treated 15 min with AG1296 followed by addition of PDGF with monensin for 30 min. Cells were then washed with PBS to remove AG1296 and incubated in serum-free medium for indicated times. Cell lysates were immunoprecipitated with rabbit anti-PDGFR antibody and subjected to immunoblot analysis using rabbit anti-EGFR, mouse anti-Grb2, and mouse anti-p85α antibodies. Controls include cells serum-starved alone or treated with PDGF, monensin, or PDGF plus monensin. **(D)** Stimulation of downstream signaling pathway proteins by activation of endosome-associated PDGFR. F442 and HepG cells were treated as in (C), and cell lysates subjected to immunoblot analysis using anti-pMAPK/Erk and anti-pAkt antibodies. Anti-MAPK and anti-Akt antibodies were used to assess total for protein levels. Figure reproduced for this thesis with permission. The immunoblots shown are representative of at least three independent experiments.

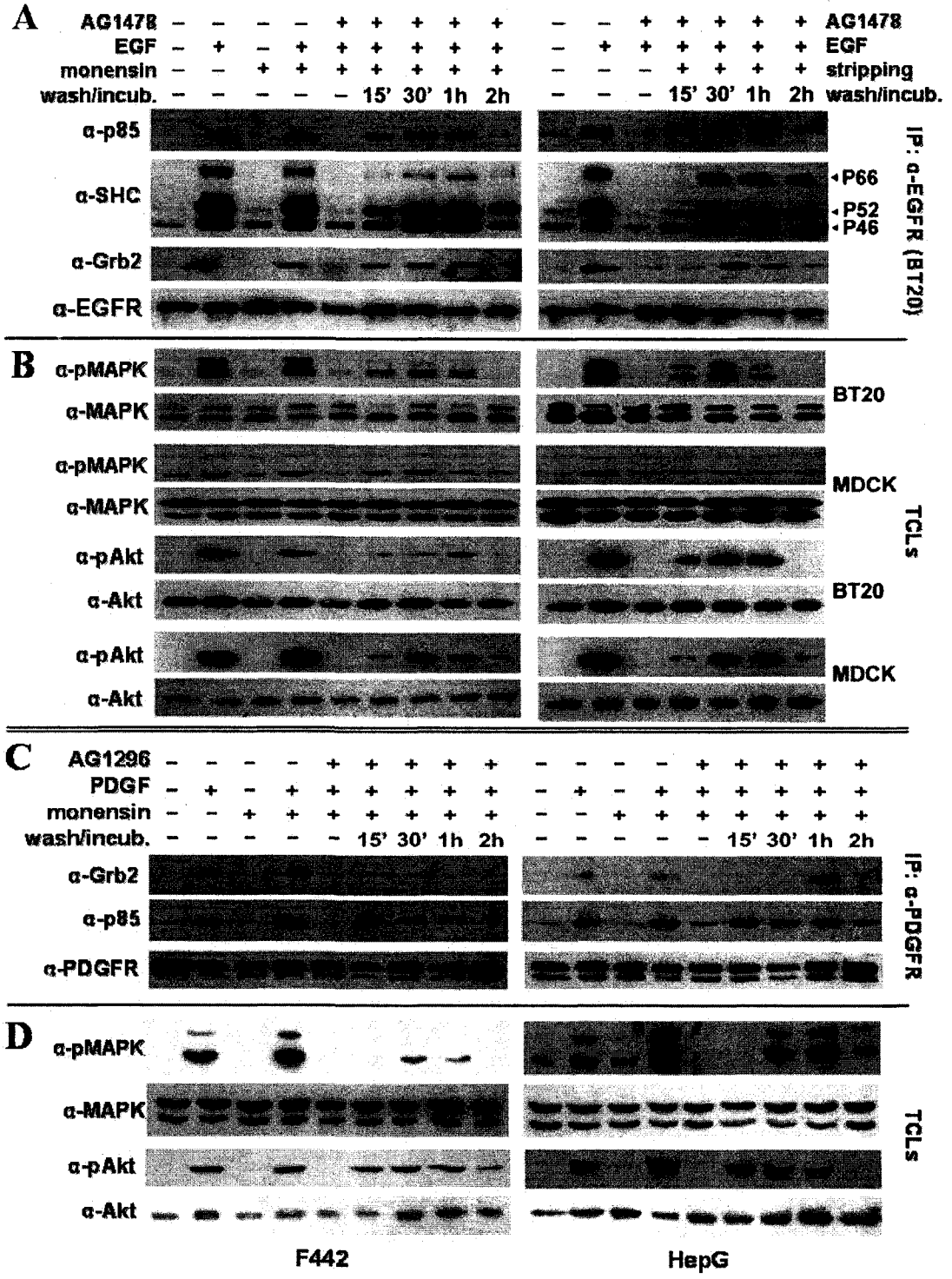
A
AG1478
EGF
monensin
wash/incub.
15' 30' 1h 2h
stripping
α-p85
α-SHC
α-Grb2
α-EGFR
P66
P52
P46
IP: α-EGFR (BT20)
B
α-pMAPK
α-MAPK
α-pAkt
α-Akt
BT20
MDCK
TCLs
C
AG1296
PDGF
α-Grb2
α-p85
α-PDGFR
IP: α-PDGFR
D
F442
HepG

that EGF and PDGF induce the stimulation of both the Ras/MAPK pathway essential for cell mitogenesis (Marshall, 1996), and the PI3K/Akt pathway that protects against apoptosis (Burgering and Coffer, 1995; Downward, 1998). As seen in Fig 3.5B and 3.5D, endosomal activation of either EGFR and PDGFR led to the phosphorylation of MAPK and Akt. It is interesting to note that while the phosphorylation of endosomally activated EGFR or PDGFR is approximately 50% of that following standard ligand stimulation (Fig 3.4A and 3.4C), the corresponding phosphorylation levels of MAPK and Akt were also approximately 50% of that following standard ligand stimulation (Fig. 3.5B and 3.5D). Thus, endosomally- and standardly –activated receptors are equally effective in activating the Ras/MAPK and PI3K/Akt pathways.

3.4 Support of Cell Survival by Endosomal RTK Signaling

I next determined whether endosome localized signaling of RTKs is sufficient to produce a biological outcome. I first assessed by TUNEL assay whether endosomal EGFR signaling could rescue BT20 and MDCK cells from apoptosis induced by serum withdrawal (Fig 3.6). For BT20 cells cultured in 10% FBS, the basal percentage of apoptotic cells was less than 5%; however, serum withdrawal for 24 h induced 54 ± 3% apoptosis (Fig 3.6A). For MDCK cells, serum-withdrawal for 72 h induced 47 ± 3% apoptosis, compared with ~4% apoptosis in 10% FBS (Fig 3.6B). To determine the effects of activation of endosome-associated EGFR on apoptosis induced by serum-withdrawal, BT20 and MDCK cells were stimulated with EGF (20 ng/ml) for 30 min in the presence of AG1478 with or without monensin to allow the internalization of inactive EGF-EGFR complexes into endosomes. After subsequent activation of endosome-localized EGFR by stripping and/or washing and incubating with serum-free medium for

Fig 3.6. Activation of endosome-associated EGFR promotes cell survival. BT20 **(A)** and MDCK **(B)** cells were incubated in serum-free medium for 48 h (BT20) or 72 h (MDCK) to induce apoptosis. The cells were then treated with AG1478 and EGF (20 ng/ml) with or without monensin followed by AG1478 washout (preceded by acid strip for monensin-free treatment) and incubated for 12 h to allow recovery from apoptotic induction. Some cells were pretreated with wortmannin (100 nM) to determine the effects of PI3K inhibition on the survival response. TUNEL assay and immunofluorescence were used to determine percentage of cell population undergoing apoptosis. Data represents the mean from triplicate experiments (1500 cells counted in total), and plotted as the number of apoptotic nuclei/total nuclei x 100 (mean ± s.d.).

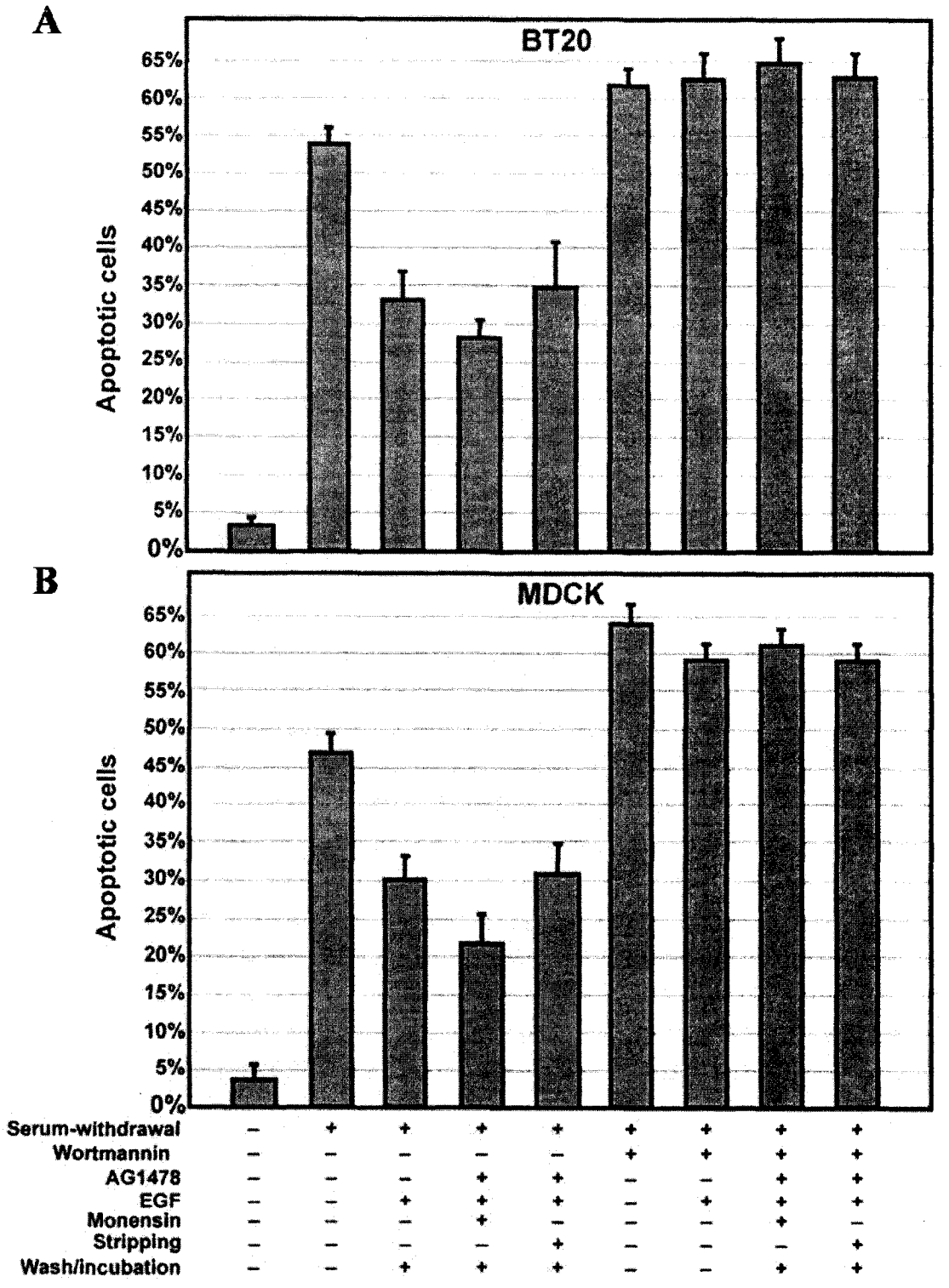
A
BT20
Apoptotic cells
65%
60%
55%
50%
45%
40%
35%
30%
25%
20%
15%
10%
5%
0%
B
MDCK
Apoptotic cells
65%
60%
55%
50%
45%
40%
35%
30%
25%
20%
15%
10%
5%
0%
Serum-withdrawal – + + + + + + + +
Wortmannin – – – – – + + + +
AG1478 – – – + + – – + +
EGF – – + + + – + + +
Monensin – – – + – – – + –
Stripping – – – – + – – – +
Wash/incubation – – + + + – – + +

12 h, the percentage of apoptotic cells was reduced to a level comparable with that following standard EGF (20 ng/ml) stimulation for 30 min (Fig 3.6). These results demonstrate that pure endosomal signaling of EGFR is sufficient to produce a biological effect. Moreover, when the cells were pretreated with wortmannin (100 nM) to block PI3K activity, activation of endosomal EGFR was unable to suppress apoptosis induced by serum-withdrawal (Fig 3.6). This indicates that, similar to standard EGFR activation, activation of endosome-associated EGFR supports cell survival by stimulating the PI3K-Akt pathway.

I next examined the effects of endosomal PDGFR signaling on serum-withdrawal induced apoptosis by using the TUNEL assay (Fig 3.7). HepG and F442 cells cultured in 10% FBS have a ~6% and ~4% basal rate of apoptosis, respectively. After 48 hours of serum withdrawal, these rates increase to ~50% in both cell types (Fig 3.7, column 3). As a control, treatment with camptothecin, a potent apoptosis-inducing drug, causes a >80% level of death in serum-fed cultures (column 2). As seen in column 4 of Fig 3.7, a brief 1 h pulse of PDGF, administered after 36 h of starvation, provides a sufficient signal to save approximately half of the cells from apoptotic death. To determine whether an anti-apoptotic effect can be similarly elicited from activating endosome-associated PDGFR, after 24 hours of starvation HepG and F442 cells were stimulated with PDGF (10 ng/ml) for 30 min in the presence of AG1296 with or without monensin to allow for the internalization of inactive PDGFR into endosomes. Following the subsequent activation of endosome-associated PDGFR by washing and incubating with serum-free medium for the remaining 12 h, the percentage of apoptotic cells was reduced to levels similar to that following 1 h of standard PDGF treatment (Fig 3.7, compare column 5 with 4). It is important to note that in both cases, the pulse of PDGFR activation is

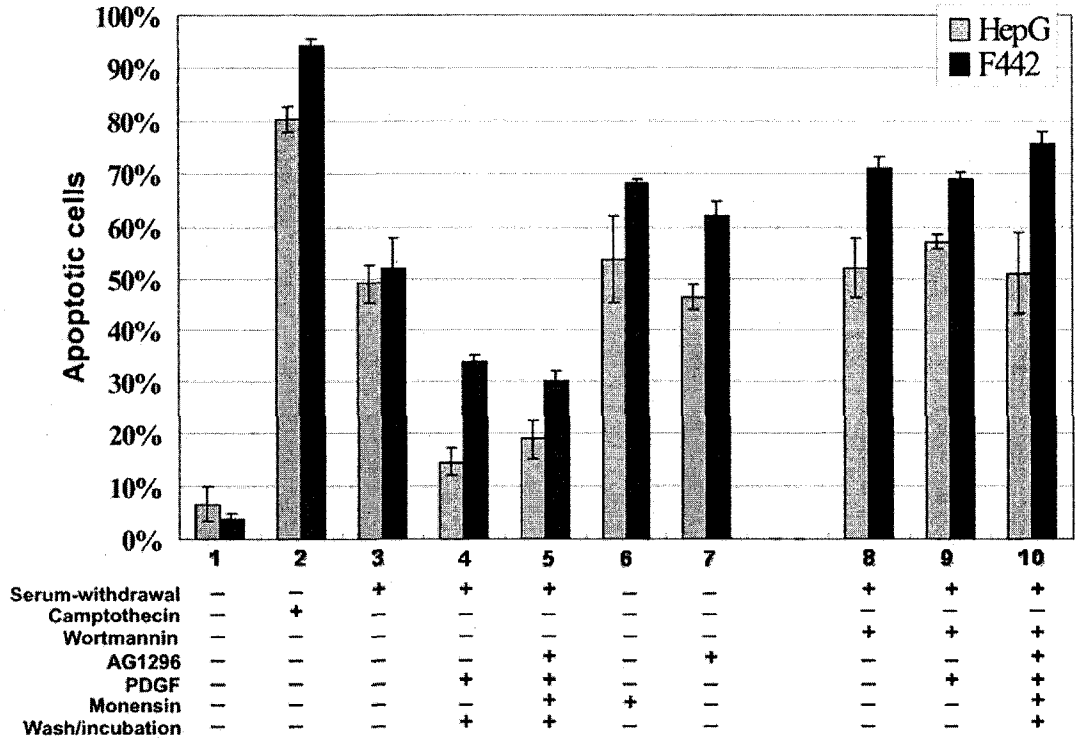

Fig 3.7. Activation of endosome-associated PDGFR promotes cell survival. HepG and F442 cells were either left in culture medium containing 10% FBS with or without camptothecin (50nM), or incubated in serum-free medium for 36 h to induce apoptosis. Some of the cells were pulsed with PDGF (10ng/ml) for 1 h, followed by ligand washout. As additional controls, cells were administered either monensin or AG1296 in place of PDGF. A low level of cell death can be observed following addition of monensin (lane 6), due to its cytotoxicity under prolonged retention (1 h) in this control. Some cells were pretreated with wortmannin (100 nM) to determine the effects of PI3K inhibition on the survival response (columns 7-10). Percentage apoptosis in cell populations determined by TUNEL assay; results represent the mean from triplicate experiments (1500 cells counted in total), and plotted as the number of apoptotic nuclei/total nuclei x 100 (mean ± s.d.).

delimited to those receptors stimulated over the treatment period, and since the growth factor is thoroughly washed out following treatment, no newly activated receptors will contribute to the anti-apoptotic "signal". I show, therefore, that endosomal PDGFR can transduce survival signals of physiological significance.

As with the EGFR system, I tested whether PDGFR-mediated survival signals depended on the PI3K/Akt pathway. If the cells were pretreated with wortmannin, 1 hour of standard PDGF stimulation did not promote cell survival (Fig 3.7, column 9). This is expected, since wortmannin inhibits PI3K and thus prevents transduction downstream necessary to inhibit initiation of the apoptotic program. To investigate whether the survival signals elicited from endosome-associated PDGFR originate from the same PI3K-Akt pathway, cells were pretreated with wortmannin (100 nM) and then treated 30 min with AG1296 and PDGF with or without monensin before washout. As can be seen in column 10 of Fig 3.7, activation of endosome-associated PDGFR is unable to suppress apoptosis induced by serum-withdrawal. This indicates that similar to standardly-activated EGFR, endosomally-activated EGFR, and standardly-activated PDGFR, activation of endosome-associated PDGFR supports cell survival by stimulating the PI3K-Akt pathway.

3.5 Stimulation of Cell Proliferation by Endosomal RTK Signaling

In the previous section I showed that endosomal EGFR/PDGFR signaling is sufficient to elicit cell survival through generation of anti-apoptotic signals that counteract starvation-induced apoptosis. This demonstrated that endosomal RTK signaling is sufficient to lead to at least one important physiological outcome. However, it was still not clear whether endosomal RTK signaling could stimulate another important

biological outcome: cell proliferation. Even though many of the underlying mechanisms remain poorly characterized, it is well established that in order for a quiescent cell to proliferate, it must be continually exposed to mitogen (e.g. serum or purified growth factors) until a few hours prior to S-phase (Pardee, 1989; Planas-Silva and Weinberg, 1997). In serum arrested epithelial cells, as well as in many other cell types, this is typically a span of 7-9 hours, entailing the initial entry into early G1-phase from the quiescent state (or G0), and on through late G1 and past the restriction point (R-point). Since the mitogenicity of RTK growth factors such as EGF and PDGF is well known, I hypothesized that endosome-generated RTK signals would be sufficient to drive quiescent cells into S-phase, thereby leading to DNA synthesis. To validate this hypothesis I chose to focus on the well-characterized EGFR system in BT20 and MDCK cells.

3.5.1 Effects of a Short Pulse of Standard/Endosomal EGFR Signaling on Cell Proliferation

I first determined whether the same duration of endosomal EGFR signaling able to support cell survival was sufficient to promote cell proliferation in BT20 and MDCK cells. Cell proliferation (DNA synthesis) was determined by BrdU incorporation. As shown in Fig 3.8, serum starvation for 24 hours arrested the growth of MDCK and BT20 cells, and addition of 10% FBS or EGF (100 ng/ml) for 12 h stimulated BrdU incorporation. However, specific activation of endosome-associated EGFR did not stimulate BrdU incorporation (Fig 3.8, column D). The specific activation of endosome-associated EGFR was achieved by treating the cells with AG1478, EGF and monensin for 30 min followed by washing and incubation with serum-free medium for 8 h. This result is not wholly unexpected, since EGFR only remained activated for less than 2 h following

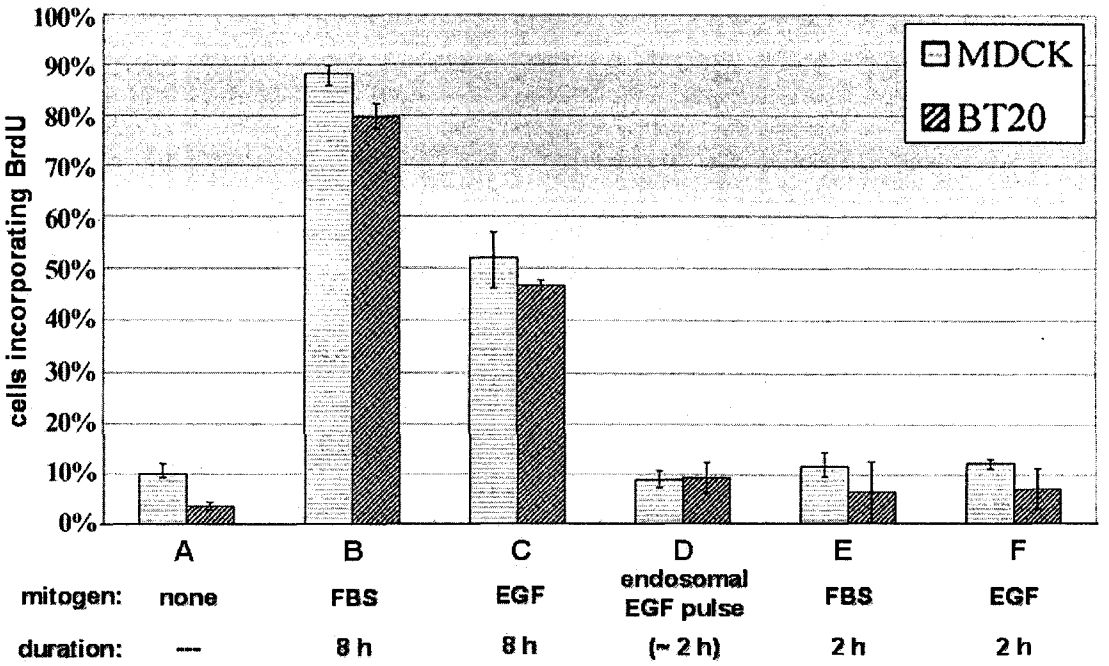

Fig 3.8. A short pulse of either standard or endosomal EGFR signaling is insufficient to stimulate cell proliferation. For standard treatment, MDCK and BT20 cells were plated at 10,000 per cover slip and serum starved to quiescence (~36 h). Cells were then stimulated for various durations using either 10% FBS (B and E), 100ng/ml EGF (C and F), or activation by a pulse of endosomal EGF (D). All treatments were performed in the presence of 25uM BrdU, after which unbound ligand was removed and cells incubated in serum-free media until assayed 18 h from the initiation of treatment. Cells were fixed and multiple random fields of cells were quantitated for BrdU incorporation (DNA synthesis) by immunofluorescence. 500 cells per sample were counted and data was obtained from triplicate experiments. Data plotted as the number of BrdU-positive nuclei/total nuclei x 100 (mean ± s.d.).

its activation at endosomes, and cells typically require 8 or more hours of continual exposure to mitogen in order to stimulate DNA synthesis (Fig 3.8, columns B & C)

(Jones and Kazlauskas, 2001c; Pardee, 1989; Planas-Silva and Weinberg, 1997; Stiles et al., 1979b). Indeed, in control experiments, stimulating cells with EGF or FBS alone for 2 h did not stimulate BrdU incorporation either (Fig 3.8, column 5 & 6). Thus, a system needed to be established to determine whether prolonged endosomal EGFR signaling is sufficient to stimulate cell proliferation.

3.5.2 Induction of Cell Proliferation via Biphasic EGF-mediated Signaling

Since it is impossible to achieve continued endosomal EGFR signaling without altering EGFR trafficking, I decided to determine whether multiple short pulses of endosomal EGFR signaling are sufficient to stimulate cell proliferation. In PDGF-induced fibroblasts, a recent study demonstrated that serum-arrested cells could be driven into S-phase using two 30 min pulses of ligand, spaced 8 hours apart (Jones and Kazlauskas, 2001c). Moreover, the kinetics of proliferation was equivalent to the case where cells were exposed to mitogen continually. However, this biphasic mitogenic signaling paradigm has not been demonstrated for EGFR. Due to the high similarity between the PDGFR and EGFR signaling systems, it is possible that a biphasic requirement for EGF may also exist in cells whose major receptor tyrosine kinase regiment included the EGFR. Therefore, I first examined if this phenomenon applied to the EGFR system in general by investigating the effects of two separated standard EGF pulses on cell proliferation in MDCK and BT20 cells.

I adopted a strategy similar to that used by Jones *et al.* (Jones and Kazlauskas, 2001a). This strategy is outlined in Fig 3.9. Over a time course of 16 h, which includes the G0 to S-phase transition, serum-arrested cells were stimulated with mitogen either

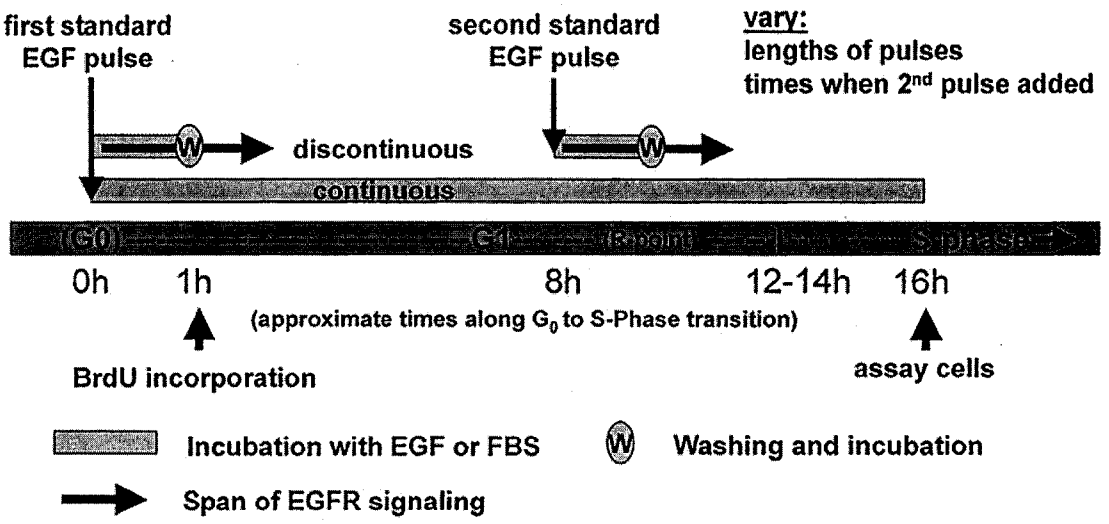

Fig 3.9. Schematic of the continuous and discontinuous EGF-stimulation assays. For discontinuous treatment, "w" indicates washout of unbound ligand, and solid arrows imply a continuation of signaling (from internalized receptors) after growth factor is removed from the media. Following the second EGF pulse under discontinuous treatment, cells are incubated in serum-free media until assayed for BrdU incorporation at 16 h (from initiation of treatment), which corresponds to S-phase in both MDCK and BT20 cells.

continuously (Fig 3.10A) or discontinuously in two temporally separate pulses (Fig 3.10B). In the latter case, the second mitogenic pulse was administered 4, 8, or 12 hours following the first. To remove excess unbound mitogen following either continuous or discontinuous stimulation periods, cells where washed several times with PBS and starvation media was added until cells were assayed for DNA synthesis. Using immunofluorescence, cell proliferation was measured by quantitating the percentage of cellular nuclei positive for BrdU incorporation (indicative of newly synthesized DNA).

As can be seen in Fig 3.10A, continual exposure to either FBS or EGF for 8 h or longer led to a marked increase in proliferating cells over unstimulated controls. Although induction using FBS appeared to elicit a ~30% greater response than when EGF was used alone, this is likely a result of compounded mitogenic signals elicited from the plethora of factors present in serum.

The results from Fig 3.10B reveal that the same mitogenic response could be induced if EGF was added in two temporally separate pulses. Two one-hour pulses of EGF, spaced 8 h apart, can drive cells into S-Phase with similar kinetics to continuous treatment (compare column E of Fig. 3.10A with column C of Fig 3.10B). Interestingly, using an initial 30 min pulse of EGF favoured proliferation only if the second pulse was 1 h (Fig 3.10B, columns A & B). Although it has been shown in fibroblast cells that two 30 min PDGF pulses are sufficient for mitogenesis, the same treatment in my cells using EGF gave only a weak response, lending to either physiological variation between cell types, and/or varying mitogenic potencies between growth factors. To distinguish between these two possibilities, cells were treated with two 30 min pulses of serum or two 1 h pulses of serum spaced eight hours apart according to the strategy outlined in Fig 3.9. As seen from columns E & F in Fig 3.10B, either pair of FBS-pulse lengths elicited

Fig 3.10. Two pulses of standard EGFR signaling are sufficient to stimulate cell proliferation. (A) DNA synthesis (S-phase entry) induced from a continuous mitogenic pulse. MDCK and BT20 cells were plated at 10,000 per cover slip and serum-starved to quiescence (~36 h). Cells were then continually stimulated for various durations using either 100ng/ml EGF (B-G) or 10% FBS (H-M) in the presence of 25μM BrdU. After expiry of duration, unbound ligand was removed and cells incubated in serum-free media. At 18 h, cells were fixed and assayed for BrdU incorporation. **(B)** DNA synthesis (S-phase entry) induced from two temporally separate EGF pulses. Cells were plated and starved as in A, then stimulated with an initial pulse of EGF or FBS for the duration indicated before removing free ligand and culturing once again in starvation media. A second pulse of mitogen was administered again at 4 h (G), 8 h (A-F), or 12 h (H) from the initiation of the first pulse, and washed out following the duration indicated. Cells were then fixed and multiple random fields of cells were quantitated for BrdU incorporation by immunofluorescence. 500 cells per sample were counted and data was obtained from triplicate experiments. Data plotted as the number of BrdU-positive nuclei/total nuclei x 100 (mean ± s.d.).

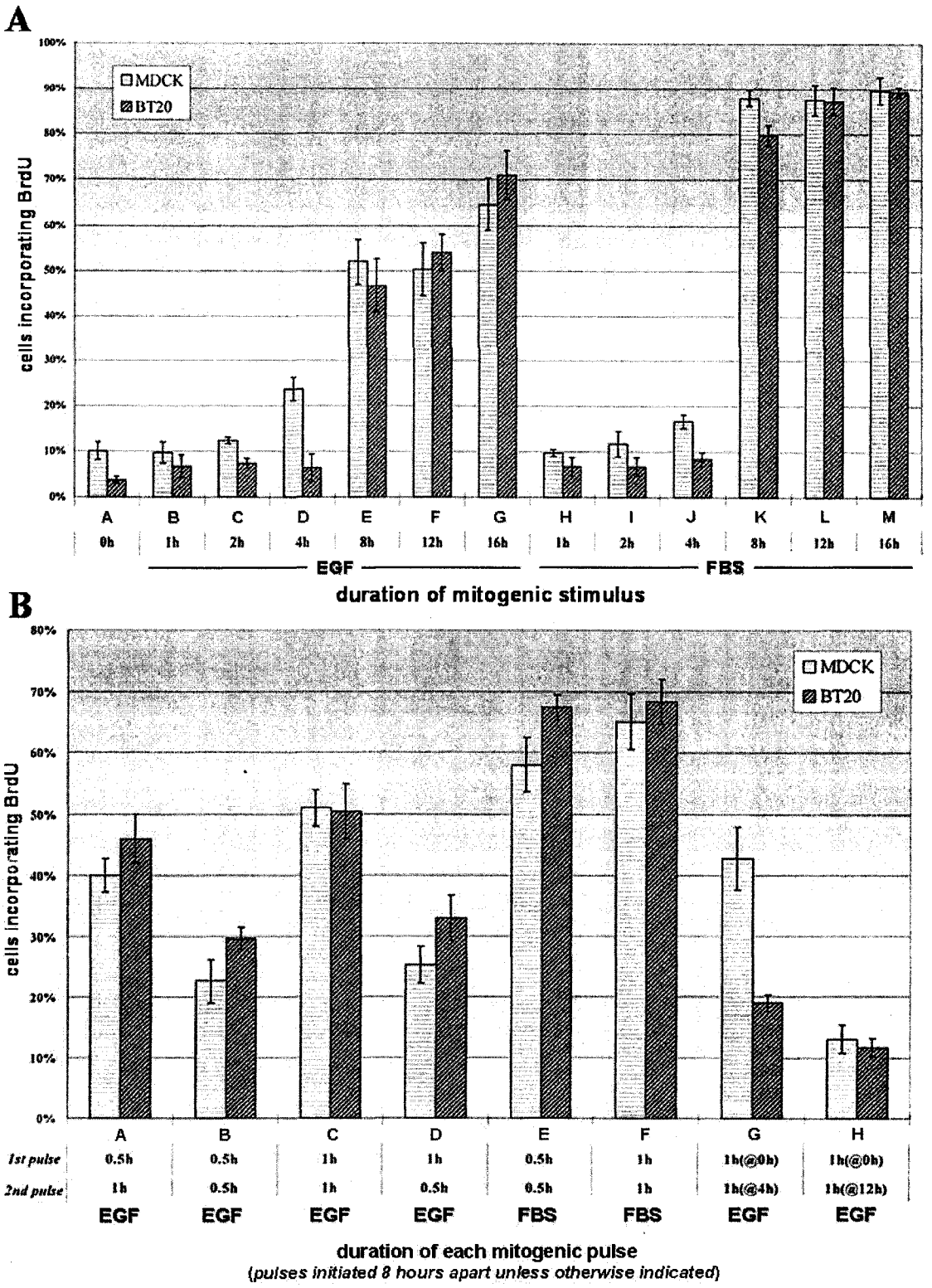
A
MDCK
BT20
cells incorporating BrdU
100%
90%
80%
70%
60%
50%
40%
30%
20%
10%
0%
A B C D E F G H I J K L M
0h 1h 2h 4h 8h 12h 16h 1h 2h 4h 8h 12h 16h
EGF
FBS
duration of mitogenic stimulus
B
MDCK
BT20
cells incorporating BrdU
80%
70%
60%
50%
40%
30%
20%
10%
0%
A B C D E F G H
1st pulse 0.5h 0.5h 1h 1h 0.5h 1h 1h(@0h) 1h(@0h)
2nd pulse 1h 0.5h 1h 0.5h 0.5h 1h 1h(@4h) 1h(@12h)
EGF EGF EGF EGF FBS FBS EGF EGF
duration of each mitogenic pulse
(pulses initiated 8 hours apart unless otherwise indicated)

proliferation in MDCK and BT20 cells, suggesting that factors present in serum, in addition to EGF, may compound the potency and/or multiplicity of mitogenic signals, therefore shortening the time required to engage downstream events necessary for mitogenesis.

I also varied the separation of the second EGF-pulse (Fig 3.10B). Both cell types were mitogenically compromised if the second pulse was extended to 12 h (column H). It seemed therefore that cells become unresponsive to further mitogenic stimulus if left too long after the initial pulse. On the other hand, there appeared to be a disparity between the two cell types if the second pulse was given only 4 hours after the first (column G). While MDCK cells showed a strong proliferative response using this timing scheme, BT20 cells showed a more subdued response. This likely reflects the difference in cell-division times (and cell-cycle lengths) between MDCK and BT20 cells, the former of which divides significantly faster under serum-growth conditions. This was not a problem, since MDCK cells remain as mitogenically responsive when the second pulse was given at 8 h, and thus both cell types could still be treated in parallel. These results therefore demonstrate that the requirement for acute EGF exposure to stimulate cell proliferation can be substituted with two short pulses of EGF.

3.5.3 Induction of Cell Proliferation by Two Pulses of Endosomal EGFR Signaling

The above results indicate that the requirement for prolonged EGF exposure to stimulate cell proliferation can be substituted with two short pulses of ligand. By integrating this two pulse paradigm with the method to generate endosomally exclusive RTK signals, I next proceeded to test the mitogenicity of endosomal EGFR.

As outlined in Fig. 3.11, I modified the discontinuous treatment assay for use with the endosomal-EGFR activation system. Cells were first pre-treated with the reversible

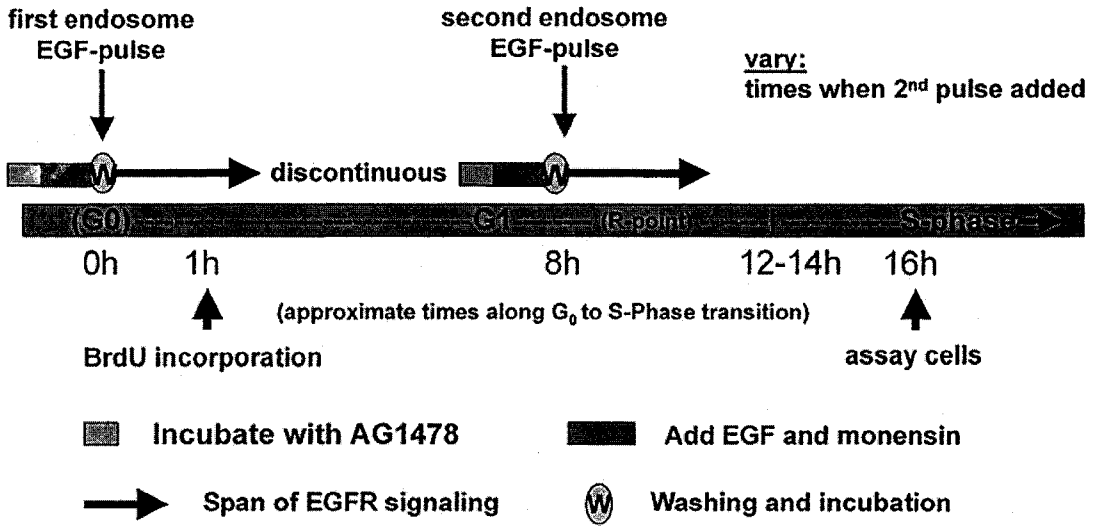

Fig 3.11. Schematic of the (discontinuous) endosome-associated EGFR stimulation assay. For each endosome-EGF pulse, the light grey bar represents pre-incubation with AG1478, the dark grey indicates incubation with EGF with or without monensin, and the "W" indicates washout of AG1478 and thus the onset of endosome-EGFR activation. Solid arrows imply the approximate extent of EGFR signaling after each wash step. Following the second endosome-EGF pulse, cells are incubated in serum-free media until assayed for BrdU incorporation at 16 h (from initiation of treatment), which corresponds to S-phase in both MDCK and BT20 cells.

kinase inhibitor AG1478, followed by addition of EGF with or without monensin for 30 min. The EGF induces the thorough internalization of kinase-blocked receptor, while monensin prevents receptor recycling to the cell surface. Upon washing out the inhibitor, endosomal-EGFR becomes activated and serves as a nucleation site for novel signaling complexes. By repeating this procedure twice within an 8 h interval, two pulses of endosomal EGFR signaling could be generated and the effects on cell proliferation assessed (Fig 3.12). Since receptor activation commences following washout of the kinase inhibitor, I define this point as the onset of a "pulse". In order to standardize the endosome-EGF pulse to a standard-EGF pulse of one hour, I adjusted the AG1478 + EGF + monensin incubation time of the endosomal-EGFR assay treatment to one hour, which equates to one hour of ligand binding. Even though the kinetics of internalization between surface-activated and kinase-blocked (inactive) receptors may differ, 30 min of ligand addition at saturating concentrations (100ng/ml) is sufficient to internalize all EGFR in either case (Wang et al., 2002a).

Two one-hour endosome-EGF pulses, spaced 8 h apart, led to a nearly identical proliferation rate as that for two equivalently timed standard-EGF pulses (compare column C in Fig 3.10B with column E in Fig 3.12). To test whether AG1478 or monensin were themselves mitogenic, I pulsed these factors without EGF at the various times indicated; as can be seen in the first two columns of Fig 3.12, neither induced proliferation. When the timing of the second endosome-EGF pulse was modulated, the outcome was similar to the standard-EGF pulse situation (Fig 3.10B). Neither MDCK nor BT20 cell types led to significant proliferation if the pulses were 12 h apart (Fig 3.12, column F). This indicates that after 8 hours of the first mitogenic pulse, cells become unresponsive to further stimulus and miss the opportunity to enter S-phase. When the

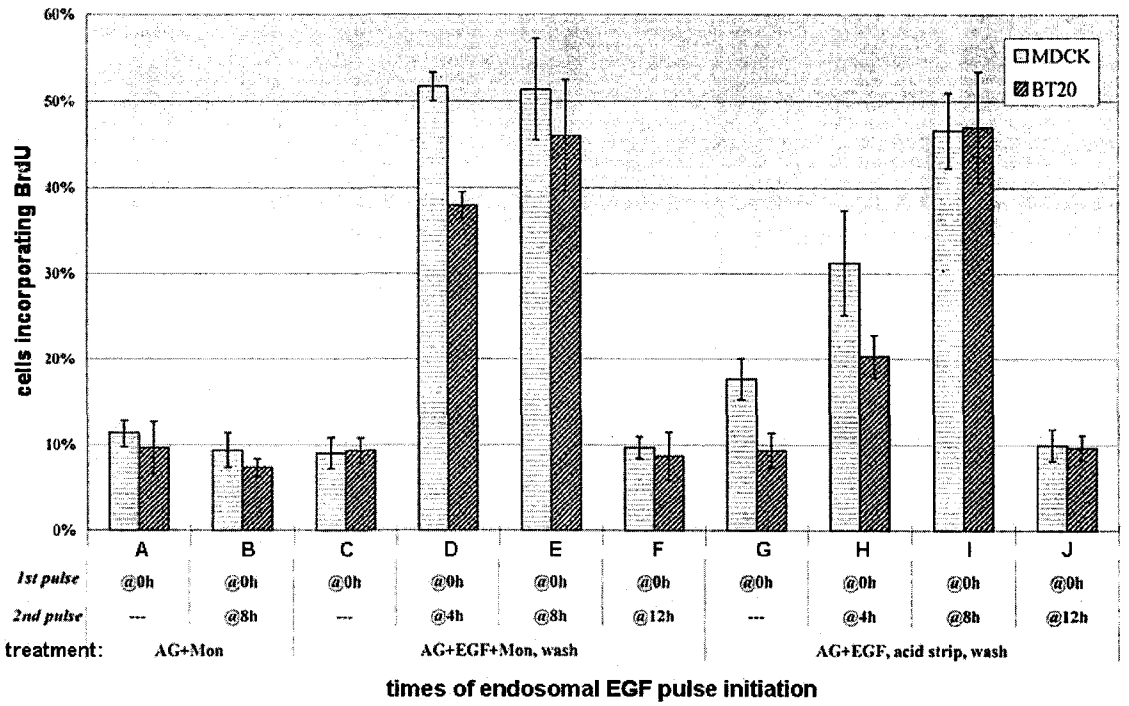

Fig 3.12. Two pulses of endosomal EGFR signaling are sufficient to stimulate cell proliferation. DNA synthesis (S-phase entry) induced from two temporally separate endosomal EGF pulses. MDCK and BT20 cells were plated at 10,000 cells per coverslip, serum-starved to quiescence (~36 h), and then treated with AG1478 and EGF (100ng/ml) with (C-F) or without (G-J) monensin followed by washing and incubation in starvation medium. Some cells were left in serum-free medium until the end of the assay (C and G), while others were pulsed a second time at 4 h (D), 8 h (E), or 12 h (F) after initiation of first pulse. Cells treated without monensin were instead stripped of plasma membrane-recycled ligand prior to EGFR activation (G-J). At 16 h, cells were fixed and multiple random fields of cells were quantitated for BrdU incorporation by immunofluorescence. 500 cells per sample were counted and data was obtained from triplicate experiments. Data plotted as the number of BrdU-positive nuclei/total nuclei x 100 (mean ± s.d.).

second pulse was administered 4 h after the first (column D), both cell type populations underwent significant S-phase entry, with the response in BT20 cells ~12% lower than MDCK. Again, this likely reflects the longer cell-cycle length of BT20 compared to MDCK cells.

Due to the concern of possible non-specific effects on cells during prolonged exposure to monensin (Doebler, 2000; Tartakoff, 1983), I employed the monensin-free strategy described earlier for endosomal-EGF treatment (chapter 3.2). Since a fraction of inactive EGF-EGFR complexes could conceivably recycle back to the surface in the absence of monensin, I stripped off surface ligand with a mild acidic buffer prior to washout of AG1478. In this manner, spacing the endosome-EGF pulses 8 h apart led to near-equal proliferative rates compared to pulsing in the presence of monensin (Fig 3.12, column I), indicating that monensin did not non-specifically alter the cell proliferation in our assay. Together, these results indicate that two pulses of endosomal EGFR signaling are sufficient to stimulate cell proliferation by driving quiescent cells into S-phase.

3.5.4 Induction of Cell Proliferation by Two Pulses of Endosomal PDGFR Signaling

In order to determine whether endosome-derived mitogenic signaling applied to other RTKs, I studied the PDGFR system in HepG and F442 cells. Stimulation of mitogenesis by biphasic PDGF-induced signaling has been previously demonstrated for quiescent NIH 3T3 cells (Jones and Kazlauskas, 2001c). However, whether this phenomenon applied also to HepG and F442 cells was not clear, so I treated these cells with PDGF continuously for 8 hours or with either a single 1 hour PDGF pulse or two PDGF pulses spaced 8 hours apart, and assayed for cell proliferation (DNA synthesis) by quantitation of nuclear BrdU incorporation (Fig 3.13). As with short term mitogen treatment in BT20 and MDCK cells, 1 h treatment with either PDGF or FBS in HepG and

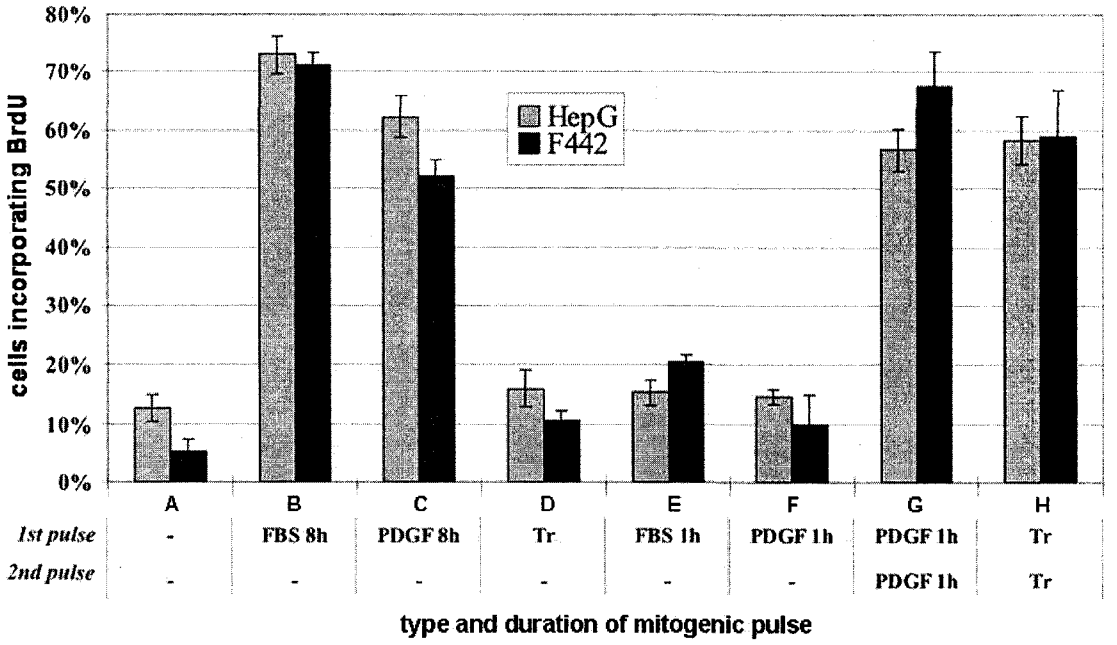

Fig 3.13. Two pulses of endosomal PDGFR signaling are sufficient to stimulate cell proliferation. HepG and F442 cells were serum-starved to quiescence (~24 h) and stimulated in the presence of BrdU with PDGF for 8 h (C), PDGF for 1 h (F), or treated with one (D) or two (H) pulses of AG1296 plus PDGF and monensin (Tr). After pulsing, cells were incubated with serum-free medium and fixed at 16 h (from initiation of treatment). Random fields of cells were quantitated for BrdU incorporation by immunofluorescence. 500 cells per sample were counted and data was obtained from triplicate experiments. Data plotted as the number of BrdU-positive nuclei/total nuclei x 100 (mean ± s.d.).

F442 cells was insufficient to cause mitogenesis (column E & F). However, both continuous and discontinuous standard PDGF stimulation over an 8 hour interval drives quiescent HepG and F442 cells into S-phase (columns C & G).

Having confirmed that the biphasic mitogenic signaling paradigm applied to these cell types, I determined whether endosomal PDGFR signaling is sufficient to stimulate their proliferation. HepG and F442 were first pre-treated with the PDGFR-specific reversible kinase inhibitor AG1296, followed by addition of PDGF with or without monensin for 1 hour. As with two endosomal EGFR pulses, one pulse of endosomal PDGFR signaling is insufficient to stimulate S phase entry (Fig 3.13, column D). However, two pulses of endosomal PDGFR signaling can drive both HepG and F442 cells into S-phase with equal efficacy as two-pulses of standard PDGFR activation (column H). Moreover, both modes of PDGF treatment (standard and endosomal) elicited a proliferative response as robust as that elicited by cells treated 8 hours with 10% FBS (compare column G & H with column B), indicating that purified PDGF is as potent a mitogen as serum in both F442 and HepG cells. These results demonstrate that PDGFR signals, derived exclusively from the endosome, can lead to cell proliferation; furthermore, the mitogenicity of endosome-derived PDGFR signaling is kinetically similar to that derived from standard PDGF-induced signaling.

3.6 Engagement of Cell Cycle Machinery by Mitogenic EGFR Signaling

Having demonstrated the mitogenic competence of either two pulses of standard EGFR signaling or two pulses of endosomal EGFR signaling, I was next interested in seeing how these two systems engage the cell cycle machinery in BT20 and MDCK cells. In order to assess the engagement of the G1 cell cycle following standard or endosomal

EGF-treatment, I investigated the induction profiles of cell cycle-regulated proteins in the G0 to S-phase transition over a 20 h span starting from the first mitogenic pulse (Fig 3.14). The transcription factor c-Myc is a major downstream target of mitogenic signaling, and has been shown to affect the cell-cycle at multiple points, both early and late in G1, including its role in regulating cyclin-D/cdk2,4 complexes (Amati et al., 1998; Kerkhoff et al., 1998; Obaya et al., 1999). To assess the activation of the G1 machinery itself, I directly investigated the induction of cyclins D1 and E, and the phosphorylation status of Rb protein (Fig 1.3B).

The 20 hour span following initial mitogenic pulsation was investigated at multiple time points by western blot analysis (Fig 3.14). The time points immediately following 0 h and 8 h are broken down into smaller intervals in correspondence to when each pulse of standard- or endosomal -EGFR signaling was initiated (Fig 3.14C & 3.14D). As controls, I analyzed proteins over the same time course, but using continuous EGF exposure for 8 h (Fig 3.14A) or a single 1 h EGF pulse without a second one (Fig 3.14B). Following initial EGF-stimulation in both cell types and under all treatments, c-Myc was rapidly induced within 1 h. For cells given only an initial EGF treatment of one hour, c-Myc protein levels gradually declined by 8 h, while for continually treated cells, the levels of c-Myc rose steadily throughout the time course, peaking at 9-10 h. In MDCK cells, this rise in c-Myc expression was more pronounced initially (compare 4 h for MDCK and BT20, Fig 3.14A), but was as prolonged as that in BT20 cells. In cells induced discontinuously with two pulses of EGF, there appeared a distinct "re-induction" of c-Myc following the second pulse. The later rise in c-Myc levels was most pronounced in BT20 cells 30 min following stimulation with the second EGF pulse (Fig 3.14C & 3.14D), though within each cell type, no difference was observed between two pulses of

Fig 3.14. Induction of G1 cell cycle proteins by continuous or discontinuous EGF stimulation. Subconfluent cultures of MDCK and BT20 cells were serum-starved to quiescence (~48 h) and treated in various ways with EGF as indicated below. For each time point indicated, cells were collected, solubilized, and equal amounts of lysate protein subjected to immunoblot analysis using antibodies to c-Myc, cyclin-D1, cyclin-E, and phospho-retinoblastoma protein (pRb). Anti-tubulin antibody was used to assess equal protein loading. MDCK lysates were not analyzed for pRb phosphorylation because the antibody didn't detect the canine protein. Black arrows represent initiation of standard EGF pulses, grey arrows are endosomal EGF pulses (conditioning via AG1478+ EGF+ acid strip followed by inhibitor washout), and "W" represents the time at which standard EGF pulses are terminated by replacement with serum-free media. **(A)** Cells were treated continuously with EGF (100ng/ml) until assayed. **(B)** Cells were treated one hour with EGF, after which unbound ligand was removed and cells cultured in starvation medium until assayed. **(C)** Cells were treated with two one hour pulses of EGF, administered a 0 and 8 h. Pulses were terminated by washing as mentioned above. **(D)** Cells were treated with AG1478 and EGF, and then acid stripped of recycled ligand and washed free of AG1478 to activate internalized EGF:EGFR complexes. At 8 h, the same treatment was repeated. The immunoblots shown are representative of at least three independent experiments.

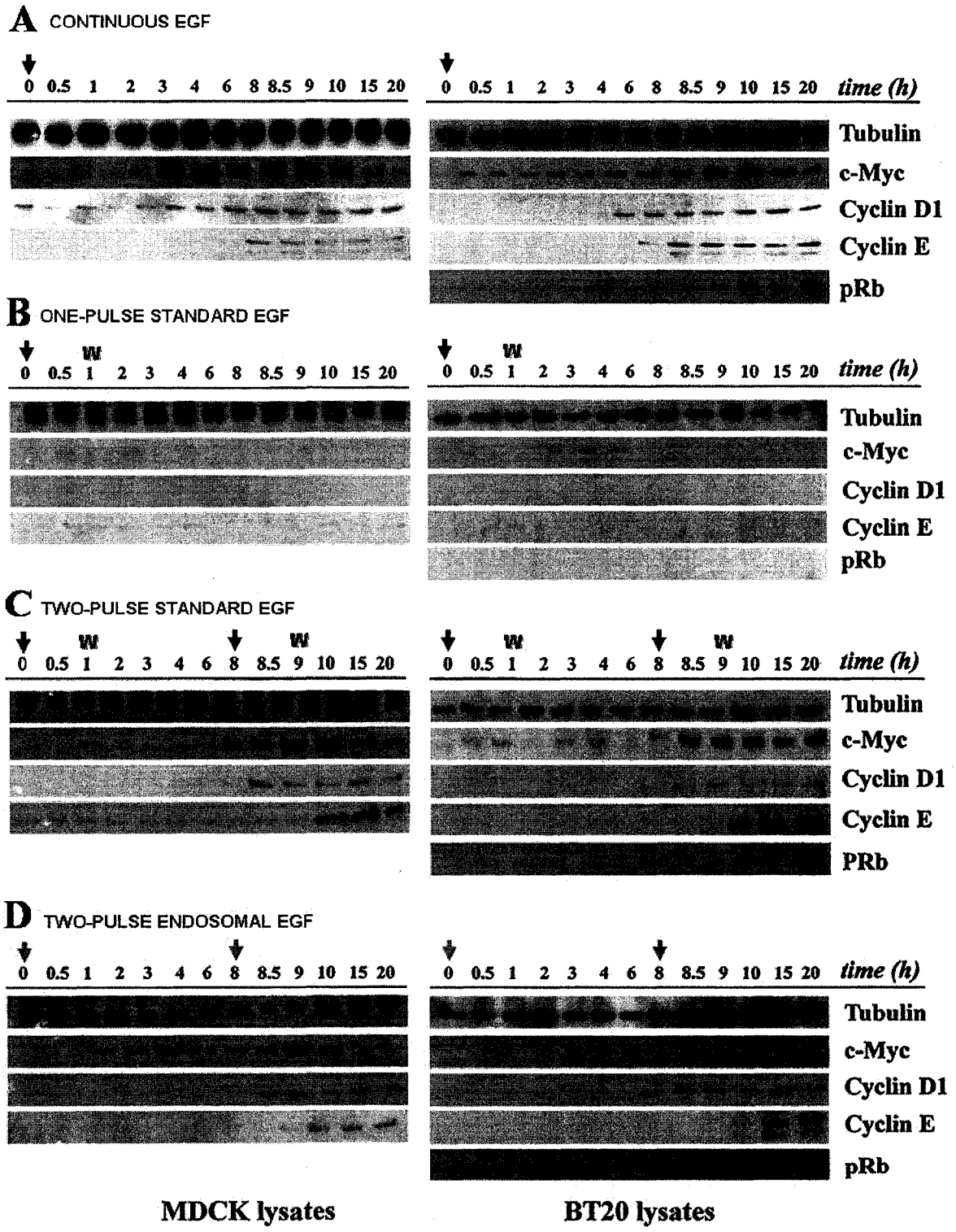
A CONTINUOUS EGF
0 0.5 1 2 3 4 6 8 8.5 9 10 15 20
0 0.5 1 2 3 4 6 8 8.5 9 10 15 20 time (h)
Tubulin
c-Myc
Cyclin D1
Cyclin E
pRb
B ONE-PULSE STANDARD EGF
W
0 0.5 1 2 3 4 6 8 8.5 9 10 15 20
0 0.5 1 2 3 4 6 8 8.5 9 10 15 20 time (h)
Tubulin
c-Myc
Cyclin D1
Cyclin E
pRb
C TWO-PULSE STANDARD EGF
W W
0 0.5 1 2 3 4 6 8 8.5 9 10 15 20
0 0.5 1 2 3 4 6 8 8.5 9 10 15 20 time (h)
Tubulin
c-Myc
Cyclin D1
Cyclin E
PRb
D TWO-PULSE ENDOSOMAL EGF
0 0.5 1 2 3 4 6 8 8.5 9 10 15 20
0 0.5 1 2 3 4 6 8 8.5 9 10 15 20 time (h)
Tubulin
c-Myc
Cyclin D1
Cyclin E
pRb
MDCK lysates
BT20 lysates

standard and endosomal EGFR signaling. Whether cells were treated with one long pulse or two short pulses over eight hours, the relative kinetics of cyclin induction and Rb phosphorylation appeared to be similar. An ordered pattern of induction can be observed, beginning with the second elevation of c-Myc levels, followed by the appearance of detectable levels of cyclin-D1, then cyclin-E, and ending in phosphorylation of Rb. In a few instances where phospho-Rb is detected prior to the appearance of cyclin-E, it can be seen that the Rb is only hypophosphorylated, presumably via cyclin-D/cdk complexes, as indicated by slightly lower mobility on SDS-PAGE. In continually stimulated cells, the G1 cell cycle machinery was engaged starting between 4-6 h, consistent with the findings comparing continuous and discontinuous PDGF-treatment in fibroblasts (Jones and Kazlauskas, 2001c). The Rb levels themselves remained constant throughout G1-S time course (data not shown). MDCK lysates were not analyzed for phosphorylation of Rb since our antibody was not reactive with canine Rb protein. These data show that the cell cycle machinery leading to S-phase is engaged to the same extent whether cells are treated continuously or in two distinct pulses. Moreover, it appears that there is little difference in cell-cycle engagement between mitogenic signals initiated from standard EGFR activation or from the activation of endosome-associated EGFR.

3.7 Comparison of Signaling Events during the First and Second EGF Pulse

I demonstrated that two pulses of endosomal EGFR signaling engaged the G1 cell-cycle machinery the same way as two pulses of standard EGFR signaling. Next, I wanted to more closely examine the signal transduction pathways downstream of EGFR under these two different stimulation conditions. Two-hour time spans following the initiation of the first pulse (0 to 2 h) or the initiation of the second pulse (8 to 10 h) were

monitored under both standard and endosomal EGFR activation conditions. For each time point, cell lysates were analyzed for activity (phosphorylation) of EGFR and other key signaling proteins. Cells acutely (continuously) stimulated with EGF typically reveal long term elevation of EGFR phosphorylation due to continual stimulation of recycling and/or newly synthesized receptors. By using this discontinuous treatment method to limit EGF-mediated activation to two widely separated times, I could therefore specifically elucidate the events at either point.

Consistent with findings presented in section 3.3 of this chapter, the first pulse of EGFR activation led to the stimulation (phosphorylation) of MAPK, Akt, and PLCγ1. Fig 3.15A shows this for BT20 cells and Fig 3.16A for MDCK cells. Additionally, Grb2 and Shc immunoprecipitated with EGFR after either standard EGFR activation or activation of endosome-associated EGFR in BT20 cells (Fig. 3.15C). The endosomal EGFR pulse resulted in the slower recruitment and activation of downstream proteins due likely to the slower activation of EGFR itself. Standard EGFR activation and activation of endosome-associated EGFR by the second pulse of EGF resulted in a very similar activation pattern of downstream signaling proteins. Fig 3.15B shows this for BT20 cells and Fig 3.16B for MDCK cells. Following either type of pulse, Akt was strongly activated, PLC-γ1 was moderately activated, and Erk (MAPK) was weakly activated in both cell types. Moreover, both standard EGFR activation and activation of endosome-associated EGFR resulted in the association of the receptor with Grb2 and Shc following initiation of the second pulse (Fig 3.15D). These results thus reveal that second-phase activation of endosome-associated EGFR stimulates downstream signaling cascades in a similar manner to the second-phase activation via standard EGFR activation.

Interestingly, the protein activity profile following the second mitogenic pulse

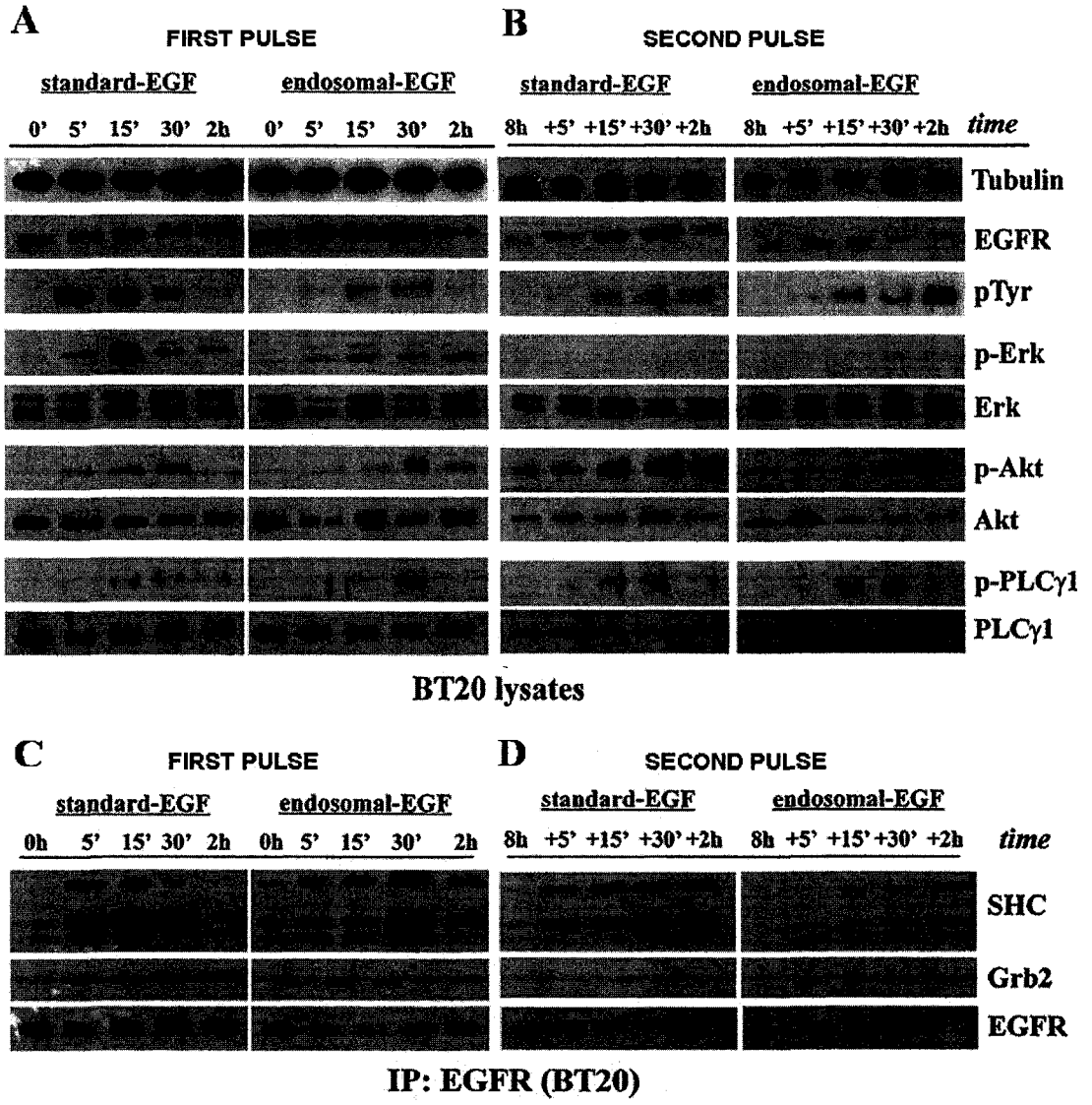

Fig 3.15. Biphasic stimulation of EGFR signal transduction following standard and endosomal EGFR activation in BT20 cells. BT20 cells were serum-starved to quiescence (~48 h) and treated discontinuously at times 0 and 8 h with one hour pulses of EGF (standard-EGF) or with pulses of endosomal-EGF (conditioning via AG1478 + EGF + acid strip followed by inhibitor washout). **(A and B)** First (A) or second pulse (B) standard/endosomal activation of EGFR and its downstream effectors. Cell lysates, collected at the times indicated, were subjected to immunoblot analysis using antibodies against EGFR, pTyr, phospho-Erk1/2 (p-MAPK), Erk1/2 (MAPK), phospho-Akt, Akt, phospho-PLCγ1, and PLCγ1. Anti-tubulin was used to assess protein loading. For the endosome-EGF pulse, samples collected at 0 h (for first pulse) and 8 h (for second pulse) preceded the acid strip step, though cells had already been pre-incubated with AG1478 and EGF. **(C and D)** First (C) or second pulse (D) standard/endosomal EGF activation induces recruitment of signaling proteins to EGFR. BT20 lysates were immuno-precipitated with anti-EGFR and subjected to immunoblot using anti-Grb2, SHC, and EGFR. The immunoblots shown are representative of three independent experiments.

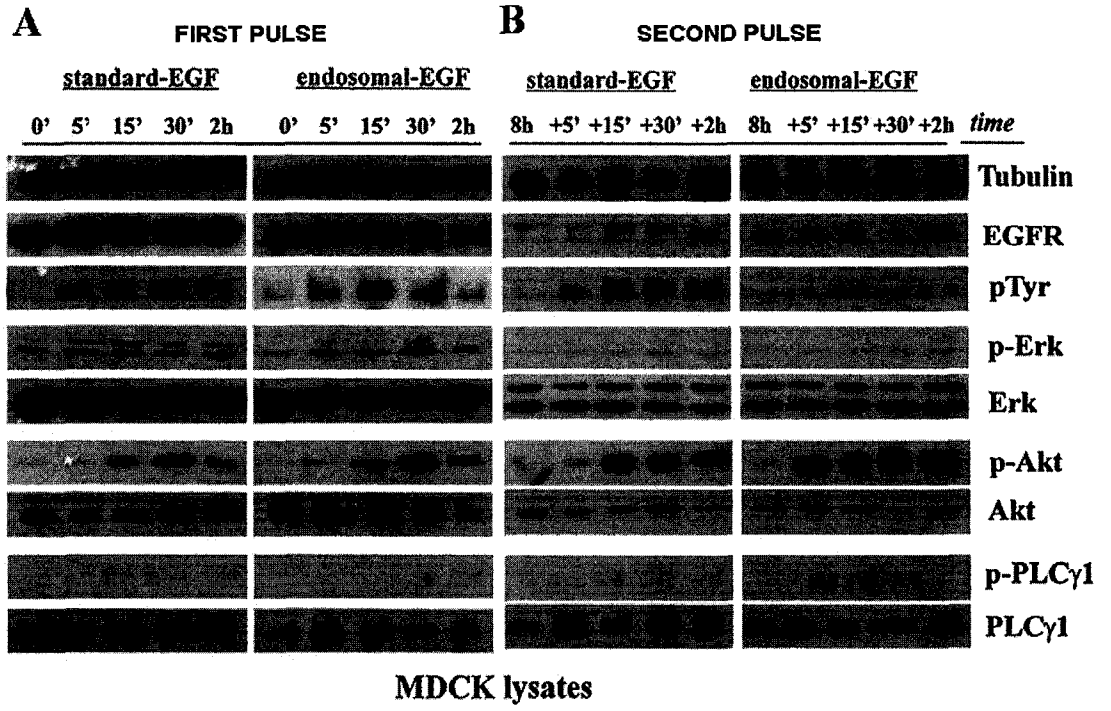

Fig 3.16. Biphasic stimulation of EGFR signal transduction following standard and endosomal EGFR activation in MDCK cells. Subconfluent cultures of MDCK cells were serum-starved to quiescence (~48 h) and treated discontinuously at times 0 and 8 h with one hour pulses of EGF (standard-EGF) or with pulses of endosomal-EGF (conditioning via AG1478+EGF+acid strip followed by inhibitor washout). **(A and B)** First pulse (A) or second pulse (B) standard/endosomal activation of EGFR and its downstream signaling effectors. Cell lysates, collected at the times indicated, were subjected to immunoblot analysis using antibodies against EGFR, pTyr, phospho-Erk1/2 (p-MAPK), Erk1/2 (MAPK), phospho-Akt, Akt, phospho-PLCγ1, and PLCγ1. Anti-tubulin was used to assess protein loading. For the endosome-EGF pulse, samples collected at 0 h (for first pulse) and 8 h (for second pulse) preceded the acid strip step, though cells had already been pre-incubated with AG1478 and EGF. The immunoblots shown are representative of at least three independent experiments.

appeared to differ quantitatively from that following induction of the first mitogenic pulse (compare Fig 3.15A with 3.15B; and Fig 3.16A with 3.16B). Receptor protein levels, analyzed over 2 h following the second EGF-pulse, were moderately less compared to initial levels. One possibility for this could be that the cell, following lysosomal degradation of EGF-EGFR complexes activated by the first induction, had not yet replenished its receptor number to initial levels. Despite this lower receptor quantity, both EGFR and downstream effectors were still significantly activated at the second pulse, though still appeared to differ kinetically from the first pulse. While the first pulse of EGF stimulation led to a rapid activation pattern of EGFR and the p85 subunit of PI3K, rising within 5-15 min and declining by 2 h, the second pulse response, in both cell types, showed a delayed pattern of activity that remained high even at 2 h. Stimulation of Akt following the second EGF pulse was not only more prolonged, but appeared significantly stronger as well. The pattern of PLC-γ stimulation appeared to be similar in both pulses, although Erk (MAPK) phosphorylation, as seen in the second pulse, was significantly lower under both standard and endosome-EGF induction. Similar levels of Erk protein over both pulses ruled out the possibility that the markedly reduced signal was due to less Erk protein present at 8 h.

Shc association with EGFR was stronger at later times following endosomal EGFR activation than compared to standard EGFR activation. This pattern was weakly paralleled by Grb2 (Fig 3.15C & 3.15D). I also showed that both Grb2 and Shc associated with EGFR following the second pulse to a lesser extent compared with that following the initial pulse, with the reduction in Grb2 association being more pronounced. Overall, these results indicate that signaling events during either the first or the second EGF-mediated pulse are similar regardless of whether EGFR is activated

standardly or endosomally, though significant differences are evident between the signaling events induced from the first and second temporal pulses.

Compared to the first pulse of EGFR activation, second-pulse activation of EGFR showed reduced Erk (MAPK) induction and reduced association of EGFR with Grb2 and Shc. Furthermore, second-pulse EGFR activation led to a stronger and more sustained stimulation of Akt compared to first-pulse EGFR activation. Overall, this implicated that Ras/MAPK pathway activation was reduced and PI3K/Akt pathway activation was increased during the second mitogenic wave compared to the first. These patterns were paralleled in both standard and endosomal EGFR activation conditions. To more precisely determine the role of Erk and PI3K activation in cell proliferation induced by two pulses of EGFR signaling, I selectively inhibited Erk and PI3K activation at each pulse of EGFR signaling and examined the effects on cell proliferation. As shown in Fig 3.17A, inhibition of either Erk activation by U1026, or PI3K activation by wortmannin following the first pulse of EGFR signaling resulted in partial inhibition of cell proliferation. On the other hand, while inhibition of PI3K activation following the second pulse of EGFR signaling significantly blocked EGF-induced cell proliferation, inhibition of Erk activation following the second pulse had no effect on EGF-induced cell proliferation. No differences were observed between EGFR signaling initiated from the PM (standard) or from endosomes, or between the cell types used. The efficacy of U1026 in inhibiting Erk activation or wortmannin in inhibiting PI3K activation, and the ability to reverse these effects after inhibitor washout, was determined with anti-p-Erk and anti-p-Akt immunoblots (Fig 3.17B&C). These results suggest that while the first phase of Erk and PI3K activation is involved in initiating the cell cycle leading to the R-point before S-phase entry, the second phase of PI3K activation plays a more important role than the

Fig 3.17. The role of Erk (MAPK) and PI3K activation on cell proliferation induced by two pulses of EGFR signaling in BT20 and MDCK cells. (A) Effect of wortmannin and U1026 on cell proliferation induced by two-pulses of EGFR signaling from both standard (A,C,E,G,I) and endosomal (B,D,F,H,J) treatments. Cells were treated discontinuously at 0 h and again at 8 h using standard-EGF ("EGF") or endosome-EGF ("endo") pulses. Proliferation (DNA synthesis) was assayed by BrdU incorporation as previously described in this chapter. Data plotted as the number of BrdU-positive nuclei/total nuclei x 100 (mean ± s.d.). "W," treatment with wortmannin (100nM). "U," treatment with U1026 (10uM). **(B and C)** Immunoblot analysis of the inhibition of Erk/MAPK phosphorylation by U1026 (B) and inhibition of Akt phosphorylation by wortmannin (C) on both MDCK and BT20 cells following an initial pulse of endosomal-EGF (treatment). Wash and recovery of Erk and Akt phosphorylation was assayed in the last column of each blot; here, cells were washed after the first pulse at 0 h and lysates assayed for recovery following the second endosome-EGF pulse treatment at 8 h. The immunoblots shown are representative of at least three independent experiments.

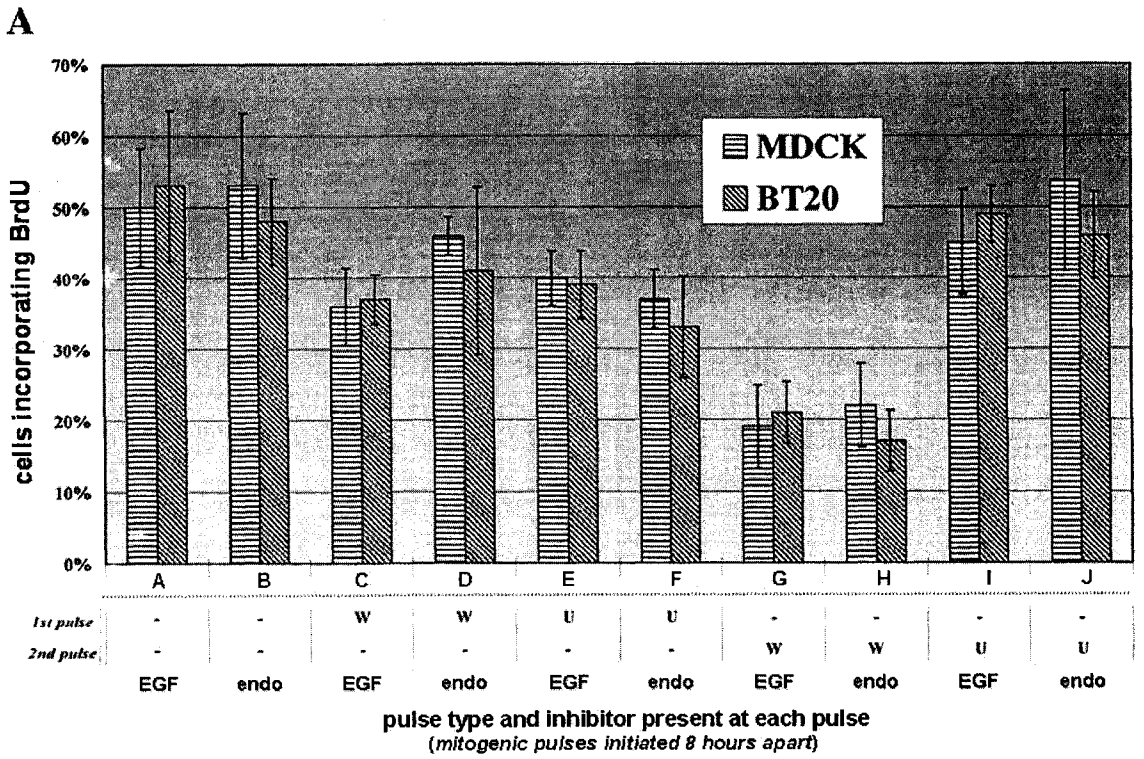
A
70%
60%
50%
40%
30%
20%
10%
0%
cells incorporating BrdU
MDCK
BT20
A B C D E F G H I J
1st pulse - - W W U U - - - -
2nd pulse - - - - - - W W U U
EGF endo EGF endo EGF endo EGF endo EGF endo
pulse type and inhibitor present at each pulse
(mitogenic pulses initiated 8 hours apart)

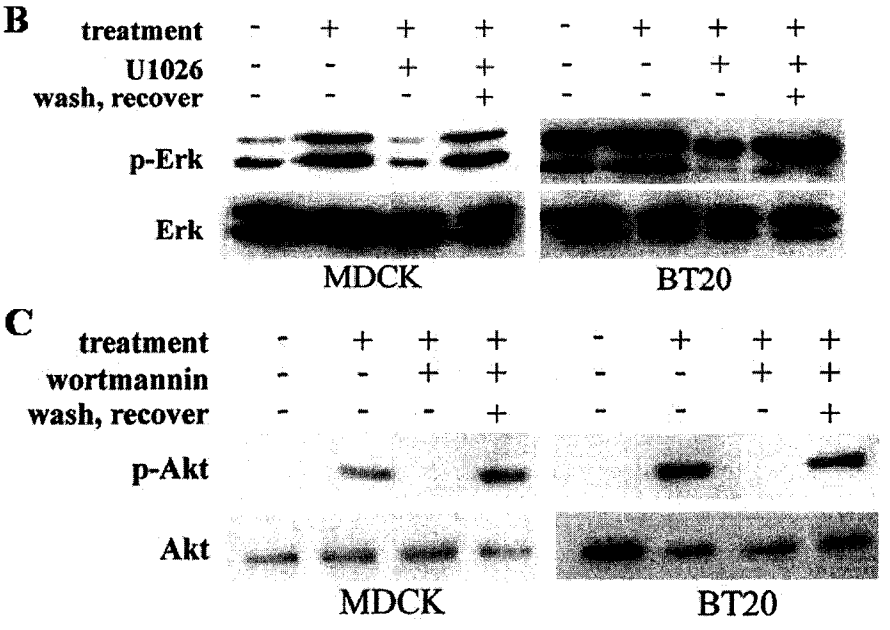
B
treatment - + + + - + + +
U1026 - - + + - - + +
wash, recover - - - + - - - +
p-Erk
Erk
MDCK
BT20
C
treatment - + + + - + + +
wortmannin - - + + - - + +
wash, recover - - - + - - - +
p-Akt
Akt
MDCK
BT20

second phase of Erk activation in driving cells into S-phase.

3.8 Summary

Here I report the development of a system whereby EGFR and PDGFR can be specifically activated at endosomes following internalization. By using this system, I demonstrated that growth factor-induced activation of EGFR and PDGFR at the endosome leads to nucleation of signaling complexes and downstream activation of the PLC-γ, PI3K/Akt, and Ras/MAPK signaling pathways. Furthermore, endosomal EGFR and PDGFR signals are sufficient to rescue cells from starvation-induced apoptosis, an important biological outcome of RTK signal transduction.

Because the same duration of endosomal EGFR and PDGFR signaling able to support cell survival was insufficient to promote cell proliferation, I next investigated the basic minimum requirements for growth factor-induced mitogenesis in my cell types. I found that the requirement for prolonged ligand exposure to stimulate cell proliferation can be substituted with two short pulses of ligand (EGF or PDGF). Integrating this two pulse paradigm with the method to generate endosomally exclusive RTK signals, I developed a system to test the mitogenicity of endosomal EGFR and PDGFR. To this end, I demonstrated that two pulses of endosome-derived RTK signaling was sufficient to drive quiescent cells into S-phase and thereby lead to cell proliferation. Since mitogenesis stimulated by biphasic signaling had not been previously observed for the EGFR system, I further characterized the events following each EGF-induced pulse in BT20 and MDCK cells: the first EGF pulse aroused cells from quiescence into G1 of the cell cycle, while the second pulse, required several hours later, drives cells through the restriction point and into S-phase. Both PM-initiated and endosome-initiated EGF pulses

transduced qualitatively similar signals from EGFR in both cell types and engaged the cell-cycle machinery in the same manner. Overall these findings demonstrate the full physiological relevance of endosomally signaling RTKs.

CHAPTER 4

Cbl-Mediated Downregulation of Epidermal Growth Factor Receptor

The majority of data presented in this chapter has been adapted into this thesis from Pennock S and Wang Z. (2007). A Tale of Two Cbls: Interplay of c-Cbl and Cbl-b in EGFR Downregulation. Submitted to *Mol. Cell. Biol.*

4.1 Overview

The precise role of Cbl in epidermal growth factor receptor (EGFR) endocytosis and trafficking remains to be fully uncovered. The Cbls are oncoproteins by virtue of their prominent role in regulating signal transduction. Understanding how they modulate upstream receptors such as EGFR is necessary to understand how they contribute to cancer. Although it is known that c-Cbl ubiquitinates EGFR and mediates its downregulation in response to EGF, the controversy endures as to whether Cbl's function on receptor downregulation is mediated at an early stage in EGFR trafficking (i.e. by enhancing EGFR internalization) and/or at a later stage (i.e. by targeting endosomal EGFR to lysosomes for degradation). It is also not clear how other Cbl isoforms, such as Cbl-b, participate with c-Cbl in EGFR downregulation. My preliminary results showed that EGFR-Y1045F, an EGFR mutant which possesses a diminished capacity to bind c-Cbl, internalizes following EGF stimulation with kinetics equivalent to that of wild-type EGFR. Although this suggests that Cbl interaction with EGFR is dispensable for EGF-mediated endocytosis, it does not completely rule out Cbl's involvement, as the Y1045F mutant still associates with Cbl, albeit to a lesser extent, via the Grb2 adaptor protein.

In this chapter, I investigate the spatiotemporal role of Cbl in EGFR downregulation. First, I employ various EGFR mutants to test whether Cbl interaction and/or Cbl-mediated ubiquitination is required for EGF-induced EGFR internalization. Next, I characterize Cbl localization, association, and EGFR ubiquitination during EGFR endocytic trafficking. Lastly, I utilize RNAi to determine the absolute requirement for Cbl in EGFR degradation.

4.2 Determination of c-Cbl's Requirement in EGFR Endocytosis

I first employed three different YFP-tagged EGFR mutants including EGFR-Y1045F, EGFR1044, and EGFR-LL/AA, along with YFP-tagged wild-type EGFR (wtEGFR), to study the role of c-Cbl interaction and c-Cbl-mediated ubiquitination of EGFR in its internalization following EGF stimulation (Fig 4.1). EGFR1044 and EGFR-LL/AA have been previously constructed by our group (Wang et al., 2005; Wang et al., 2007), while EGFR-Y1045F was newly constructed for this study. EGFR-Y1045F has a single phenylalanine substitution at tyrosine 1045 shown to abolish its ability to directly interact with c-Cbl, while EGFR1044 (a mutant truncated from its C-terminus to residue 1044) should conceivably lack both direct c-Cbl interaction as well and indirect interaction at phosphotyrosines 1068 and 1086 through the Grb2 adaptor (Levkowitz et al., 1999; Schlessinger, 2000). The third mutant, EGFR-LL/AA, replaces two critical leucines for alanines at residues 1010 and 1011. Our group has previously reported that this mutant is deficient in ligand induced internalization (Wang et al., 2007). As Y1045, Y1068, and Y1068 are all retained on this non-internalizing EGFR, this construct would also allow me to determine the sufficiency of Cbl interaction on EGFR internalization.

293T cells were transiently transfected with wtEGFR, EGFR-Y1045F, EGFR-1044 and EGFR-LL/AA, serum starved overnight, and then either treated with 100ng/ml EGF for 10 min (+E) or left untreated (sf). I showed by immunoblotting that EGFR was expressed at similar levels for all constructs (Fig 4.2A). No endogenous EGFR was detectable—this was expected as 293T cells express very low levels of the receptor. As can also be seen in Fig 4.2A, endogenous c-Cbl was expressed at similar levels in all transfectants. Immunoblotting for phosphotyrosine demonstrated that EGFR was activated by EGF to similar levels in EGFR-Y1045F and EGFR-LL/AA-expressing cells, and to a lesser extent in cells expressing EGFR1044 (Fig 4.2A). Densitometric analysis

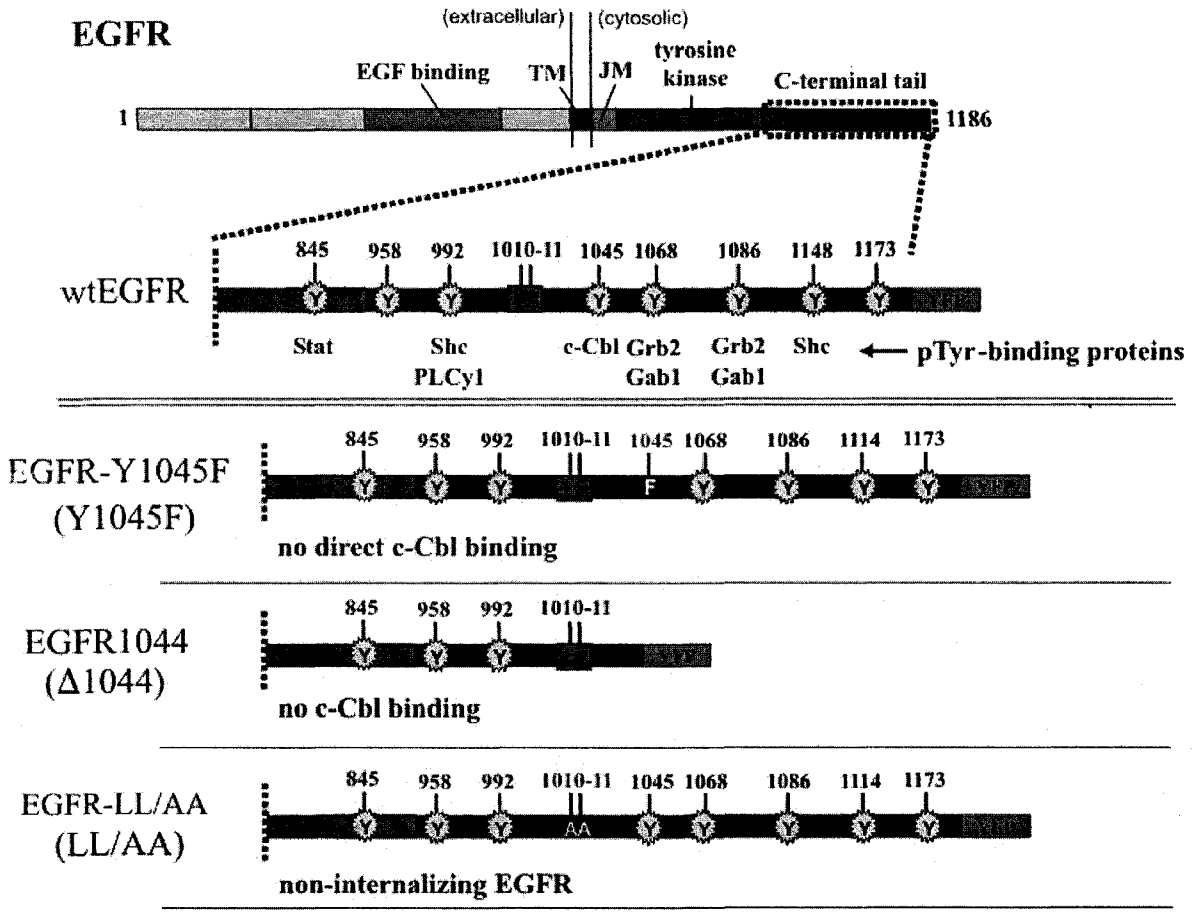

Fig 4.1. EGFR constructs employed in Chapter 4. Each construct was tagged at its C-terminus with yellow fluorescent protein (YFP). EGFR-Y1045F (abbreviated Y1045F) contains a single phenylalanine substitution at tyrosine 1045 which has been shown to abolish its ability to directly interact with c-Cbl. EGFR1044 (abbreviated Δ1044), an EGFR truncated after residue 1044, should conceivably lack both direct c-Cbl interaction (via phosphotyrosine 1045) and indirect interaction at phosphotyrosines 1068 and 1086 via Grb2. The EGFR-LL/AA mutant (abbreviated LL/AA), which replaces two critical leucines for alanines at residues 1010 and 1011, is deficient in ligand-induced internalization.

Fig 4.2. Cbl-mediated ubiquitination of wtEGFR and Cbl-binding deficient EGFR. 293T cells were transiently transfected with YFP-tagged wtEGFR, Δ1044 (EGFR1044), or LL/AA (EGFR- LL/AA). Following overnight removal of serum, cells were treated 10 min with 100ng/ml EGF (+E) or left untreated (sf). Total cell lysates (TCLs) were immunoblotted directly **(A)**, or first immunoprecipitated with anti-YFP and then immunoblotted with the indicated antibodies **(C)**. **(B and D)** Graphical representation of immunoblot data. The immunoprecipitations and immunoblots shown in (A) and (C) were performed in triplicate and their corresponding band intensities quantified by densitometry. **(B)** Graphical representation of the anti-pEGFR/anti-EGFR band intensity ratio taken from TCL immunoblots in (A). **(D)** Graphical representation of anti-Cbl/anti-EGFR and anti-Ub/anti-EGFR band intensity ratios taken from triplicate immunoblots representative of (C). Data was normalized to EGFR and arbitrarily scaled to 100 (mean ± s.d.). Size markers run adjacent to sample lanes were used to confirm the location of ubiquitinated EGFR (~180 kD). The immunoblots shown are representative of at least three independent experiments.

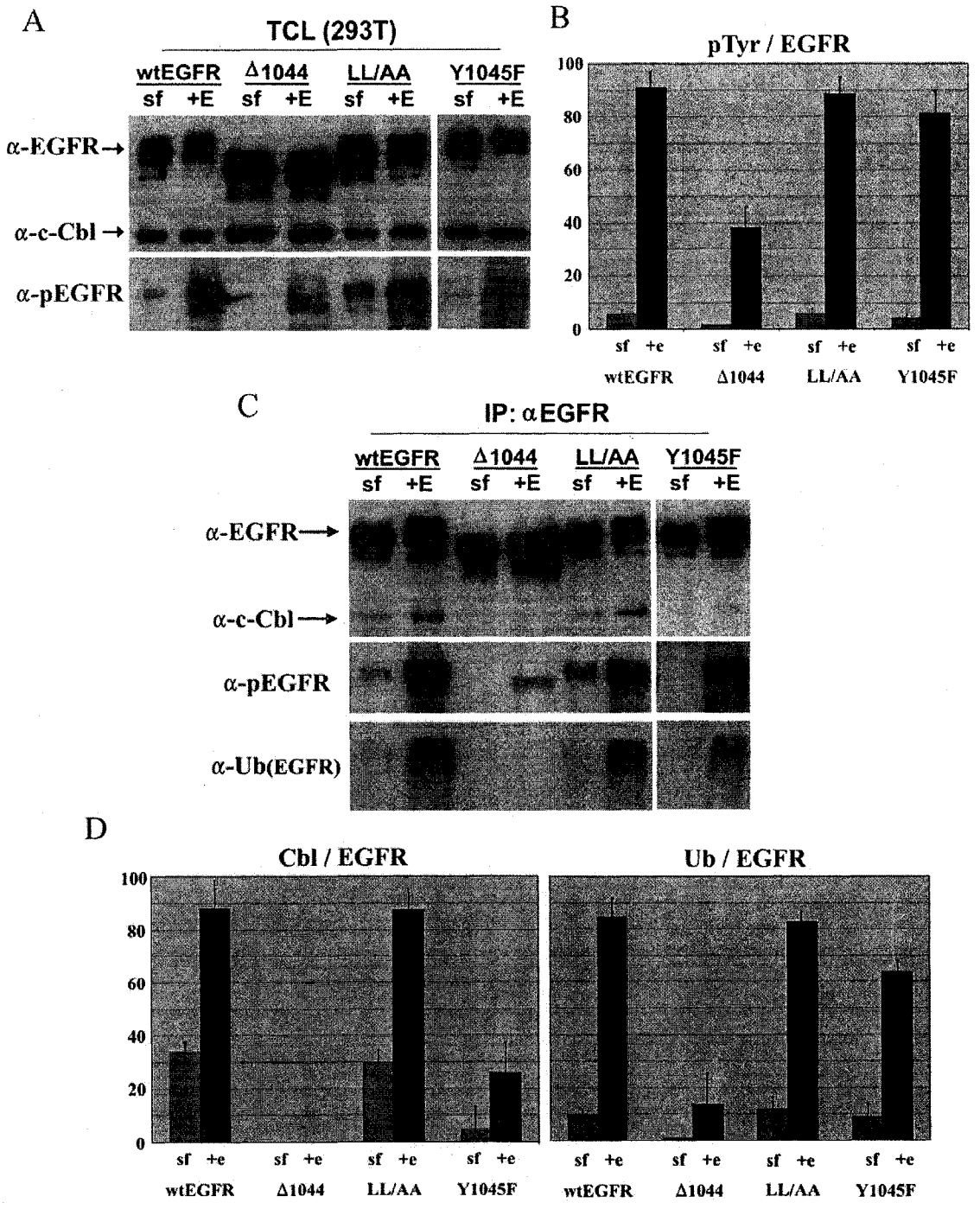
A
TCL (293T)
wtEGFR
Δ1044
LL/AA
Y1045F
sf +E sf +E sf +E sf +E
α-EGFR→
α-c-Cbl →
α-pEGFR
B
pTyr / EGFR
100
80
60
40
20
0
sf +e sf +e sf +e sf +e
wtEGFR Δ1044 LL/AA Y1045F
C
IP: αEGFR
wtEGFR
Δ1044
LL/AA
Y1045F
sf +E sf +E sf +E sf +E
α-EGFR→
α-c-Cbl→
α-pEGFR
α-Ub(EGFR)
D
Cbl / EGFR
Ub / EGFR
100
80
60
40
20
0
sf +e sf +e sf +e sf +e
wtEGFR Δ1044 LL/AA Y1045F
sf +e sf +e sf +e sf +e
wtEGFR Δ1044 LL/AA Y1045F

of phosphotyrosine immunoblots show EGFR1044 phosphorylation was approximately 45% the level of wtEGFR phosphorylation (Fig 4.2B). This is likely due to the lack of phosphorylated tyrosines downstream of residue 1044.

In order to assess the state of Cbl interaction with and Cbl-mediated ubiquitination of the various EGFR mutants, I immunoprecipitated the same cell lysates with an anti-YFP antibody and probed for c-Cbl and ubiquitin (Ub) (Fig 4.2C & 4.2D). Both wtEGFR and EGFR-LL/AA interacted with c-Cbl and was ubiquitinated to a similar extent following EGF stimulation (Fig 4.2C). c-Cbl association with EGFR-Y1045F was significantly reduced (~30% the level of Cbl-wtEGFR association). However, EGFR-Y1045F ubiquitination was unexpectedly high—approximately 75% the level of wtEGFR. Neither c-Cbl association with EGFR1044, nor c-Cbl-mediated ubiquitination of EGFR1044 was observed by immunoblot in response to 10 min EGF. I then kinetically analyzed the EGF-induced internalization rates of the EGFR mutants by flow cytometry. 293T cells were transiently transfected with wtEGFR, EGFR1044, EGFR-LL/AA or EGFR-Y1045F, serum starved overnight, and treated with 100ng/ml of fluorescently labeled EGF for various times. I also assessed the internalization rate of endogenous EGFR in BT20 cells. Fig 4.3 compares the rates of internalization of these receptors over a 1 h time course following EGF. By 30 min stimulation, ~80% of wild-type overexpressed and endogenous EGFR were internalized. Interestingly, both EGFR-Y1045F and EGFR1044 internalized to the same extent as wtEGFR. These results demonstrate that neither c-Cbl association with EGFR, nor Cbl-mediated ubiquitination of EGFR, is required for EGF-mediated receptor internalization. EGFR-LL/AA, as previously reported, showed minimal internalization, and this was not due to rapid receptor recycling (Wang et al., 2007). Thus, neither c-Cbl association with EGFR, nor

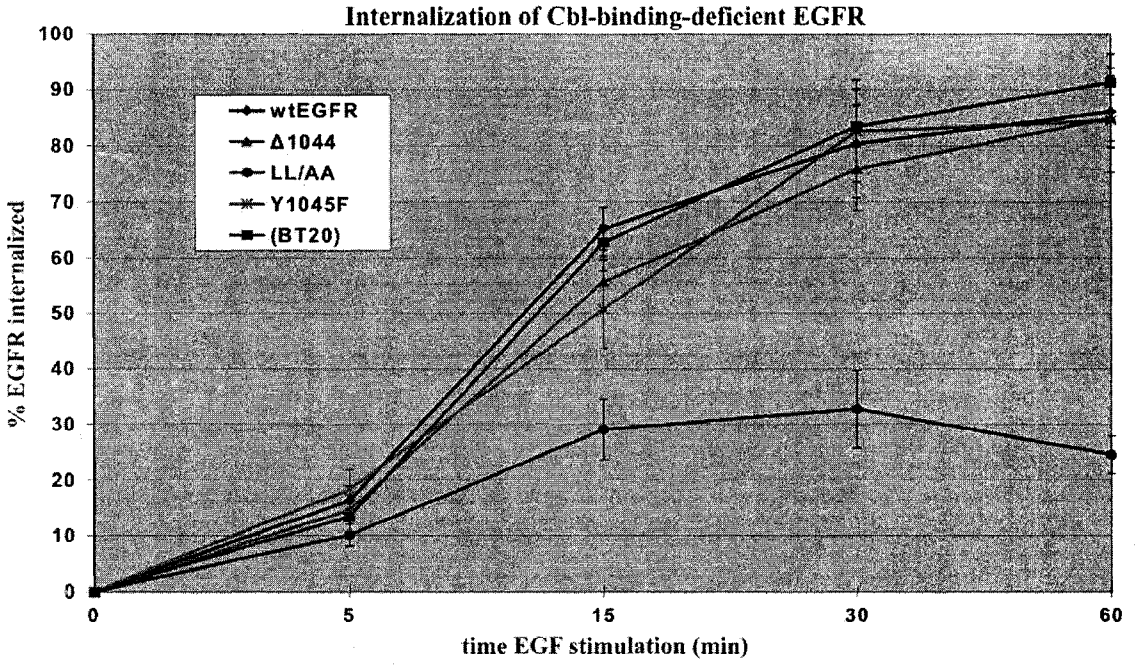

Fig 4.3. Quantitative analysis of EGF-mediated internalization of Cbl-binding-deficient EGFR by flow cytometry. 293T cells were transiently transfected with YFP-tagged wtEGFR, Δ1044 (EGFR1044), or LL/AA (EGFR-LL/AA). BT20 cells were used to assess internalization of endogenous EGFR. Following overnight removal of serum, cells were treated with 100ng/ml Alexa Fluor 647-labelled EGF for the times indicated and their rates of internalization measured by flow cytometry. Data represent the mean (± s.d.) of at least three experiments performed in triplicate.

Cbl-mediated ubiquitination of EGFR, is sufficient for EGF-mediated receptor internalization.

4.3 Characterization of Cbl-EGFR interaction during EGFR trafficking.

Despite Cbl's established role as a downregulator of EGFR signaling, my results suggested that Cbl does not exert its negative regulatory role at the level of EGFR internalization. Other investigations have proposed a more downstream role for Cbl in EGFR trafficking (de Melker et al., 2001; Duan et al., 2003; Grovdal et al., 2004; Longva et al., 2002; Thien et al., 2001). I therefore decided to characterize Cbl-EGFR interaction during the receptor's internal trafficking following ligand stimulation.

I first investigated the general state of c-Cbl membrane localization using subcellular fractionation. BT20 cells, or 293T cells transfected with YFP-tagged wtEGFR, EGFR1044, or EGFR-LL/AA were starved of serum overnight and then treated with EGF at various times over a 1 h time course. At each time point, cell homogenates were collected, pre-cleared of nuclei, and the resulting post-nuclear supernatant (PNS) fractionated into total membrane (TM) and cytosolic (CY) fractions. These fractions were then solubilized and immunoblotted with anti-c-Cbl antibody. Fig 4.4A represents one of three fractionation experiments performed for quantification by densitometry. Ratios of TM to CY Cbl band intensities were calculated and the data graphically presented as a percentage of the wtEGFR TM/CY ratio at 5 min EGF (Fig 4.4B). As gauged from this graph, c-Cbl maximally localizes to membranes within 5-15 min of EGF stimulation in cells expressing wtEGFR and EGFR-LL/AA. Interestingly, c-Cbl remained associated with EGFR-LL/AA-containing membranes ~15 min longer than wtEGFR-containing membranes, though both lose a significant portion of c-Cbl by 1 h

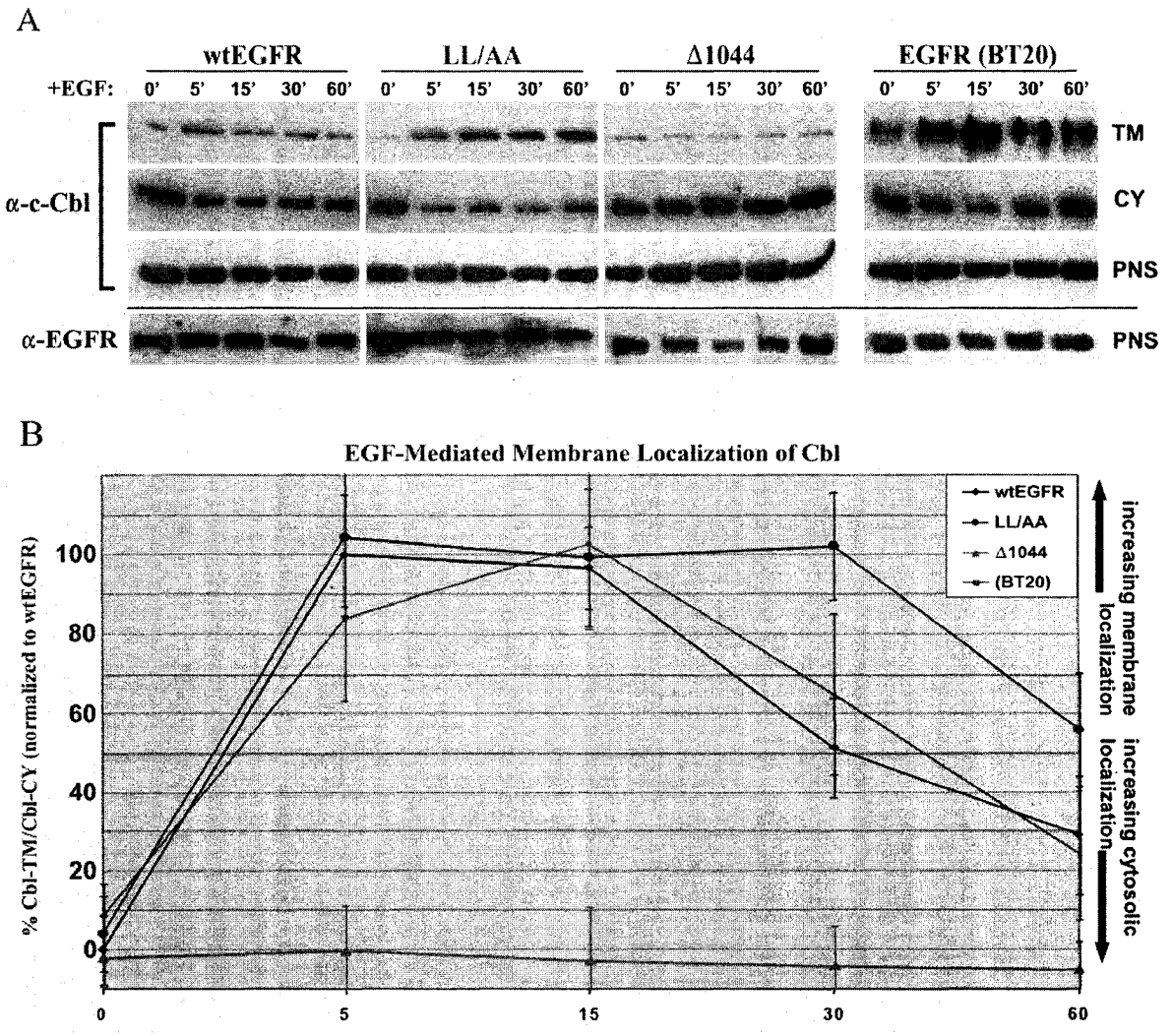

Fig 4.4. EGF-mediated membrane localization of Cbl. 293T cells were transiently transfected with YFP-tagged wtEGFR, Δ1044 (EGFR1044), or LL/AA (EGFR-LL/AA). BT20 cells were also used to assess the role of endogenous EGFR (BT20). Following overnight removal of serum, cells were treated with 100ng/ml EGF for the times indicated. Cell homogenates were pre-cleared of nuclei and the resulting post-nuclear supernatant (PNS) was fractionated into total membrane (TM) and cytosolic (CY) fractions. **(A)** Subcellular fractions were solubilized and immunoblotted with anti-Cbl. A non-transfected control showed Cbl retention in cytosol during the time course of EGF stimulation (not shown). **(B)** Graphical analysis of Cbl localization over 1 h time course of EGF treatment. Immunoblots depicted in (A) were performed in triplicate and their band intensities quantified by densitometry. Data represents the mean (± s.d.) percentage ratios of membrane-bound (TM) to cytosolic (CY) Cbl, normalized to wtEGFR ratios. The immunoblots shown are representative of at least three independent experiments.

EGF. The possibility that membrane-associated Cbl is lost by degradation and not re-localization to the cytosol can be ruled out because (1) the total level of c-Cbl, shown in the PNS fraction, does not change over the EGF stimulation time course, and (2) there is a corresponding increase in cytosolic c-Cbl levels at later times of stimulation (Fig 4.4A). In cells expressing EGFR1044, c-Cbl does not localize to membranes following EGF stimulation, a result in agreement with the immunoprecipitation experiment in Fig 4.2C. Moreover, the lack of c-Cbl membrane localization in EGFR1044-expressing cells strongly argues against the possibility that Cbl is indirectly involved in EGFR internalization via interaction with a membrane-bound complex, such as the CIN85-endophilin regulatory complex found associated with clathrin-coated vesicles (Petrelli et al., 2002; Soubeyran et al., 2002; Szymkiewicz et al., 2002).

To directly assess c-Cbl-EGFR interaction during EGFR trafficking, I performed immunoprecipitation experiments. 293T cells transfected with YFP-tagged wtEGFR, EGFR-LL/AA, or EGFR1044 were stimulated with EGF over the same 1 h time course used for Fig 4.4. At each time point, cell lysates were immunoprecipitated using anti-YFP antibody and immunoblotted with antibodies to EGFR and c-Cbl (Fig 4.5A). c-Cbl association with wtEGFR was strongest within the first 15 min following EGF. After this time the level of c-Cbl interaction decreased rapidly and was virtually undetectable by 60 min EGF. In EGFR-LL/AA-expressing cells, c-Cbl disassociation was delayed approximately 15 min, while in EGFR1044-expressing cells no c-Cbl interaction with the receptor was observed. These results are in agreement with my subcellular fractionation data. To ensure that my observations were not limited to 293T cells exogenously overexpressing an EGFR, I performed the same experiments in BT20 cells using a monoclonal EGFR antibody to immunoprecipitate the endogenous receptor (Fig 4.5A,

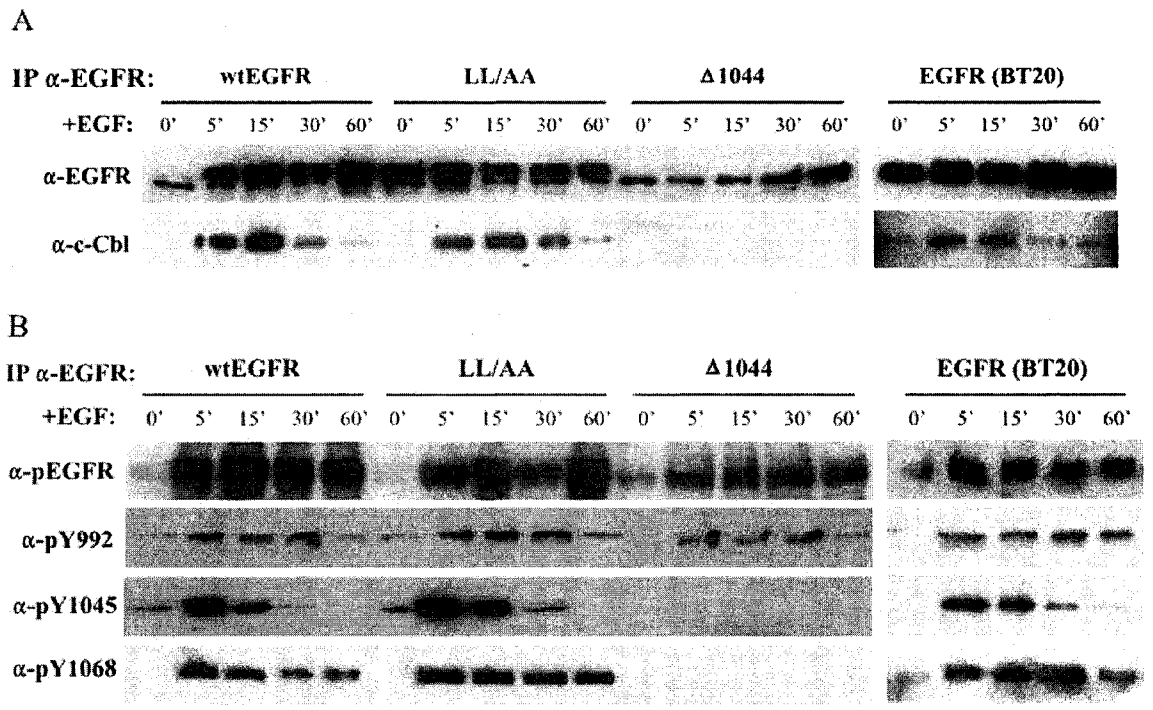

Fig 4.5. Cbl-EGFR association during EGF-mediated EGFR trafficking. 293T cells were transiently transfected with YFP-tagged wtEGFR, Δ1044 (EGFR1044), or LL/AA (EGFR-LL/AA), serum starved overnight, and then treated with 100ng/mlEGF for the times indicated. Cell lysates were immunoprecipitated using anti-YFP (shown as α-EGFR in the figure) and then immunoblotted with anti-EGFR and anti-Cbl **(A)** or antibodies to EGFR phosphotyrosines **(B)**. BT20 cells were treated in parallel to assess association of Cbl with endogenous EGFR. The immunoblots shown are representative of at least three independent experiments.

rightmost panels). Immunoblotting for c-Cbl revealed that endogenous EGFR interacts with Cbl similarly to wtEGFR in 293T cells. In these experiments it is also important to note that no degradation of EGFR was observed by 1 h. To eliminate the possibility that repletion of EGFR levels by new protein synthesis was not interfering with the interpretation of our data, I performed the same experiments in the presence of 50ug/ul of cycloheximide (CHX), but found no difference in the levels of EGFR or in the pattern of c-Cbl interaction (the lack of affect over 1 h EGF can be seen in Fig 4.6A, panel 19).

My results demonstrate that a significant portion of c-Cbl disassociates from EGFR between 15 and 30 min EGF, a time well in advance of receptor degradation. Indeed, I observed no appreciable EGFR degradation over the first hour of EGF stimulation (Fig 4.5A, top row). Nor was the loss of c-Cbl association due to the loss of c-Cbl itself, as c-Cbl levels remained constant over the same 1 h time course (Fig 4A, bottom row). In fact, total cellular c-Cbl levels were not significantly changed even after 2 h EGF stimulation, a time when EGFR degradation begins to occur (Fig 4.6A, panels 1 & 2). Together this suggested that c-Cbl disassociation preceded EGFR degradation and prompted me to investigate specific mechanisms of c-Cbl disassociation.

I examined whether c-Cbl disassociation resulted from specific alterations to EGFR. The immunoprecipitates from Fig 4.5A were screened with a panel of antibodies specific to major EGFR phosphotyrosines (α-pY992, α-pY1045, and α-pY1068) and an antibody that recognizes all phosphotyrosines on EGFR (α-pEGFR) (Fig 4.5B). Interestingly, Y1045 phosphorylation of either transiently expressed or endogenous EGFR significantly decreased after 15 min EGF, contemporaneous with c-Cbl disassociation. The delay in Y1045F dephosphorylation of EGFR-LL/AA compared with wtEGFR was roughly paralleled by the delayed c-Cbl disassociation observed for EGFR-

LL/AA compared to wtEGFR. The dephosphorylation at Y1045F on EGFR was not a result of total receptor dephosphorylation, as immunoblotting for total phosphotyrosine showed no change in overall EGFR hyperphosphorylation over 1 h EGF (Fig 4.5B, top lane panels). Furthermore, dephosphorylation at Y1045 appeared specific, since the levels of Y992 and Y1068 phosphorylation remained constant over the time when dephosphorylation at Y1045 occurred. Y992 also appeared to be specifically dephosphorylated, though this occurred later than Y1045 dephosphorylation. Although pY1045 is the major Cbl docking site, Cbl can also interact with EGFR via Grb2 at pY1068 on the receptor; interestingly, I did not observe significant dephosphorylation at this site. Together these results suggest a potential mechanism for Cbl disassociation involving specific dephosphorylation of the EGFR at Y1045.

4.4 Cbl-mediated ubiquitination and degradation of EGFR.

To elucidate the role of Cbl in EGFR downregulation at the post-internalization stage of receptor trafficking, I investigated wtEGFR levels by western blot of total cell lysates over an extended time course of EGF stimulation in order to profile the receptor's degradation (Fig 4.6A, panel 1). In wtEGFR-transfected 293T cells I observed significant receptor degradation after 2 h EGF. By 4 h EGF, wtEGFR levels were virtually undetectable, while c-Cbl levels remained unchanged (panel 2). A similar pattern of degradation was observed for the endogenous receptor and c-Cbl in BT20 cells (panels 17 & 18). All these experiments were performed in the presence of cycloheximide in order to inhibit new protein synthesis; parallel experiments performed without inhibition still showed EGFR degradation after 2h EGF, though the effect was less pronounced (panel 19). I next assessed the state of wtEGFR ubiquitination over the

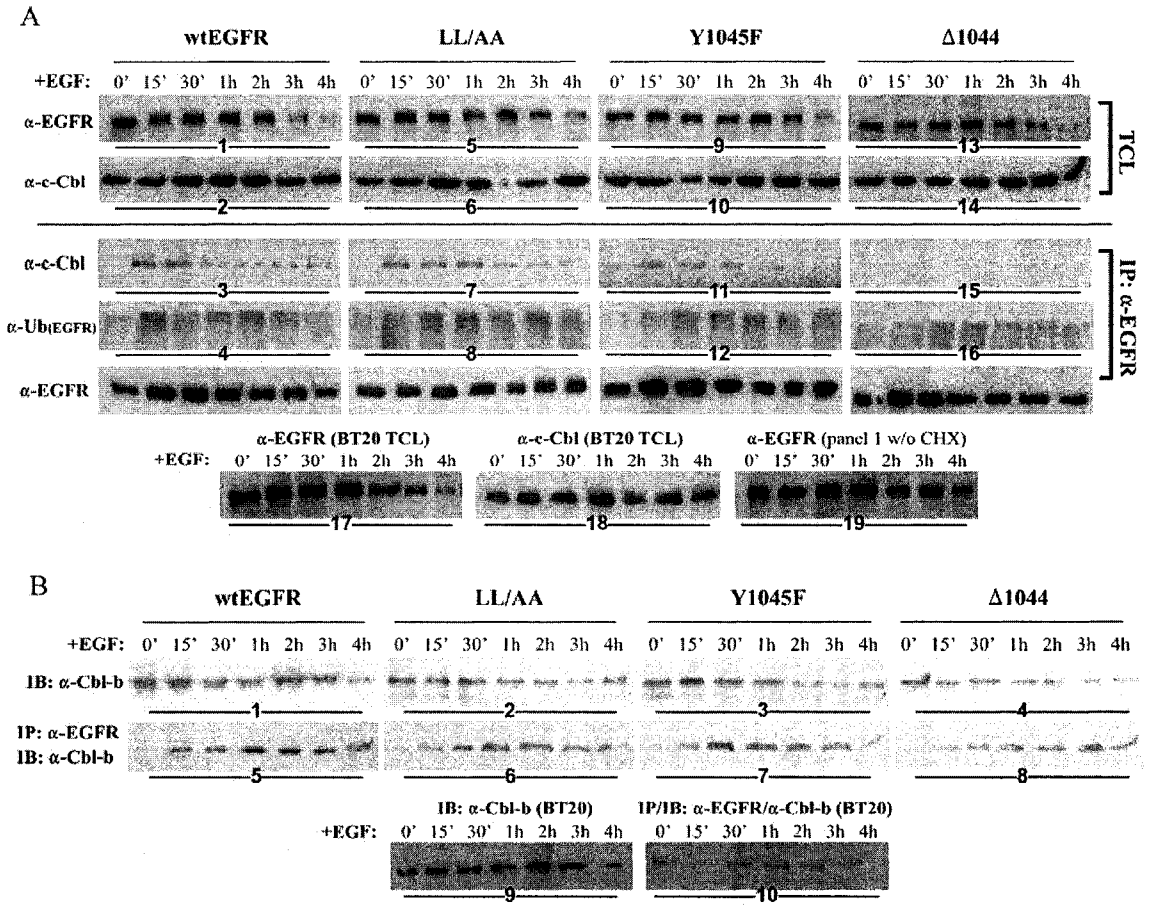

Fig 4.6. Cbl-mediated degradation and ubiquitination of EGFR. 293T cells were transiently transfected with YFP-tagged wtEGFR, LL/AA (EGFR1010LL/AA), Y1045F (EGFR-Y1045F), or Δ1044 (EGFR1044). Cells were serum starved overnight and then treated with 100ng/ml EGF for the times indicated. Total cell lysates (TCLs) were either immunoblotted directly or immunoprecipitated first with anti-YFP and then immunoblotted with anti-EGFR, anti-c-Cbl, anti-Ub **(A)**, or anti-Cbl-b **(B)**. CHX, cycloheximide (panel 19). The immunoblots shown are representative of at least three independent experiments.

same extended time course. As I was unable to confidently assess the ubiquitination of EGFR using the EGFR antibody alone, I instead immunoprecipitated EGFR and probed the precipitates with the same antibody used for Fig 4.2 that recognizes both monomeric ubiquitin and polyubiquitin (panel 4). Receptor ubiquitination rose strongly to reach a peak around 15 min EGF, after which ubiquitination levels fell by ~30%. To my surprise, a second smaller rise in receptor ubiquitination appeared after 30 min EGF, peaking at sometime between 1-2 h EGF: a time when c-Cbl interaction was already very low, as shown in the corresponding c-Cbl immunoblot of immunoprecipitated EGFR (panel 3).

I next performed parallel experiments using 293T cells transfected with EGFR-LL/AA or EGFR-Y1045F (Fig 4.6A, panels 5-12). The profile of EGFR-Y1045F degradation was similar to wtEGFR (panel 9), although EGFR-LL/AA degradation occurred later than wtEGFR (compare panel 5 with panel 1). This delay in EGFR-LL/AA degradation is not surprising, as its inability to undergo ligand-induced endocytosis would mean it relies primarily on constitutive endocytic mechanisms to internally accumulate in endosomes. I then looked at the ubiquitination of these two mutants. The initial ubiquitination level of EGFR-Y1045F was expectedly less than wtEGFR but increased significantly after 15 min EGF to peak around 1 h EGF. The delayed rise in ubiquitination was unanticipated since c-Cbl association was already very low at this time (panels 7 & 11). This result extended the previously observed disparity between the unexpectedly high level of EGFR-Y1045F ubiquitination relative to c-Cbl association (Fig 4.2B). When I looked at EGFR-LL/AA ubiquitination, what seemed to be a two wave pattern of ubiquitination was observed. Unlike the two wave pattern observed for wtEGFR however, the first rise in EGFR-LL/AA ubiquitination occurred

slowly (over the first hour of EGF), then, following a small fall in ubiquitination, rose again at ~3 h EGF. I also noticed the overall intensity of EGFR-LL/AA ubiquitination was greater than wtEGFR (panel 8). A longer time of c-Cbl retention with the plasma membrane-bound receptor can only partially explain this higher level of ubiquitination, as the latter wave of ubiquitination occurs well after c-Cbl disassociation.

I also transfected 293T cells with truncated EGFR1044; surprisingly, this mutant was not only significantly degraded but also ubiquitinated (Fig 4.6A, panels 13 & 16), despite the complete lack of c-Cbl interaction (panel 15). Earlier I observed very low levels of EGFR1044 ubiquitination following 10 min EGF (Fig 4.2D). As gauged from the extended EGF time course in Fig 4.6, EGFR1044 undergoes significant ubiquitination after this early time, eventually peaking at 1 h EGF. Together these results strongly implicated that another E3 ubiquitin ligase, in addition to c-Cbl, was acting to effect the ubiquitination and degradation of EGFR. A strong candidate for investigation was Cbl-b, another major Cbl isoform. Cbl-b is roughly the same size as c-Cbl and possesses the same N-terminal domains involved in RTK regulation (Fig 1.5A). Like c-Cbl, Cbl-b is also known to bind EGFR and regulate its signaling in response to EGF (Davies et al., 2004; Ettenberg et al., 1999a; Ettenberg et al., 2001). I therefore first obtained an antibody specific to Cbl-b and determined the total protein levels of Cbl-b by western blotting the lysates prepared in Fig 4.6A (Fig 4.6B, panels 1-4). Cbl-b was significantly expressed in all 293T transfectants, though unlike c-Cbl levels, Cbl-b levels did not remain constant during the EGF-stimulation time course. I was unable to explain the small degree of fluctuation observed in Cbl-b levels at later times of EGF, though the general trend reveals a decrease of the protein by 3-4 h EGF, contemporaneous with EGFR degradation. In BT20 cells, Cbl-b levels were on average ~50% higher than in our

293T transfectants at early times of EGF, but rapidly decreased after 2 h EGF (Fig 4.6B, panel 9).

I next tested Cbl-b association with EGFR by probing the EGFR immunoprecipitates prepared in Fig 4.6A with anti-Cbl-b (Fig 4.6B, panels 5-8). Cbl-b interacts with wtEGFR, EGFR-LL/AA, EGFR-Y1045F, and EGFR1044 following EGF stimulation. Significantly, Cbl-b association with EGFR was weak at early times of EGF stimulation in all transfectants. The highest level of association with wtEGFR and EGFR-LL/AA occurred between 1 and 2 hours EGF, which is what I also observed for endogenous EGFR in BT20 immunoprecipitates blotted with anti-Cbl-b (Fig 4.6B, panel 10). In contrast to wtEGFR, peak Cbl-b association with EGFR-Y1045F occurred markedly earlier, at ~30 min. Most striking was that Cbl-b associated with the EGFR1044 truncation (Fig 4.6B, panel 8). Cbl-b association with this mutant was weaker compared to the other EGFRs but remained EGF-dependent. Moreover, Cbl-b's association with EGFR1044 rose gradually and did not display a discernible peak. Lastly, I observed that unlike c-Cbl, Cbl-b's association with EGFR is prolonged and retained even during the receptor's degradation. Overall, these results reveal a previously unacknowledged interplay of two major Cbl homologues—c-Cbl and Cbl-b—with the trafficking EGFR.

4.5 Requirement for c-Cbl and Cbl-b in EGFR Downregulation

To conclusively define the role of c-Cbl and Cbl-b in EGFR ubiquitination and degradation, I employed RNA interference (RNAi) experiments (Fig 4.7). Strong candidate sequences in the coding region of both Cbls were chosen and used to design small interfering RNA duplexes (siRNAs) for use in all subsequent RNAi experiments.

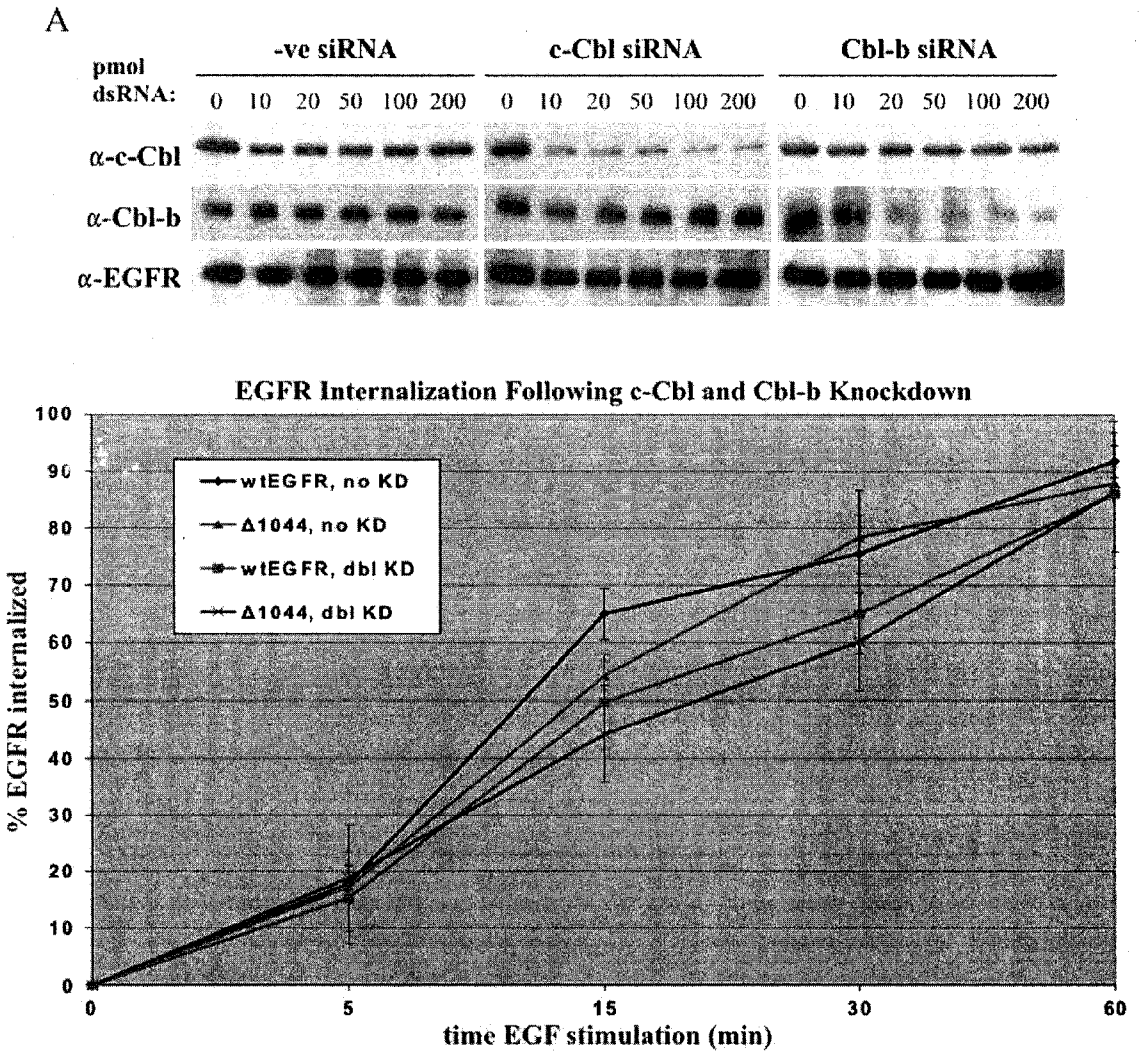

Fig 4.7. RNAi-mediated knockdown of c-Cbl+Cbl-b does not affect EGF-induced EGFR internalization. (A) 293T cells were transfected with wtEGFR and the indicated duplex RNA (dsRNA) at varying amounts for 48 hours. Optimal amounts of dsRNA for knockdown were 100 pmol for c-Cbl and 200 pmol for Cbl-b. A control duplex was employed (-ve siRNA) to assess non-specific effects on protein expression. **(B)** Quantitative analysis by flow cytometry of EGF-mediated internalization following c-Cbl/Cbl-b knockdown of BT20 cells or 293T cells transfected with wtEGFR or Δ1044 (EGFR1044). Data represent the mean (± s.d.) of triplicate experiments. $p > 0.05$ for all data pairs at each time point, as determined by Bonferroni two-way analysis. The immunoblots shown are representative of at least three independent experiments.

To first assess the degree of mRNA knockdown, candidate c-Cbl and Cbl-b siRNAs, along with a non-specific control siRNA, were cotransfected with wtEGFR in 293T cells. The immunoblots in Fig 4.7A demonstrate significant and Cbl-specific knockdown (>90%) at 48 h post-transfection. The highest level of Cbl knockdown was observed using 100 pmol of c-Cbl dsRNA or 200 pmol of Cbl-b dsRNA. Neither Cbl siRNA duplex, nor the control siRNA duplex, showed non-specific interference effects.

Using the optimized conditions established from these experiments, I employed RNAi to address the absolute requirement of Cbl interaction and Cbl-mediated ubiquitination in EGFR downregulation. I began by first revisiting Cbl's role in EGFR internalization, now in the context of both Cbls. 293T cells were transfected with wtEGFR or EGFR1044 along with siRNA duplexes to both Cbls or the control siRNA. Following 48 h knockdown, in which the levels of both Cbl were reduced >90% as seen in Fig 4.7A, cells were serum starved overnight and treated with 100ng/ml of fluorescently labeled EGF for various times. EGFR internalization was then analyzed by flow cytometry (Fig 4.7B). Overall, the c-Cbl+Cbl-b double knockdown (dbl KD) had little effect on EGF-mediated internalization of either wtEGFR or EGFR1044. Initial internalization rates were nearly identical for all transfectants (between 15-20% internalized EGFR at 5 min EGF), though there was a noticeable dip in receptor internalization rates in the dbl KD transfectants compared with the no KD transfectants during the middle of the stimulation, this was statistically insignificant ($p > 0.05$ for all data pairs). Nevertheless, by 60 min EGF the internalization levels of normal and Cbl-deficient transfectants are virtually identical. This suggests that Cbl knockdown does not significantly alter EGFR internalization. Since the levels of EGFR internalization by 1 h EGF were nearly identical in all our transfectants regardless of the presence or absence of

Cbl, I remained convinced that Cbl's function in EGFR downregulation was to induce receptor degradation later during trafficking.

To assert this hypothesis, 293T cells cotransfected with either YFP-tagged wtEGFR or EGFR1044 along with control siRNA (no KD), c-Cbl siRNA (c-Cbl KD), Cbl-b siRNA (Cbl-b KD), or c-Cbl+Cbl-b siRNAs (dbl KD) were treated with EGF and analyzed over a 4 h time course by western blot (Fig 4.8). Total cell lysates (TCLs) from each time point were either immunoblotted directly or immunoprecipitated first with anti-YFP and then immunoblotted with various antibodies. The results from the no-KD transfectants (expressing a non-specific siRNA) fully agreed with the data presented in Fig 4.6. EGF-stimulated wtEGFR underwent two distinct waves of ubiquitination: the first wave was coincident with the strongest c-Cbl-EGFR interaction (~15 min EGF) while the later wave was coincident with the strongest Cbl-b-EGFR interaction (~1 h EGF). EGFR1044, on the other hand, showed only a single rise in ubiquitination and this occurred only after 15 min EGF, corresponding to peak Cbl-b interaction. Despite the difference in ubiquitination patterns, both receptors were significantly degraded by 4 h EGF. I next turned to the immunoblots from the Cbl knockdown transfectants. Probing TCLs from these transfectants in order to assess knockdown efficiency of c-Cbl and/or Cbl-b revealed a >90% disappearance in both homologues. Furthermore, neither Cbl protein could be appreciably detected in the corresponding EGFR immunoprecipitates, thus minimizing the possibility that even low levels of Cbl could effect EGFR downregulation In c-Cbl KD cells, ubiquitination of wtEGFR was delayed and appeared strongest when Cbl-b interaction was at its peak (~30 min EGF). In contrast, wtEGFR expressed in Cbl-b KD cells showed only an initial rise in ubiquitination following EGF. Despite these differences, significant degradation of wtEGFR (~50%) occurred by 4 h

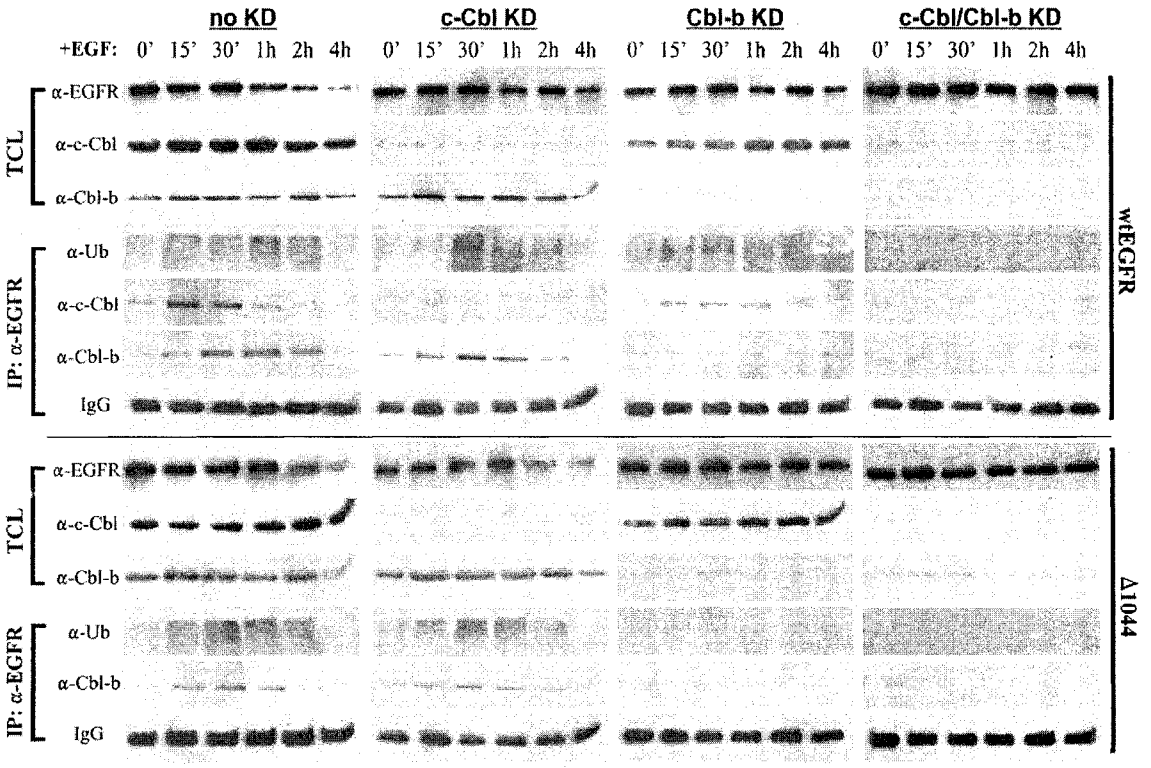

Fig 4.8. c-Cbl and Cbl-b together account for total EGFR ubiquitination and degradation. 293T cells were transfected with YFP-tagged wtEGFR or Δ1044 (EGFR1044) and one of the following RNAi duplexes: 200 pmol non-specific control dsRNA (no KD), 100 pmol c-Cbl dsRNA (c-Cbl KD), 200 pmol Cbl-b dsRNA (Cbl-b KD), or 100 pmol c-Cbl and 200 pmol Cbl-b dsRNAs (c-Cbl/Cbl-b KD). Following 48hr transfection, cells were serum starved overnight and then treated with 100ng/ml EGF for the times indicated. Total cell lysates (TCLs) were either immunoblotted directly or immunoprecipitated first with anti-YFP and then immunoblotted with the indicated antibodies. The immunoblots shown are representative of at least three independent experiments.

EGF in both c-Cbl KD and Cbl-b KD cells. Most importantly, both ubiquitination and degradation of wtEGFR was eliminated in the double-Cbl knockdown cells (Fig 4.8, rightmost column). When I looked at the immunoblots from EGFR1044 c-Cbl KD cells, the pattern of receptor ubiquitination and degradation was nearly similar to the no KD condition. This is not surprising, as c-Cbl cannot directly influence the truncated receptor. Under Cbl-b KD conditions however, both receptor ubiquitination and degradation are virtually abolished, revealing that Cbl-b is alone necessary for these events in the truncated receptor.

I wanted to present the above data in a comparative and consistent manner. To this end, I performed all anti-EGFR and anti-Ub immunoblots from Fig 4.8 in triplicate and quantified band intensities by densitometry. In order to normalize the data for graphical analysis, the sample corresponding to 0 min EGF no KD was run alongside each anti-Ub immunoblot of immunoprecipitated EGFR (for Fig 4.9A), while the sample corresponding to 0 min EGF no KD was run alongside each anti-EGFR immunoblot (for Fig 4.9B). Fig 4.9A compares the ubiquitination levels of wtEGFR and EGFR1044 in response to EGF. Under no KD conditions, the two wave ubiquitination pattern of wtEGFR is seen as an initial strong rise peaking at 15 min EGF, followed by a ~25% decline in signal and then another small rise of 5-10% at 1 h EGF. The degree of receptor deubiquitination following the initial rise is clearly evident: ubiquitination levels at 30 min have fallen by ~30% from 15 min EGF. The meaningfulness of the second ubiquitination wave can be statistically disputed (Fig 4.9A, top left graph: $p>0.05$ comparing 30 min and 1 h), though it is possible that different receptors in the same sample are being ubiquitinated by c-Cbl and Cbl-b concurrently, which would serve to blunt the two-wave pattern. However, in the single Cbl knockdowns, this overlap is

Fig 4.9. Graphical analysis of Cbl-mediated ubiquitination and EGFR degradation. 293T cells were transfected and treated as in Fig 8. **(A)** Analysis of Cbl-mediated EGFR ubiquitination. Anti-Ub blots of EGFR immunoprecipitates as shown in Fig 8 were performed in triplicate and their corresponding band intensities quantified by densitometry and normalized to the anti-Ub band at 0'. Data represent the mean (± s.d.). **(B)** Analysis of Cbl-mediated EGFR degradation. Anti-EGFR blots of TCLs as shown in Fig 8 were prepared in triplicate, densitometrically quantified, and normalized to the anti-EGFR band at 0'. Data represent the mean (± s.d.). Stars and circles mark values of insignificant variance ($p>0.05$) with EGFR levels at 0' and 60' respectively, as determined by Newman-Keuls one-way analysis.

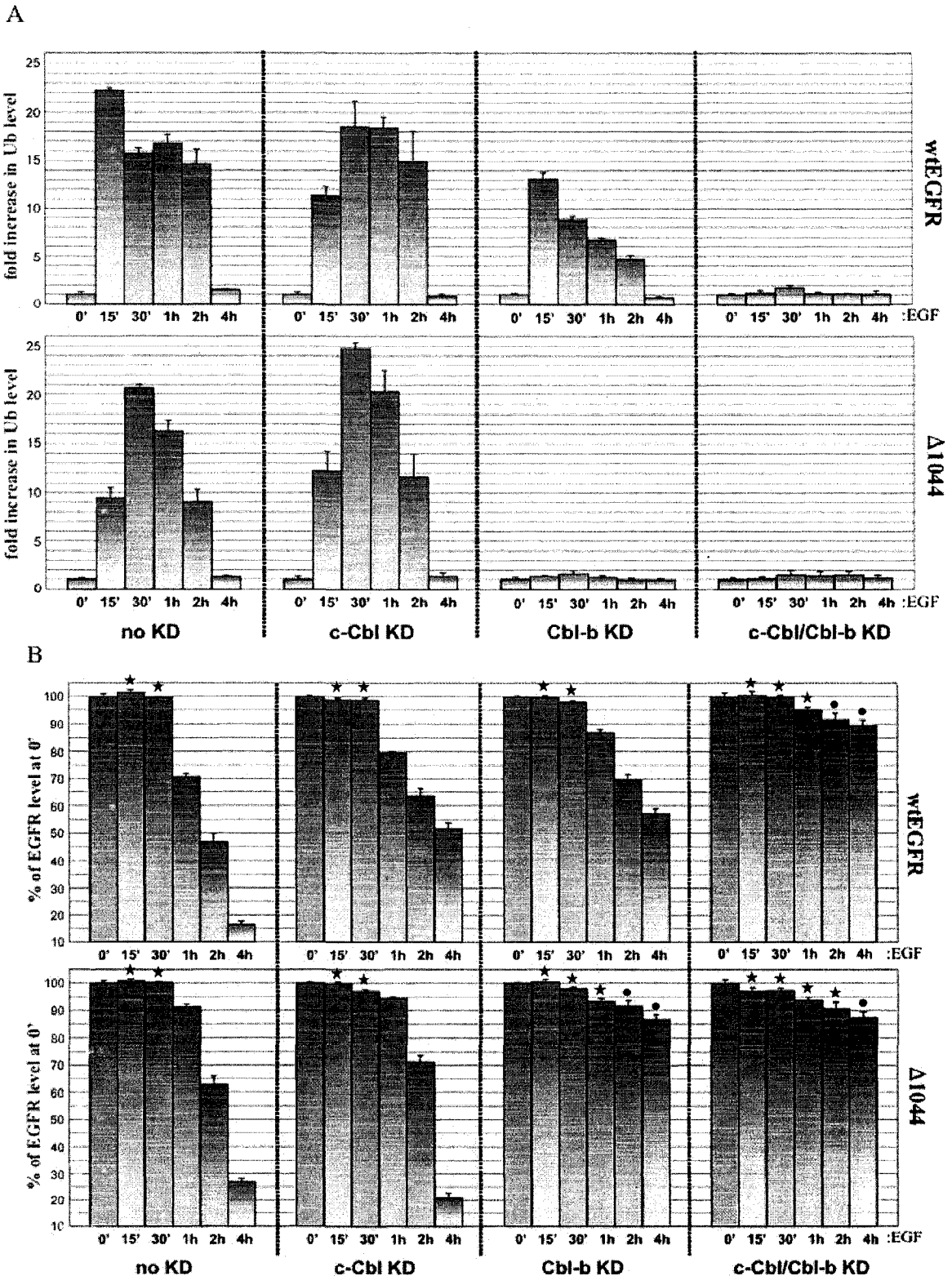
A
fold increase in Ub level
wtEGFR
Δ1044
0' 15' 30' 1h 2h 4h :EGF
no KD
c-Cbl KD
Cbl-b KD
c-Cbl/Cbl-b KD
B
% of EGFR level at 0'
wtEGFR
Δ1044
0' 15' 30' 1h 2h 4h :EGF
no KD
c-Cbl KD
Cbl-b KD
c-Cbl/Cbl-b KD

eliminated and each wave is clearly evident. Comparing these two graphs reveals that the first ubiquitination wave is still ~20% stronger than the second wave. It is also significant to note that either wave is lower than the waves under no KD conditions, perhaps suggesting that a small fraction of Cbl-b ubiquitinates EGFR at early times of EGF and a small fraction of c-Cbl continues to ubiquitinate EGFR at latter times. Interestingly, the trend of Cbl-b-mediated EGFR1044 ubiquitination shows a pronounced rise similar to the first wave of wtEGFR. Aside from these subtle kinetic differences, it can be clearly seen that both Cbls account for total EGFR ubiquitination, as elimination of both Cbl homologues virtually abolishes the ubiquitin signal (Fig 4.9A, top right graph). Furthermore, both Cbls are required for EGFR degradation (Fig 4.9B, top right graph), while eliminating either only serves to delay this event (Fig 4.9B, top middle graphs). As both Cbls account for total EGFR ubiquitination and degradation, this also confirmed my assumption, based on what is known of Cbl-3, that this smaller homologue plays no role in EGFR downregulation (Keane et al., 1999). Taken together, my results reveal that (1) Cbl downregulates EGFR through ubiquitination, and (2) either c-Cbl and Cbl-b are sufficient to effect EGFR degradation, and together both are necessary.

4.6 Summary

In this chapter I demonstrate that Cbl plays its role in EGFR downregulation at the level of ubiquitin-mediated degradation and not internalization. Both Cbl interaction with EGFR and Cbl-mediated EGFR ubiquitination were found to be neither necessary nor sufficient for EGF-mediated EGFR internalization. Rather Cbl's negative regulation occurs at the level of EGFR degradation. Although c-Cbl was not degraded in complex with EGFR, Cbl-mediated ubiquitination was required for receptor degradation. Either c-

Cbl- or Cbl-b-mediated ubiquitination was sufficient to cause EGFR degradation, and together both were necessary. Furthermore, by utilizing RNAi methods to knockdown either Cbl, I uncovered two temporally distinct "waves" of EGFR ubiquitination. Either wave corresponded to a high level of EGFR association with a particular Cbl protein. c-Cbl interaction with EGFR was strongest at an earlier stage of EGFR trafficking while Cbl-b's peak association occurred later. In addition, I found specific dephosphorylation of EGFR at Y1045 to occur concomitantly with c-Cbl disassociation. I conclude that Cbl acts as a negative regulator of EGFR via ubiquitin-mediated degradation, not internalization, and that there exists a temporal interplay of two Cbl isoforms with EGFR during the receptor's internal trafficking route.

CHAPTER 5:

Discussion

Intuitively, the endosome must be an important location for RTK signal transduction. Following ligand binding, receptors undergo clathrin-mediated endocytosis in a matter of minutes and yet can spend hours trafficking along the endocytic route in a kinase-active state before being degraded. As this would appear to indicate that RTKs transduce a large proportion of their signals intracellularly, it is therefore important to characterize this phenomenon in a physiological context. In this thesis, I studied both RTK signal transduction from endosomes and the intracellular regulation of EGFR by Cbl.

5.1 Physiologically Relevant Signaling from Endosomal RTKs

For many years investigators have debated the existence of endosomal signaling (Burke et al., 2001; Ceresa and Schmid, 2000; Clague and Urbe, 2001; Felder et al., 1992; Bevan et al., 1996). Initially, endocytosis of ligand-activated receptors has generally been considered a mechanism to attenuate signaling. Recent evidence suggests that internalized receptors maintain their ability to generate cellular signals after endocytosis to endosomes. However, in spite of intensified efforts in understanding cell signaling from endosomes (Downward, 1998; Felder et al., 1990; Lanzetti et al., 2000; McPherson et al., 2001; Vieira et al., 1996), no direct evidence exists to demonstrate the activation of signal transduction pathways from this location, nor to support the physiological relevance of endosomal signaling (Di Fiore and De Camilli, 2001). This deficiency is largely due to the lack of methods allowing exclusive separation and characterization of endosome-generated signaling without contribution from signaling at the cell surface. A system is needed to provide definitive evidence that RTKs can initiate, generate, and propagate signals from endosomal compartments.

This thesis reports the establishment of a system that allows RTKs to be specifically activated in endosomes without initial activation at the cell surface (Chapter 3.1). This system was tested on both EGFR and PDGFR systems. Cells were pretreated with a RTK-specific kinase inhibitor to block cell surface activation of receptor and then ligand was added for a time sufficient to cause complete internalization of inactive ligand-receptor complexes. These ligand-bound, kinase-inhibited receptors internalized in a manner kinetically similar to ligand-bound kinase-active receptors (i.e. via standard ligand activation), and entered the same population of early endosomes. This ensured that subsequent endosomal RTK activation would occur in a physiological context. It also suggested that the requirement for RTK internalization was invested in ligand-binding and not ligand-induced kinase activation, a point which has been long debated.

Because it has been reported that kinase-inactive EGFR preferentially recycles back to the PM following internalization, monensin was employed to inhibit receptor recycling and thus ensure that following kinase activation, all signals would originate from endosomes (Doebler, 2000; Tartakoff, 1983). An alternative system was also adapted without monensin, and though the level of receptor recycling following ligand-induced internalization of kinase inhibited receptors was ~10% of the total internalized amount, a brief acid wash effectively removed any cell surface ligand, ensuring no cell surface activation would occur when kinase inhibitor was removed.

After removal of kinase inhibitor (AG1478 for EGFR and AG1296 for PDGFR), endosomal receptor was autophosphorylated. Although receptors remained phosphorylated for similar times (1-2 h) following either standard ligand activation or endosomal activation, the level of endosomally activated receptor was approximately half that of standardly activated receptors. Low levels of EGF dissociation at endosomes and

incomplete washout of kinase inhibitor may both attribute to this observed decrease in endosomal receptor phosphorylation. Nevertheless, this did not compromise the effectiveness of endosomal receptor activity, as signaling substrates for endosomal receptors were also activated at half the level of substrates stimulated by standard receptor activation.

Next it was shown that endosomally-activated EGFR/PDGFR can recruit signaling proteins, including Grb2, Shc, and the p85 regulatory subunit of PI3K, and can stimulate components of major signaling pathways, including Erk/MAPK and Akt. This demonstrates that the endosome is not only a site where receptors can continue to coordinate signaling events initiated at the PM, but is also a site where signaling-competent complexes can be nucleated.

In order to determine if endosomal RTKs were fully capable of eliciting a biological outcome, the effects of endosomal EGFR/PDGFR signaling on serum-withdrawal induced apoptosis was examined by TUNEL assay (Fig 3.6 & 3.7). Endosomally-activated EGFR/PDGFR generated signals sufficient to suppress apoptosis induced by serum-withdrawal. In addition, this anti-apoptotic effect was inhibited by wortmannin, indicating that, similar to standard RTK survival signaling, endosome-derived survival signaling required the PI3K-Akt pathway. I showed, therefore, that both endosomal EGFR and PDGFR can transduce survival signals of physiological significance.

These results argue against the role of endocytosis as a means of signal attenuation. Although initial RTK signaling from the cell surface is dispensable for EGF- and PDGF-induced signaling outcomes, the PM remains the site where ligand binding occurs and thus cannot be disregarded as unimportant. Nonetheless, there are other ways to activate RTKs that do not require ligand binding. For instance, RTKs can be transactivated by

other receptors (e.g. GPCRs) or non-receptor enzymes (e.g. Src kinases) (Carpenter, 1999; Ozcan et al., 2006; Wada et al., 1990). Ultraviolet radiation and peroxide are also known to activate RTKs in the absence of ligand (Peus et al., 1999; von Montfort et al., 2006). Since many of these factors can affect receptors intracellularly, it is conceivable that they can activate RTKs intracellularly as well, and thus in some situations, the PM may be completely dispensable for signal transduction. Another point in favour of endosomal signaling is intuitive: ligand activated RTKs remain on the PM only briefly and spend the majority of their lifetimes trafficking along the endosomal route.

It is also reasonable to assume that the relative physiological contributions of PM and endosome-localized signaling may vary among different cell types and receptor systems. For instance, a recent finding in neuronal cells revealed that endocytosis of nerve growth factor (NGF) is dispensable for activation of survival pathways via its cognate receptor, TrkA (MacInnis and Campenot, 2002). Nevertheless, the results in this thesis provide evidence strongly supporting the biological significance of endosomal signaling from two RTKs: EGFR and PDGFR.

5.2 Mitogenicity of endosomally signaling RTKs

The second part of chapter 3 addressed the important but difficult question of whether endosomal RTK signaling is sufficient to stimulate cell proliferation. By activating EGFR/PDGFR at the endosome, I showed that a pulse of activity equivalent to that following 1 hour of standard EGF/PDGF stimulation generated signals sufficient to suppress apoptosis induced by serum-withdrawal (Fig 3.6). However, a similar 1 hour pulse was unable to induce cell proliferation from EGFR in MDCK and BT20 cells (Fig 3.8).

The difficulty in addressing this question is due to the insufficient activation time of endosome-associated EGFR. EGFR remains activated for 1-2 h following its activation at endosomes before it is ultimately degraded in lysosomes. It is generally accepted that in order to elicit a proliferative response, quiescent cells typically require ligand exposure until about two hours prior to S-phase, which generally corresponds to 7-9 hours (Pardee, 1989). A single span of endosomal EGFR signaling, following washout of kinase inhibitor, lasted approximately one hour and was insufficient to stimulate DNA synthesis in BT20 and MDCK cells (Fig 3.8). This was also true for 1 hour standard treatment with EGF, though unlike standard treatment, I could not prolong signaling from endosomes without integrating newly synthesized and/or recycling receptors in the process. In order to validate the mitogenicity of endosomal EGFR therefore, I needed to establish a means to assure that additional signals (enough to effect cell proliferation) would be exclusively endosomal.

A recent finding by Jones *et al.* (Jones and Kazlauskas, 2001c) revealed that the prolonged requirement for PDGF to stimulate proliferation of fibroblasts can be replaced with two short pulses of PDGF, corresponding to the times when mitogen is required to drive cells from quiescence, and then later through the R-point of G1 phase. This insight allowed me to adapt and test a strategy to determine whether two pulses of EGFR signaling is sufficient to stimulate cell proliferation (Fig 3.9 & 3.11). In PDGF-induced fibroblasts, it was found that a full mitogenic outcome is elicited when mitogenic pulses were administered 7-9 hours apart. Applying this finding to the EGF receptor system, I found that EGF-induced mitogenesis in epithelial and breast carcinoma cells followed a similar biphasic mechanism, corresponding to times when the cells require growth factor for cell-cycle progression. Two short pulses of standard EGF-induced signaling, spaced

8 hours apart, was sufficient to elicit proliferation with kinetics similar to 8 h of continuous EGF treatment (Fig 3.10). More importantly, two pulses of endosomal EGFR signaling, spaced 8 hour apart, is also sufficient to stimulate cell proliferation in a similar way as two pulses of standard EGFR signaling (Fig. 3.12). Interestingly, for cell proliferation induced by two pulses of endosomal EGFR signaling, the response was reduced when the second pulse was given at 4 h under monensin-free conditions versus conditions in which monensin was included. I am not completely clear what causes this discrepancy. However, it is possible that in the presence of monensin, more EGFR is accumulated in the endosome, thus the endosomal EGFR signaling is proportionally stronger. Alternatively, the acidic wash used to strip EGF from surface EGFR in the monensin-free system may cause unanticipated side effects from which cells need to recover.

I next determined whether endosome-derived mitogenic signaling applied to PDGFR in HepG and F442 cells (Fig 3.13). Standard stimulation of mitogenesis by biphasic PDGF-induced signaling has been previously demonstrated in NIH 3T3 cells (Jones et al., 1999). HepG and F442 cells could also be driven into S-phase via two standard PDGF pulses (column G). Most importantly for the aim of this investigation, I found that two pulses of endosomal PDGFR signaling, spaced 8 hours apart, led to cell proliferation in both cell types (column H). Moreover, the mitogenicity of two pulses of endosome-derived PDGFR signaling is kinetically similar to that derived 8 h of continual treatment with serum (compare columns H with B). Thus, PDGF itself is as an extremely potent mitogen from endosomes in F442 and HepG cells.

Underlying support for the physiological relevance of endosomal RTK signaling comes from the proliferation experiments following standard discontinuous EGF

treatment (Fig 3.10B). If the duration of either EGF pulse was 30 min or less, the proliferative response was compromised (column B), while two one-hour pulses were as proliferative as continuous 8 h EGF treatment (compare Fig 3.10B column C with Fig 3.10A column E). This implicates the minimum time required for ligand exposure (and thus the minimal signaling requirement) is at least 30 minutes, a span well exceeding the occupancy time of activated EGFR at the plasma membrane. It is therefore likely that the majority of standard EGF-induced mitogenic signals are actually endosomally derived. Furthermore, eliminating the initial plasma membrane component from the total mitogenic signal quantity does not compromise the proliferative response.

I then returned to EGFR to study mitogenic signaling events in more detail. Upon investigating the time course of G1-cell cycle events using either standard or endosomal EGF treatments, I found no differences in how the G1-machinery was engaged (Fig 3.14). In both cases, the transcription factor c-Myc was induced early on (0.5-2 h) in response to the first pulse and more strongly following the second pulse (8.5 h) (Fig 3.14C & 3.14D). Even under continuous EGF treatment, c-Myc induction appeared to follow a biphasic pattern (Fig 3.14B), albeit not as pronounced as for the discontinuous systems. Likewise, an ordered sequence of cell-cycle events followed the second pulse under either standard or endosomal EGF-treatment: beginning with elevation in cyclin-D1 levels a half an hour after the onset of the second pulse, followed by an increase in cyclin-E levels, and finally with the hyperphosphorylation of Rb protein, an event defining the R-point (Jones and Kazlauskas, 2001b; Peeper et al., 1997).

I then investigated the specific signaling events effected from each mitogenic pulse following both standard and endosome EGF treatments (Fig 3.15 for BT20 cells and Fig 3.16 for MDCK cells). In addition to EGFR and its' phosphorylation state, I

analyzed the activation profiles of three important signaling pathway components: Erk/MAPK, Akt, and PLCγ1 (Figs 3.15 & 3.16). Though it is well established that under standard EGF treatment all three of these proteins are activated/phosphorylated (Di Fiore and Gill, 1999; Downward, 1998; Pawson, 1995; Peeper et al., 1997), I wanted to determine whether different levels of activity existed depending on location (standard signaling compared to endosomal signaling) or time (first pulse compared to second pulse). In most cases, differences between standard and endosome-stimulated systems were kinetic (i.e. quantitative). Activation of proteins under endosome-EGF induction was generally more delayed than standard EGFR activation. This may reflect the incomplete removal of AG1478 and delayed activation of the internalized receptor following endosomal EGFR activation. Although phosphorylation of these three proteins was qualitatively similar whether EGFR was activated in a standard manner or from endosomes, I did observe differences in protein activity between the two pulses themselves. Following the second pulse, activation of Akt was higher and more prolonged compared to the first pulse. Moreover, Erk/MAPK activity was significantly less during the second pulse even though the protein levels were similar to those of the first pulse. This observation may be partially explained by the corresponding immunoprecipitation experiments performed in BT20 cells (Fig 3.15C & 3.15D). Activated EGFR communicates with Ras through a signaling complex containing Grb2, Shc, and mSos, the latter of which acts as a Ras-specific guanine nucleotide exchange factor (Bar-Sagi et al., 1993; Downward, 1994; Schlessinger, 1994). Comparing the EGFR immunoprecipitates from both pulses, less Grb2 and Shc were recruited to the receptor following the second EGF-induction. Additionally, EGFR levels themselves were reduced at this time, as seen by EGFR immunoblots of both cell lysates and

immunoprecipitated protein. These observations, and perhaps a lower level of available Grb2 and Shc (consequent of previous proteolytic degradation), would help to explain the lower Erk/MAPK activity. These results are consistent with both cell types used. Overall, these differences lend to the emerging idea that temporally distinct, though not necessarily exclusive events, are needed to drive cells into S-phase. Furthermore, these events are activated equally well from EGFR signaling initiated at either the endosome or the plasma membrane.

Lastly I carried out experiments to determine which specific signaling pathways are responsible for mediating the biphasic proliferative response. I inhibited PI3K activation and/or Erk/MAPK activation induced during the first or second EGFR pulse and then examined the effects on cell proliferation (Fig 3.16). My results suggest that while both Erk and PI3K activation are important in initiating events leading to the S-phase entry following the first pulse of EGFR activation, PI3K activation, though not Erk activation, is required for driving S-phase entry following the second pulse of EGFR activation. These findings are in agreement with previous reports regarding PDGFR (Jones et al., 1999).

In this thesis, I elucidated the biphasic nature of EGF-induced proliferative signaling in order to address the mitogenic role of endosomal EGFR. Linking this with the system to allow for the specific activation of endosome-associated EGFR without initial activation at the plasma membrane, I have validated the mitogenic function of endosomal EGFR. Endosomal EGFR signaling thus appears to be fully competent for transducing biological outcomes.

5.3 Cbl's Role in EGFR Downregulation

The oncogenic potential of Cbl is invested in its role as negative regulator of many upstream signaling proteins, among them EGFR, PDGFR, c-Src, insulin receptor, and many others [reviewed in (Thien and Langdon, 2001)]. An exact understanding of how Cbl downregulates these proteins is vital to delineating exactly how it contributes to cancer. Cbl functions as an E3 ligase to ubiquitinate EGFR and mediate its downregulation in response to EGF. However, considerable controversy exists as to whether Cbl's function on EGFR downregulation occurs by enhancing EGFR internalization or by lysosomal sorting during receptor trafficking: substantial evidence supporting either view continues to emerge in the literature.

Chapter 4 of this thesis investigates Cbl's role in EGFR downregulation. I found that the absolute requirement for Cbl is at the level of ubiquitin-mediated degradation and not internalization. In order to determine whether Cbl interaction with and Cbl-mediated ubiquitination of EGFR is required for ligand-induced EGFR internalization, various mutant EGFRs with distinct characteristics were expressed in 293T cells (Fig 4.1). These included an internalization-deficient EGFR (EGFR-LL/AA), and two mutants deficient for binding Cbl: EGFR-Y1045F, which lacks direct c-Cbl binding, and EGFR1044, which completely lacks c-Cbl binding. Both western analysis and kinetic analysis of receptor internalization showed that EGFR internalization does not depend on its interaction with c-Cbl or c-Cbl-mediated ubiquitination (Figs 4.2 & 4.3). Firstly, I showed that EGFR1044 was not associated with c-Cbl and its ubiquitination was not detectable at 10 min of EGF stimulation; yet, EGFR1044 was internalized similarly to wild type EGFR in response to EGF. This demonstrates that neither c-Cbl association with EGFR, nor Cbl-mediated ubiquitination of EGFR, is necessary for EGF-induced EGFR internalization. Secondly, EGFR-LL/AA still associated with c-Cbl and was

ubiquitinated to the same extent as wild type EGFR even though it showed only minimal internalization. This indicates that neither c-Cbl association with EGFR, nor Cbl-mediated ubiquitination of EGFR is sufficient for EGF-induced EGFR internalization.

I then turned my query to downstream stages of EGFR trafficking and revealed that c-Cbl disassociated from EGFR well in advance of EGFR degradation (Figs 4.4 and 4.5). c-Cbl disassociation from EGFR-LL/AA was delayed compared to wtEGFR, and since both EGFRs exhibit the same level of receptor functionality, this suggests that subcellular environment is important to the disassociation mechanism of c-Cbl (Fig 4.4 & 4.5A). Since EGFR-LL/AA is mostly restricted to the plasma membrane, it may have poor access to machinery responsible for c-Cbl's disassociation. Interestingly, loss of c-Cbl binding to EGFR corresponded to the specific dephosphorylation of Y1045 on the receptor, shedding light on a potential mechanism for Cbl's disassociation (Fig 4.5B). Also, there was a delay in EGFR-LL/AA dephosphorylation at Y1045 (compared to wtEGFR) that paralleled its delay in c-Cbl disassociation. Whether these dephosphorylation events are the cause or consequence of c-Cbl disassociation however, remains to be clarified. It is reasonable to suppose that the phosphatase(s) responsible for this event would require exposure of the phosphotyrosine at 1045, and this would require c-Cbl to first be disassociated. Several studies have also shown that Cbl is recruited by soluble factors at later times of EGF stimulation (Bao et al., 2003; Buday et al., 1996; Fukazawa et al., 1996; Kassenbrock et al., 2002; Tanaka et al., 1995; Wu et al., 2003). One example is a recent finding demonstrating that EGF-activated Cdc42 is able to recruit c-Cbl via Cool-1, thereby preventing Cbl association with the EGFR (Wu et al., 2003; Feng et al., 2006).

I next looked at receptor ubiquitination and degradation over a longer time course of EGF stimulation (Fig 4.6). Every EGFR studied, including the truncated EGFR1044, was degraded and ubiquitinated. As EGFR1044 should completely lack c-Cbl binding and c-Cbl mediated ubiquitination, I searched for alternative E3 ubiquitin ligases that might be responsible. The strongest candidates were the two other major Cbl isoforms: Cbl-b and Cbl-3. Both homologues bind EGFR and regulate its signaling in an EGF-dependent fashion, though only Cbl-b's ubiquitin ligase activity has been demonstrated (Ettenberg et al., 1999a; Keane et al., 1995; Keane et al., 1999). Cbl-3 possesses the TKB and RING finger domains necessary to function as an E3 ligase, though it lacks the C-terminal tail possessed by c-Cbl and Cbl-b, which contains a wide range of regulatory sites, including multiple SH3-domain-binding motifs and an ubiquitin associated (UBA) domain. Cbl-3 also has a limited expression profile. While its expression is highest in tissues of the liver, pancreas, prostate, and intestine, in most other tissue types expression of this protein is low or altogether absent (Keane et al., 1999). It therefore seemed that Cbl-b was the stronger candidate to investigate.

My analysis indeed revealed that Cbl-b was working in conjunction with c-Cbl to bind and ubiquitinate wtEGFR, EGFR-LL/AA, and EGFR-Y1045F, while Cbl-b alone was acting to ubiquitinate EGFR1044. c-Cbl and Cbl-b function was not simply redundant, as each appeared to act on EGFR at temporally distinct times during EGF-mediated trafficking (Fig 4.6). In order to conclusively establish the overall role of Cbl in EGFR downregulation, I employed RNAi experiments to knockdown either or both Cbl homologues (Figs 4.7 & 4.8). My data showed that either c-Cbl or Cbl-b is capable of ubiquitinating EGFR (Fig 4.9A). In addition, either Cbl alone was sufficient to cause EGFR degradation (Fig 4.9B). In the absence of both Cbls, however, EGFR is neither

ubiquitinated nor degraded (Fig 4.9). Moreover, double knockdown of both Cbls did not significantly affect EGF-mediated internalization (Fig 4.7B), indicating that both Cbls, not only c-Cbl, was dispensable for EGFR endocytosis.

My findings implicate a molecular mechanism by which the interplay of c-Cbl and Cbl-b with EGFR regulates the receptor's ubiquitination and degradation (Fig 4.8). Within 15 min EGF stimulation, EGFR interacts primarily with c-Cbl, thus mediating its ubiquitination. At this stage Cbl-b binding appears inhibited. This may be due to locational constraints, competition with c-Cbl for binding sites of the receptor, and/or some other requirement for additional EGFR modifications. Following peak c-Cbl association and the initial rise in receptor ubiquitination, EGFR is partially deubiquitinated (Ub levels drop ~30% between 15 and 30 min EGF). This is likely due to the action of Ub-specific protease Y (UBPY), previously shown to be a key deubiquitinating enzyme for EGFR (Mizuno et al., 2005). Consistent with my findings, this study showed a similar drop in EGFR ubiquitination after 15 min EGF. Moreover, EGFR ubiquitination was completely abolished when UBPY was overexpressed.

The onset of the next "stage" of c-Cbl and Cbl-b interplay with EGFR (i.e. following ~30 min EGF-induced trafficking) is marked by several contemporaneous events, including c-Cbl disassociation from EGFR, specific dephosphorylation at Y1045, and a strong rise in Cbl-b association with EGFR. It is the latter event that most likely accounts for the second rise in EGFR ubiquitination observed at ~ 1h EGF (Fig 4.6, panel 4). c-Cbl and Cbl-b are thought to bind the same phosphotyrosine sites on EGFR, and I have also shown that Cbl-b, and not c-Cbl, can bind at one or more other sites upstream of residue 1044. Whether these Cbl-b-exclusive sites are phosphotyrosine-based is however unclear. Many prominent EGF-dependent phosphotyrosines exist upstream of

1044, though why c-Cbl is incapable of binding the same sites is puzzling, given the high functional and sequence homology between these homologues. A recent insight revealing a key difference between the C-terminal UBA domains of c-Cbl and Cbl-b may provide a partial explanation (Davies et al., 2004). The UBA domain recognizes and interacts with both mono- and polyubiquitinated proteins, including the EGFR. While c-Cbl's UBA domain was unable to interact with ubiquitinated proteins altogether, Cbl-b's UBA domain interacted with a wide variety of them, thus revealing a qualitative, not a quantitative, distinction in the functions of these UBA domains. Furthermore, overexpression of Cbl-b's UBA acted in a dominant-negative manner to inhibit EGFR degradation, suggesting Cbl-b directly interacts with EGFR via ubiquitin moieties. Thus, Cbl-b might be interacting with ubiquitinated residue(s) upstream of 1044 in an EGF-dependent manner. This insight does not completely explain the observed Cbl-b association pattern, and the real situation is likely a mixture of both c-Cbl-dependent (competitive) and c-Cbl-independent (non-competitive) Cbl-b binding. Whatever the case, I have conclusively demonstrated that the ubiquitination of EGFR, whether mediated by c-Cbl, Cbl-b, or both together, leads to EGFR degradation (Fig 4.9B).

5.4 Conclusions

Mammalian cells risk becoming cancerous when proteins that transduce proliferative signals are mutated, causing loss of their downstream signalling control. Receptor tyrosine kinases are such a group of potentially tumorigenic proteins. For RTKs, endocytosis has been considered a means of quickly turning off their signaling activity after being stimulated by growth factors at the plasma membrane. Once endocytosed, the internalized receptor is routed along the endosomal pathway and

eventually degraded in the lysosome (Carpenter, 1987). A flaw of this simplistic model is that many important biological pathways stemming from RTKs require prolonged signaling activity, and yet, most RTKs are cleared from the cell surface within minutes of growth factor induction (Ceresa et al., 1998). It is now realized however, that the amount of time an RTK spends along the endosomal route is much longer than what is required for its degradation (Wang et al., 2002a). I therefore pursued an investigation into the physiological role of RTK signal transduction from the level of the endosome.

The first part of my thesis investigated regulation of RTK signal transduction by endocytosis (Chapter 3). Through devising a system to specifically activate EGFR or PDGFR at endosomes, I was able to show endosomal RTK signals effected full biological outcomes. Upon stimulation at the endosome, RTKs autophosphorylate and nucleate signaling complexes capable of transducing downstream signals which lead to cell survival. I then attempted to demonstrate that endosomal RTK signaling was mitogenic. In doing so, I revealed the requirement for prolonged ligand exposure to stimulate cell proliferation in my cells can be substituted with two short pulses of ligand. By adapting this biphasic paradigm to the endosomal activation method, I showed that endosome-derived RTK signals cause cell proliferation. The events following each EGF-induced pulse engaged the G1 cell cycle machinery: the first pulse arouses cells from the resting state into G1 and renders them responsive to subsequent stimulus. The second pulse (i.e. the subsequent stimulus), was required several hours later and drove cells through the restriction point by engaging a regiment of cell cycle specific events. Furthermore, both PM-derived and endosome-derived RTK pulses transduced similar signals though events following first-pulse and second-pulse stimulation revealed some interesting differences. For instance, PI3K/Akt pathway stimulation following the second

EGFR pulse was necessary for cell proliferation while Ras/MAPK pathway activation was not. Overall these findings reveal the full physiological relevance of endosomally signaling EGFR and PDGFR. It can be hoped, that in light of the multitude of receptor tyrosine kinases that exist, future investigations will reveal analogous receptor systems which function at the endosomal level, and lend further credence to the importance of endosomal signal transduction.

The second part of my thesis investigated Cbl-mediated downregulation of EGFR (Chapter 4). I found that Cbl acts as a negative regulator of EGFR at the level of its degradation, not its internalization. Based on RNAi knockdown of both c-Cbl and Cbl-b, either c-Cbl or Cbl-b is sufficient to ubiquitinate and cause the degradation of EGFR, and together they are necessary, as elimination of both homologues abolishes EGFR ubiquitination, and consequently, prevents it degradation. Through detailed analysis of EGFR trafficking, I have also unveiled a temporal interplay of these two Cbls with EGFR during its internal trafficking route. It remains to be seen whether this downregulatory dualism of Cbl is shared among cell types and other receptor systems. Given the multitude of Cbl substrates known and the complexity of their regulatory networks, it seems a distinct possibility.

In conclusion, the results presented from both parts of my thesis ultimately argue against the role of endocytosis as a means of signal attenuation and receptor downregulation. The plasma membrane, though necessary for ligand recruitment, is neither a privileged site for EGFR signaling, nor the exclusive location where receptor fate is determined.

5.5 Future Directions

5.5.1 Ubiquity and Variability of Endosomal Signal Transduction

It is clear that at least two RTKs (EGFR and PDGFR) can generate signals of physiological significance from endosomes. Numerous other receptors, and not only other RTKs, possess characteristics that make them likely transducers from endosomes. Hormone receptors (e.g. prolactin and insulin receptors), antigen receptors (e.g. T-cell, B-cell receptors), cytokine receptors (e.g. IL-2, IL-3R, IL4R, Erythropoietin receptors), as well as other RTKs (nerve growth factor receptor (NGFR), fibroblast growth factor receptor (FGFR), hepatocyte growth factor receptor (HGFR), ErbB4, etc.) are all, in one way or another, subjected to activation-based turnover at the PM, have prolonged endocytic occupancy times, and are upstream to multiple signaling cascades (Ahn et al., 1999; Burden and Yarden, 1997; Chow et al., 1998; Clague and Urbe, 2001; Goldstein et al., 1985; McPherson et al., 2001). By using the endosomal receptor activation method outlined in this dissertation, it will be possible to study the endocytic signaling capacity of these receptor systems in their different contexts, and ultimately validate the universality (or semi-universality) of endosomal signal transduction.

Another unresolved issue which can be addressed by studying multiple receptor systems is whether the subcellular location of RTK signaling (i.e. cell surface compared to endosomal signaling) can dictate the specificity of output (Marshall, 1995). Some findings implicate, for instance, that receptor internalization is required for the activation of certain signaling components, while others demonstrate that PM-localized receptors transduce full outcomes despite their inability to internalize. A reasonable first step in studying qualitative/quantitative variability in receptor signaling therefore, is to physically demarcate PM-associated from endosome-associated signaling events. This

can be accomplished by combining established methods to stabilize receptors at the cell surface with the method presented in this thesis which allows specific activation of receptors at the endosome. By comparing the proteomes and biological outputs of receptors in these two subcellular contexts, it can be truly determined whether cells utilize endocytosis as a means to modulate signal transduction from receptors.

5.5.2 Bridging the Gap in the Biphasic Signaling Paradigm.

The growth factors that drive cell proliferation are well characterized, and the signaling pathways directly transduced upon stimulation have been elucidated. With the revealment of biphasic growth factor-induced signaling, however, many new questions arise (Obaya et al., 1999; Jones and Kazlauskas, 2001a). The G1 phase consists of two distinct growth factor-dependent stages: an initial "priming" stage in which cells are aroused from the quiescent state and attain the ability to engage the cell cycle, and a later "completion" stage in which cell cycle events necessary for exit from G1 occur. The events immediately following the second growth factor-induced pulse of signaling are known well (i.e. engagement of cell cycle machinery), though the molecular events that entail priming and render cells competent to engage the later completion stage are unknown. Moreover, the necessity of a precise molecular definition is vital in understanding hyperproliferative diseases involving hyperplasia (e.g. asthma) and neoplasia (e.g. cancer). Therefore, it is important to molecularly define the events of priming that bridge the two growth factor-dependent stages required for cell proliferation. A suitable approach to defining these events could involve differential proteomics. Due to the high number of mitogenic factors likely involved, specific proteomes could be compared first, such as those pertaining to specific protein modifications. Recently, a

powerful systemic approach to isolating and identifying tyrosine phosphorylated proteins has emerged (Rush et al., 2005). As phosphorylation is a key element in signaling downstream from RTKs, such a method would be quite applicable for distinguishing events that bridge the gap of the two mitogenic signaling pulses.

5.5.3 Elucidating the Regulatory Interplay of c-Cbl and Cbl-b

Based on RNAi knockdown experiments, I have demonstrated that both c-Cbl and Cbl-b are sufficient to ubiquitinate and cause the degradation of EGFR. However, the specific roles played by either Cbl in EGFR modification during the receptor's endosomal trafficking remain subtle and unclear. Many straightforward experiments can be performed to better define the temporal interplay of these two Cbls with EGFR. For instance, the question of whether both Cbls can simultaneously interact with the same receptor molecule can be addressed by co-immunoprecipitation experiments. At different stages of EGFR trafficking, either Cbl can be immunoprecipitated and the presence of the other Cbl tested. In conjunction with far western analysis, the interrelationship between c-Cbl, Cbl-b, and EGFR could be even further clarified. Furthermore, systemic identification of Cbl binding partners other than EGFR over the time course of EGF stimulation may reveal possible factors that delay Cbl-b association with the receptor (compared to c-Cbl). Another pending area of focus regards the different functionalities of c-Cbl and Cbl-b's UBA domain. As Cbl-b's UBA is capable of binding a wide array of ubiquitinated proteins and c-Cbl's UBA domain is not, it remains to be determined how many of these protein associations regulate Cbl-b-EGFR interactions (Davies et al., 2004). It is indeed interesting that Cbl-b can bind to EGFR at sites inaccessible to c-Cbl (upstream of residue 1045), and whether this involves the Cbl-b UBA domain can be

easily addressed by studying Cbl-b mutants either lacking this motif or possessing c-Cbl's.

Another question left unresolved regards the differential fates of the two Cbl proteins (c-Cbl and Cbl-b). Based on western analysis of Cbl interaction with EGFR over a prolonged time course (Fig 4.6), it seems that total Cbl-b levels fall during EGFR degradation while c-Cbl levels remain stable. This finding, as well as the later association of Cbl-b, suggest that Cbl-b undergoes degradation with the EGFR, while c-Cbl, already dissociated from the receptor, remains undegraded in the cytosol. Indeed, it has been shown that Cbl-b is involved in coordinating EGFR degradation at later endocytic compartments, though interestingly, both Cbls are known to undergo ligand-induced autoubiquitination during their routing with RTKs (Ettenberg et al., 1999b; Ettenberg et al., 2001; Wang et al., 1996a). If c-Cbl is eventually degraded, then it will most likely occur via the proteasome. That the two Cbls possess different degradative fates is in itself a curious possibility, given their homology and functional redundancy, though added to this is the observation that EGFR degradation is dependant on a functioning proteasome (Ettenberg et al., 1999b). Does c-Cbl somehow act in a signaling relay linking the proteasome to RTK regulation? And if so, why is c-Cbl not itself degraded at a similar time as the receptor? These questions can be addressed in part by studying RTK trafficking in the presence of proteasomal and/or lysosomal inhibition. Understanding the interplay between c-Cbl and Cbl-b might possibly lead to understanding a larger interplay between lysosomal and proteasomal mechanisms.

CHAPTER 6

REFERENCES

Reference List

Ahn,S., Maudsley,S., Luttrell,L.M., Lefkowitz,R.J., and Daaka,Y. (1999). Src-mediated tyrosine phosphorylation of dynamin is required for beta2-adrenergic receptor internalization and mitogen-activated protein kinase signaling. J. Biol. Chem. *274*, 1185-1188.

Aktas,H., Cai,H., and Cooper,G.M. (1997). Ras links growth factor signaling to the cell cycle machinery via regulation of cyclin D1 and the Cdk inhibitor p27KIP1. Mol. Cell Biol. *17*, 3850-3857.

Amati,B., Alevizopoulos,K., and Vlach,J. (1998). Myc and the cell cycle. Front Biosci. *3:d250-68.*, d250-d268.

Arteaga,C.L. (2001). The epidermal growth factor receptor: from mutant oncogene in nonhuman cancers to therapeutic target in human neoplasia. J. Clin. Oncol. *19*, 32S-40S.

Balciunaite,E., Jones,S., Toker,A., and Kazlauskas,A. (2000). PDGF initiates two distinct phases of protein kinase C activity that make unequal contributions to the G0 to S transition. Curr. Biol. *10*, 261-267.

Bao,J., Gur,G., and Yarden,Y. (2003). Src promotes destruction of c-Cbl: implications for oncogenic synergy between Src and growth factor receptors. Proc. Natl. Acad. Sci. U. S. A. *100*, 2438-2443.

Bar-Sagi,D., Rotin,D., Batzer,A., Mandiyan,V., and Schlessinger,J. (1993). SH3 domains direct cellular localization of signaling molecules. Cell. *74*, 83-91.

Barbieri,M.A., Roberts,R.L., Gumusboga,A., Highfield,H., varez-Dominguez,C., Wells,A., and Stahl,P.D. (2000). Epidermal growth factor and membrane trafficking. EGF receptor activation of endocytosis requires Rab5a. J. Cell Biol. *151*, 539-550.

Basu,S.K., Goldstein,J.L., Anderson,R.G., and Brown,M.S. (1981). Monensin interrupts the recycling of low density lipoprotein receptors in human fibroblasts. Cell *24*, 493-502.

Bennett,A.M., Hausdorff,S.F., O'Reilly,A.M., Freeman,R.M., and Neel,B.G. (1996). Multiple requirements for SHPTP2 in epidermal growth factor-mediated cell cycle progression. Mol. Cell Biol. *16*, 1189-1202.

Betsholtz,C. (2003). Biology of platelet-derived growth factors in development. Birth Defects Res. C. Embryo. Today. *69*, 272-285.

Bevan,A.P., Drake,P.G., Bergeron,J.J.M., and Posner,B.I. (1996). Intracellular signal transduction: The role of endosomes. Trends in Endocrinology and Metabolism *7*, 13-21.

Bottger,G., Nagelkerken,B., and van der Sluijs,P. (1996). Rab4 and Rab7 define distinct nonoverlapping endosomal compartments. J. Biol. Chem. *271*, 29191-29197.

Bowtell,D.D. and Langdon,W.Y. (1995). The protein product of the c-cbl oncogene rapidly complexes with the EGF receptor and is tyrosine phosphorylated following EGF stimulation. Oncogene. *19;11*, 1561-1567.

Bradford,M.M. (1976). A rapid and sensitive method for the quantitation of microgram quantities of protein utilizing the principle of protein-dye binding. Anal. Biochem. *72:248-54.*, 248-254.

Brunet,A., Bonni,A., Zigmond,M.J., Lin,M.Z., Juo,P., Hu,L.S., Anderson,M.J., Arden,K.C., Blenis,J., and Greenberg,M.E. (1999). Akt promotes cell survival by phosphorylating and inhibiting a Forkhead transcription factor. Cell. *19;96*, 857-868.

Bucci,C., Parton,R.G., Mather,I.H., Stunnenberg,H., Simons,K., Hoflack,B., and Zerial,M. (1992). The small GTPase rab5 functions as a regulatory factor in the early endocytic pathway. Cell. *70*, 715-728.

Buday,L., Khwaja,A., Sipeki,S., Farago,A., and Downward,J. (1996). Interactions of Cbl with two adapter proteins, Grb2 and Crk, upon T cell activation. J. Biol. Chem. *271*, 6159-6163.

Burden,S. and Yarden,Y. (1997). Neuregulins and their receptors: a versatile signaling module in organogenesis and oncogenesis. Neuron. *18*, 847-855.

Burgering,B.M. and Coffer,P.J. (1995). Protein kinase B (c-Akt) in phosphatidylinositol-3-OH kinase signal transduction. Nature. *376*, 599-602.

Burgess,G.M., Irvine,R.F., Berridge,M.J., McKinney,J.S., and Putney,J.W., Jr. (1984). Actions of inositol phosphates on Ca2+ pools in guinea-pig hepatocytes. Biochem. J. *224*, 741-746.

Burke,P., Schooler,K., and Wiley,H.S. (2001). Regulation of epidermal growth factor receptor signaling by endocytosis and intracellular trafficking. Mol. Biol. Cell. *12*, 1897-1910.

Carpenter,G. (1987). Receptors for epidermal growth factor and other polypeptide mitogens. Annu. Rev. Biochem. *56:881-914.*, 881-914.

Carpenter,G. (1999). Employment of the epidermal growth factor receptor in growth factor- independent signaling pathways. Journal of Cell Biology *146*, 697-702.

Carpenter,G. and Cohen,S. (1990). Epidermal growth factor. J. Biol. Chem. *265*, 7709-7712.

Carpenter,G., King,L., Jr., and Cohen,S. (1978). Epidermal growth factor stimulates phosphorylation in membrane preparations in vitro. Nature. *276*, 409-410.

Carpenter,G., King,L., Jr., and Cohen,S. (1979). Rapid enhancement of protein phosphorylation in A-431 cell membrane preparations by epidermal growth factor. J. Biol. Chem. *254*, 4884-4891.

Ceresa,B.P., Kao,A.W., Santeler,S.R., and Pessin,J.E. (1998). Inhibition of clathrin-mediated endocytosis selectively attenuates specific insulin receptor signal transduction pathways. Mol. Cell Biol. *18*, 3862-3870.

Ceresa,B.P. and Schmid,S.L. (2000). Regulation of signal transduction by endocytosis. Curr. Opin. Cell Biol. *12*, 204-210.

Chen,W.S., Lazar,C.S., Lund,K.A., Welsh,J.B., Chang,C.P., Walton,G.M., Der,C.J., Wiley,H.S., Gill,G.N., and Rosenfeld,M.G. (1989). Functional independence of the epidermal growth factor receptor from a domain required for ligand-induced internalization and calcium regulation. Cell. *59*, 33-43.

Cheng,M., Sexl,V., Sherr,C.J., and Roussel,M.F. (1998). Assembly of cyclin D-dependent kinase and titration of p27Kip1 regulated by mitogen-activated protein kinase kinase (MEK1). Proc. Natl. Acad. Sci. U. S. A. *95*, 1091-1096.

Chow,J.C., Condorelli,G., and Smith,R.J. (1998). Insulin-like growth factor-I receptor internalization regulates signaling via the Shc/Mitogen-activated protein kinase pathway, but not the insulin receptor substrate-1 pathway. Journal of Biological Chemistry *273*, 4672-4680.

Clague,M.J. and Urbe,S. (2001). The interface of receptor trafficking and signalling. J. Cell Sci. *114*, 3075-3081.

Cohen,S. (1962). Isolation of a mouse submaxillary gland protein accelerating incisor eruption and eyelid opening in the new-born animal. J. Biol. Chem. *237:1555-62.*, 1555-1562.

Cross,D.A., Alessi,D.R., Cohen,P., Andjelkovich,M., and Hemmings,B.A. (1995). Inhibition of glycogen synthase kinase-3 by insulin mediated by protein kinase B. Nature. *378*, 785-789.

Datta,S.R., Dudek,H., Tao,X., Masters,S., Fu,H., Gotoh,Y., and Greenberg,M.E. (1997). Akt phosphorylation of BAD couples survival signals to the cell-intrinsic death machinery. Cell. *91*, 231-241.

Davies,G.C., Ettenberg,S.A., Coats,A.O., Mussante,M., Ravichandran,S., Collins,J., Nau,M.M., and Lipkowitz,S. (2004). Cbl-b interacts with ubiquitinated proteins; differential functions of the UBA domains of c-Cbl and Cbl-b. Oncogene. *23*, 7104-7115.

de Melker,A.A., van der Horst,G., and Borst,J. (2004). Ubiquitin ligase activity of c-Cbl guides the epidermal growth factor receptor into clathrin-coated pits by two distinct modes of Eps15 recruitment. J. Biol. Chem. *279*, 55465-55473.

de Melker,A.A., van der Horst,G., Calafat,J., Jansen,H., and Borst,J. (2001). c-Cbl ubiquitinates the EGF receptor at the plasma membrane and remains receptor associated throughout the endocytic route. J. Cell Sci. *114*, 2167-2178.

Di Fiore,P.P. and De Camilli,P. (2001). Endocytosis and signaling. an inseparable partnership. Cell. *106*, 1-4.

Di Fiore,P.P. and Gill,G.N. (1999). Endocytosis and mitogenic signaling. Curr. Opin. Cell Biol. *11*, 483-488.

Di Guglielmo,G.M., Baass,P.C., Ou,W.J., Posner,B.I., and Bergeron,J.J. (1994). Compartmentalization of SHC, GRB2 and mSOS, and hyperphosphorylation of Raf-1 by EGF but not insulin in liver parenchyma. EMBO J. *13*, 4269-4277.

Di Guglielmo,G.M., Drake,P.G., Baass,P.C., Authier,F., Posner,B.I., and Bergeron,J.J.M. (1998). Insulin receptor internalization and signalling. Molecular and Cellular Biochemistry *182*, 59-63.

Dobrowolski,S., Harter,M., and Stacey,D.W. (1994). Cellular ras activity is required for passage through multiple points of the G0/G1 phase in BALB/c 3T3 cells. Mol. Cell Biol. *14*, 5441-5449.

Doebler,J.A. (2000). Comparative effects of carboxylic ionophores on membrane potential and resistance of NG108-15 cells. Toxicol. In Vitro. *14*, 235-243.

Downward,J. (1994). The GRB2/Sem-5 adaptor protein. FEBS Lett. *338*, 113-117.

Downward,J. (1998). Mechanisms and consequences of activation of protein kinase B/Akt. Curr. Opin. Cell Biol. *10*, 262-267.

Duan,L., Miura,Y., Dimri,M., Majumder,B., Dodge,I.L., Reddi,A.L., Ghosh,A., Fernandes,N., Zhou,P., Mullane-Robinson,K., Rao,N., Donoghue,S., Rogers,R.A.,

Bowtell,D., Naramura,M., Gu,H., Band,V., and Band,H. (2003). Cbl-mediated ubiquitinylation is required for lysosomal sorting of epidermal growth factor receptor but is dispensable for endocytosis. J. Biol. Chem. *278*, 28950-28960.

Ettenberg,S.A., Keane,M.M., Nau,M.M., Frankel,M., Wang,L.M., Pierce,J.H., and Lipkowitz,S. (1999a). cbl-b inhibits epidermal growth factor receptor signaling. Oncogene. *18*, 1855-1866.

Ettenberg,S.A., Magnifico,A., Cuello,M., Nau,M.M., Rubinstein,Y.R., Yarden,Y., Weissman,A.M., and Lipkowitz,S. (2001). Cbl-b-dependent coordinated degradation of the epidermal growth factor receptor signaling complex. J. Biol. Chem. *20;276*, 27677-27684.

Ettenberg,S.A., Rubinstein,Y.R., Banerjee,P., Nau,M.M., Keane,M.M., and Lipkowitz,S. (1999b). cbl-b inhibits EGF-receptor-induced apoptosis by enhancing ubiquitination and degradation of activated receptors. Mol. Cell Biol. Res. Commun. *2*, 111-118.

Felder,S., LaVin,J., Ullrich,A., and Schlessinger,J. (1992). Kinetics of binding, endocytosis, and recycling of EGF receptor mutants. J. Cell Biol. *117*, 203-212.

Felder,S., Miller,K., Moehren,G., Ullrich,A., Schlessinger,J., and Hopkins,C.R. (1990). Kinase activity controls the sorting of the epidermal growth factor receptor within the multivesicular body. Cell. *61*, 623-634.

Feng,Q., Baird,D., Peng,X., Wang,J., Ly,T., Guan,J.L., and Cerione,R.A. (2006). Cool-1 functions as an essential regulatory node for EGF receptor- and Src-mediated cell growth. Nat. Cell Biol. *8*, 945-956.

Feng,Y., Press,B., and Wandinger-Ness,A. (1995). Rab 7: an important regulator of late endocytic membrane traffic. J. Cell Biol. *131*, 1435-1452.

Ferguson,K.M., Darling,P.J., Mohan,M.J., Macatee,T.L., and Lemmon,M.A. (2000). Extracellular domains drive homo- but not hetero-dimerization of erbB receptors. EMBO J. *19*, 4632-4643.

Ferguson,K.M., Lemmon,M.A., Sigler,P.B., and Schlessinger,J. (1995). Scratching the surface with the PH domain. Nat. Struct. Biol. *2*, 715-718.

Frykberg,L., Palmieri,S., Beug,H., Graf,T., Hayman,M.J., and Vennstrom,B. (1983). Transforming capacities of avian erythroblastosis virus mutants deleted in the erbA or erbB oncogenes. Cell. *32*, 227-238.

Fukazawa,T., Miyake,S., Band,V., and Band,H. (1996). Tyrosine phosphorylation of Cbl upon epidermal growth factor (EGF) stimulation and its association with EGF receptor and downstream signaling proteins. J. Biol. Chem. *271*, 14554-14559.

Galisteo,M.L., Dikic,I., Batzer,A.G., Langdon,W.Y., and Schlessinger,J. (1995). Tyrosine phosphorylation of the c-cbl proto-oncogene protein product and association with epidermal growth factor (EGF) receptor upon EGF stimulation. J. Biol. Chem. *270*, 20242-20245.

Gille,H. and Downward,J. (1999). Multiple ras effector pathways contribute to G(1) cell cycle progression. J. Biol. Chem. *274*, 22033-22040.

Glenney,J.R., Jr., Chen,W.S., Lazar,C.S., Walton,G.M., Zokas,L.M., Rosenfeld,M.G., and Gill,G.N. (1988). Ligand-induced endocytosis of the EGF receptor is blocked by mutational inactivation and by microinjection of anti-phosphotyrosine antibodies. Cell. *52*, 675-684.

Goldstein,J.L., Brown,M.S., Anderson,R.G., Russell,D.W., and Schneider,W.J. (1985). Receptor-mediated endocytosis: concepts emerging from the LDL receptor system. Annu. Rev. Cell Biol. *1:1-39.*, 1-39.

Grovdal,L.M., Stang,E., Sorkin,A., and Madshus,I.H. (2004). Direct interaction of Cbl with pTyr 1045 of the EGF receptor (EGFR) is required to sort the EGFR to lysosomes for degradation. Exp. Cell Res. *300*, 388-395.

Gullick,W.J. and Srinivasan,R. (1998). The type 1 growth factor receptor family: new ligands and receptors and their role in breast cancer. Breast Cancer Res. Treat. *52*, 43-53.

Haglund,K., Di Fiore,P.P., and Dikic,I. (2003a). Distinct monoubiquitin signals in receptor endocytosis. Trends Biochem. Sci. *28*, 598-603.

Haglund,K., Shimokawa,N., Szymkiewicz,I., and Dikic,I. (2002). Cbl-directed monoubiquitination of CIN85 is involved in regulation of ligand-induced degradation of EGF receptors. Proc. Natl. Acad. Sci. U. S. A. *99*, 12191-12196.

Haglund,K., Sigismund,S., Polo,S., Szymkiewicz,I., Di Fiore,P.P., and Dikic,I. (2003b). Multiple monoubiquitination of RTKs is sufficient for their endocytosis and degradation. Nat. Cell Biol. *5*, 461-466.

Hart,C.E., Forstrom,J.W., Kelly,J.D., Seifert,R.A., Smith,R.A., Ross,R., Murray,M.J., and Bowen-Pope,D.F. (1988). Two classes of PDGF receptor recognize different isoforms of PDGF. Science. *240*, 1529-1531.

Hashimoto,Y., Katayama,H., Kiyokawa,E., Ota,S., Kurata,T., Gotoh,N., Otsuka,N., Shibata,M., and Matsuda,M. (1998). Phosphorylation of CrkII adaptor protein at tyrosine 221 by epidermal growth factor receptor. J. Biol. Chem. *273*, 17186-17191.

Haugh,J.M., Huang,A.C., Wiley,H.S., Wells,A., and Lauffenburger,D.A. (1999). Internalized epidermal growth factor receptors participate in the activation of p21(ras) in fibroblasts. J. Biol. Chem. *274*, 34350-34360.

He,C., Hobert,M., Friend,L., and Carlin,C. (2002). The epidermal growth factor receptor juxtamembrane domain has multiple basolateral plasma membrane localization determinants, including a dominant signal with a polyproline core. J. Biol. Chem. *277*, 38284-38293.

Heldin,C.H., Ostman,A., and Ronnstrand,L. (1998). Signal transduction via platelet-derived growth factor receptors. Biochim. Biophys. Acta. *19;1378*, F79-113.

Heldin,C.H. and Westermark,B. (1989). Platelet-derived growth factor: three isoforms and two receptor types. Trends Genet. *5*, 108-111.

Heldin,C.H. and Westermark,B. (1999). Mechanism of action and in vivo role of platelet-derived growth factor. Physiol Rev. *79*, 1283-1316.

Hicke,L. and Riezman,H. (1996). Ubiquitination of a yeast plasma membrane receptor signals its ligand-stimulated endocytosis. Cell. *84*, 277-287.

Hobert,M.E., Kil,S.J., Medof,M.E., and Carlin,C.R. (1997). The cytoplasmic juxtamembrane domain of the epidermal growth factor receptor contains a novel autonomous basolateral sorting determinant. J. Biol. Chem. *272*, 32901-32909.

Honegger,A.M., Schmidt,A., Ullrich,A., and Schlessinger,J. (1990a). Evidence for epidermal growth factor (EGF)-induced intermolecular autophosphorylation of the EGF receptors in living cells. Mol. Cell Biol. *10*, 4035-4044.

Honegger,A.M., Schmidt,A., Ullrich,A., and Schlessinger,J. (1990b). Separate endocytic pathways of kinase-defective and -active EGF receptor mutants expressed in same cells. J. Cell Biol. *110*, 1541-1548.

Huang,F. and Sorkin,A. (2005). Growth factor receptor binding protein 2-mediated recruitment of the RING domain of Cbl to the epidermal growth factor receptor is essential and sufficient to support receptor endocytosis. Mol. Biol. Cell. *16*, 1268-1281.

Hubbard,S.R., Mohammadi,M., and Schlessinger,J. (1998). Autoregulatory mechanisms in protein-tyrosine kinases. J. Biol. Chem. *273*, 11987-11990.

Hubbard,S.R. and Till,J.H. (2000). Protein tyrosine kinase structure and function. Annu. Rev. Biochem. *69:373-98.*, 373-398.

Hunter,T. (1998). The Croonian Lecture 1997. The phosphorylation of proteins on tyrosine: its role in cell growth and disease. Philos. Trans. R. Soc. Lond B Biol. Sci. *353*, 583-605.

Hunter,T. (2000). Signaling--2000 and beyond. Cell. *100*, 113-127.

Hunter,T. and Cooper,J.A. (1981). Epidermal growth factor induces rapid tyrosine phosphorylation of proteins in A431 human tumor cells. Cell. *24*, 741-752.

Jiang,G. and Hunter,T. (1999). Receptor signaling: when dimerization is not enough. Curr. Biol. *9*, R568-R571.

Jiang,X., Huang,F., Marusyk,A., and Sorkin,A. (2003). Grb2 regulates internalization of EGF receptors through clathrin-coated pits. Mol. Biol. Cell. *14*, 858-870.

Joazeiro,C.A., Wing,S.S., Huang,H., Leverson,J.D., Hunter,T., and Liu,Y.C. (1999). The tyrosine kinase negative regulator c-Cbl as a RING-type, E2-dependent ubiquitin-protein ligase. Science. *286*, 309-312.

Jones,S.M. and Kazlauskas,A. (2000). Connecting signaling and cell cycle progression in growth factor-stimulated cells. Oncogene. *20;19*, 5558-5567.

Jones,S.M. and Kazlauskas,A. (2001b). Growth factor-dependent signaling and cell cycle progression. Chem. Rev. *101*, 2413-2423.

Jones,S.M. and Kazlauskas,A. (2001a). Growth factor-dependent signaling and cell cycle progression. FEBS Lett. *490*, 110-116.

Jones,S.M. and Kazlauskas,A. (2001c). Growth-factor-dependent mitogenesis requires two distinct phases of signalling. Nat. Cell Biol. *3*, 165-172.

Jones,S.M., Klinghoffer,R., Prestwich,G.D., Toker,A., and Kazlauskas,A. (1999). PDGF induces an early and a late wave of PI 3-kinase activity, and only the late wave is required for progression through G1. Curr. Biol. *20;9*, 512-521.

Kamat,A. and Carpenter,G. (1997). Phospholipase C-gamma1: regulation of enzyme function and role in growth factor-dependent signal transduction. Cytokine Growth Factor Rev. *8*, 109-117.

Kao,A.W., Ceresa,B.P., Santeler,S.R., and Pessin,J.E. (1998). Expression of a dominant interfering dynamin mutant in 3T3L1 adipocytes inhibits GLUT4 endocytosis without affecting insulin signaling. J. Biol. Chem. *273*, 25450-25457.

Karin,M. and Hunter,T. (1995). Transcriptional control by protein phosphorylation: signal transmission from the cell surface to the nucleus. Curr. Biol. *5*, 747-757.

Kassenbrock,C.K., Hunter,S., Garl,P., Johnson,G.L., and Anderson,S.M. (2002). Inhibition of Src family kinases blocks epidermal growth factor (EGF)-induced activation of Akt, phosphorylation of c-Cbl, and ubiquitination of the EGF receptor. J. Biol. Chem. *277*, 24967-24975.

Keane,M.M., Ettenberg,S.A., Nau,M.M., Banerjee,P., Cuello,M., Penninger,J., and Lipkowitz,S. (1999). cbl-3: a new mammalian cbl family protein. Oncogene. *18*, 3365-3375.

Keane,M.M., Rivero-Lezcano,O.M., Mitchell,J.A., Robbins,K.C., and Lipkowitz,S. (1995). Cloning and characterization of cbl-b: a SH3 binding protein with homology to the c-cbl proto-oncogene. Oncogene. *10*, 2367-2377.

Keilhack,H., Tenev,T., Nyakatura,E., Godovac-Zimmermann,J., Nielsen,L., Seedorf,K., and Bohmer,F.D. (1998). Phosphotyrosine 1173 mediates binding of the protein-tyrosine phosphatase SHP-1 to the epidermal growth factor receptor and attenuation of receptor signaling. J. Biol. Chem. *273*, 24839-24846.

Kelly,J.D., Haldeman,B.A., Grant,F.J., Murray,M.J., Seifert,R.A., Bowen-Pope,D.F., Cooper,J.A., and Kazlauskas,A. (1991). Platelet-derived growth factor (PDGF) stimulates PDGF receptor subunit dimerization and intersubunit trans-phosphorylation. J. Biol. Chem. *266*, 8987-8992.

Kerkhoff,E., Houben,R., Loffler,S., Troppmair,J., Lee,J.E., and Rapp,U.R. (1998). Regulation of c-myc expression by Ras/Raf signalling. Oncogene. *16*, 211-216.

Kerkhoff,E. and Rapp,U.R. (1997). Induction of cell proliferation in quiescent NIH 3T3 cells by oncogenic c-Raf-1. Mol. Cell Biol. *17*, 2576-2586.

Kerkhoff,E. and Rapp,U.R. (1998). Cell cycle targets of Ras/Raf signalling. Oncogene. *17*, 1457-1462.

Kil,S.J., Hobert,M., and Carlin,C. (1999). A leucine-based determinant in the epidermal growth factor receptor juxtamembrane domain is required for the efficient transport of ligand-receptor complexes to lysosomes. J. Biol. Chem. *274*, 3141-3150.

Kohler,N. and Lipton,A. (1974). Platelets as a source of fibroblast growth-promoting activity. Exp. Cell Res. *87*, 297-301.

Kondo,I. and Shimizu,N. (1983). Mapping of the human gene for epidermal growth factor receptor (EGFR) on the p13 leads to q22 region of chromosome 7. Cytogenet. Cell Genet. *35*, 9-14.

Kouhara,H., Hadari,Y.R., Spivak-Kroizman,T., Schilling,J., Bar-Sagi,D., Lax,I., and Schlessinger,J. (1997). A lipid-anchored Grb2-binding protein that links FGF-receptor activation to the Ras/MAPK signaling pathway. Cell. *89*, 693-702.

Kranenburg,O., Verlaan,I., and Moolenaar,W.H. (1999). Dynamin is required for the activation of mitogen-activated protein (MAP) kinase by MAP kinase kinase. J. Biol. Chem. *274*, 35301-35304.

Kuriyan,J. and Cowburn,D. (1997). Modular peptide recognition domains in eukaryotic signaling. Annu. Rev. Biophys. Biomol. Struct. *26:259-88.*, 259-288.

Kurten,R.C., Cadena,D.L., and Gill,G.N. (1996). Enhanced degradation of EGF receptors by a sorting nexin, SNX1. Science. *272*, 1008-1010.

Kuruvilla,R., Ye,H., and Ginty,D.D. (2000). Spatially and functionally distinct roles of the PI3-K effector pathway during NGF signaling in sympathetic neurons. Neuron. *27*, 499-512.

Lanzetti,L., Rybin,V., Malabarba,M.G., Christoforidis,S., Scita,G., Zerial,M., and Di Fiore,P.P. (2000). The Eps8 protein coordinates EGF receptor signalling through Rac and trafficking through Rab5. Nature. *408*, 374-377.

Lavoie,J.N., L'Allemain,G., Brunet,A., Muller,R., and Pouyssegur,J. (1996). Cyclin D1 expression is regulated positively by the p42/p44MAPK and negatively by the p38/HOGMAPK pathway. J. Biol. Chem. *271*, 20608-20616.

Lee,P.S., Wang,Y., Dominguez,M.G., Yeung,Y.G., Murphy,M.A., Bowtell,D.D., and Stanley,E.R. (1999). The Cbl protooncoprotein stimulates CSF-1 receptor multiubiquitination and endocytosis, and attenuates macrophage proliferation. EMBO J. *18*, 3616-3628.

Lemmon,M.A., Bu,Z., Ladbury,J.E., Zhou,M., Pinchasi,D., Lax,I., Engelman,D.M., and Schlessinger,J. (1997). Two EGF molecules contribute additively to stabilization of the EGFR dimer. EMBO J. *16*, 281-294.

Lemmon,M.A., Ferguson,K.M., O'Brien,R., Sigler,P.B., and Schlessinger,J. (1995). Specific and high-affinity binding of inositol phosphates to an isolated pleckstrin homology domain. Proc. Natl. Acad. Sci. U. S. A. *92*, 10472-10476.

Lemmon,M.A. and Schlessinger,J. (1994). Regulation of signal transduction and signal diversity by receptor oligomerization. Trends Biochem. Sci. *19*, 459-463.

Leof,E.B. (2000). Growth factor receptor signalling: location, location, location. Trends Cell Biol. *10*, 343-348.

Leone,G., DeGregori,J., Sears,R., Jakoi,L., and Nevins,J.R. (1997). Myc and Ras collaborate in inducing accumulation of active cyclin E/Cdk2 and E2F. Nature. *387*, 422-426.

Levkowitz,G., Waterman,H., Ettenberg,S.A., Katz,M., Tsygankov,A.Y., Alroy,I., Lavi,S., Iwai,K., Reiss,Y., Ciechanover,A., Lipkowitz,S., and Yarden,Y. (1999). Ubiquitin ligase activity and tyrosine phosphorylation underlie suppression of growth factor signaling by c-Cbl/Sli-1. Mol. Cell. *4*, 1029-1040.

Levkowitz,G., Waterman,H., Zamir,E., Kam,Z., Oved,S., Langdon,W.Y., Beguinot,L., Geiger,B., and Yarden,Y. (1998). c-Cbl/Sli-1 regulates endocytic sorting and ubiquitination of the epidermal growth factor receptor. Genes Dev. *12*, 3663-3674.

Lill,N.L., Douillard,P., Awwad,R.A., Ota,S., Lupher,M.L., Jr., Miyake,S., Meissner-Lula,N., Hsu,V.W., and Band,H. (2000). The evolutionarily conserved N-terminal region of Cbl is sufficient to enhance down-regulation of the epidermal growth factor receptor. J. Biol. Chem. *275*, 367-377.

Longva,K.E., Blystad,F.D., Stang,E., Larsen,A.M., Johannessen,L.E., and Madshus,I.H. (2002). Ubiquitination and proteasomal activity is required for transport of the EGF receptor to inner membranes of multivesicular bodies. J. Cell Biol. *156*, 843-854.

Lupher,M.L., Jr., Reedquist,K.A., Miyake,S., Langdon,W.Y., and Band,H. (1996). A novel phosphotyrosine-binding domain in the N-terminal transforming region of Cbl interacts directly and selectively with ZAP-70 in T cells. J. Biol. Chem. *271*, 24063-24068.

MacInnis,B.L. and Campenot,R.B. (2002). Retrograde support of neuronal survival without retrograde transport of nerve growth factor. Science. *295*, 1536-1539.

Madhani,H.D. and Fink,G.R. (1998). The riddle of MAP kinase signaling specificity. Trends Genet. *14*, 151-155.

Margolis,B. (1999). The PTB Domain: The Name Doesn't Say It All. Trends Endocrinol. Metab. *10*, 262-267.

Margolis,B.L., Lax,I., Kris,R., Dombalagian,M., Honegger,A.M., Howk,R., Givol,D., Ullrich,A., and Schlessinger,J. (1989). All autophosphorylation sites of epidermal growth factor (EGF) receptor and HER2/neu are located in their carboxyl-terminal tails. Identification of a novel site in EGF receptor. J. Biol. Chem. *264*, 10667-10671.

Marmor,M.D. and Yarden,Y. (2004). Role of protein ubiquitylation in regulating endocytosis of receptor tyrosine kinases. Oncogene. *23*, 2057-2070.

Marshall,C.J. (1994). MAP kinase kinase kinase, MAP kinase kinase and MAP kinase. Curr. Opin. Genet. Dev. *4*, 82-89.

Marshall,C.J. (1995). Specificity of receptor tyrosine kinase signaling: transient versus sustained extracellular signal-regulated kinase activation. Cell. *80*, 179-185.

Marshall,C.J. (1996). Cell signalling. Raf gets it together. Nature. *383*, 127-128.

Matsui,T., Heidaran,M., Miki,T., Popescu,N., La,R.W., Kraus,M., Pierce,J., and Aaronson,S. (1989). Isolation of a novel receptor cDNA establishes the existence of two PDGF receptor genes. Science. *243*, 800-804.

McCarty,J.H. (1998). The Nck SH2/SH3 adaptor protein: a regulator of multiple intracellular signal transduction events. Bioessays. *20*, 913-921.

McCune,B.K. and Earp,H.S. (1989). The epidermal growth factor receptor tyrosine kinase in liver epithelial cells. The effect of ligand-dependent changes in cellular location. Journal of Biological Chemistry *264*, 15501-15507.

McPherson,P.S., Kay,B.K., and Hussain,N.K. (2001). Signaling on the endocytic pathway. Traffic. *2*, 375-384.

Milarski,K.L., Zhu,G., Pearl,C.G., McNamara,D.J., Dobrusin,E.M., MacLean,D., Thieme-Sefler,A., Zhang,Z.Y., Sawyer,T., Decker,S.J., and . (1993). Sequence specificity in recognition of the epidermal growth factor receptor by protein tyrosine phosphatase 1B. J. Biol. Chem. *268*, 23634-23639.

Miyake,S., Lupher,M.L., Jr., Druker,B., and Band,H. (1998). The tyrosine kinase regulator Cbl enhances the ubiquitination and degradation of the platelet-derived growth factor receptor alpha. Proc. Natl. Acad. Sci. U. S. A. *95*, 7927-7932.

Mizuno,E., Iura,T., Mukai,A., Yoshimori,T., Kitamura,N., and Komada,M. (2005). Regulation of epidermal growth factor receptor down-regulation by UBPY-mediated deubiquitination at endosomes. Mol. Biol. Cell. *16*, 5163-5174.

Mosesson,Y., Shtiegman,K., Katz,M., Zwang,Y., Vereb,G., Szollosi,J., and Yarden,Y. (2003). Endocytosis of receptor tyrosine kinases is driven by monoubiquitylation, not polyubiquitylation. J. Biol. Chem. *278*, 21323-21326.

Mulcahy,L.S., Smith,M.R., and Stacey,D.W. (1985). Requirement for ras proto-oncogene function during serum-stimulated growth of NIH 3T3 cells. Nature *313*, 241-243.

Nishizuka,Y. (1992). Intracellular signaling by hydrolysis of phospholipids and activation of protein kinase C. Science. *258*, 607-614.

Obaya,A.J., Mateyak,M.K., and Sedivy,J.M. (1999). Mysterious liaisons: the relationship between c-Myc and the cell cycle. Oncogene. *18*, 2934-2941.

Okutani,T., Okabayashi,Y., Kido,Y., Sugimoto,Y., Sakaguchi,K., Matuoka,K., Takenawa,T., and Kasuga,M. (1994). Grb2/Ash binds directly to tyrosines 1068 and 1086 and indirectly to tyrosine 1148 of activated human epidermal growth factor receptors in intact cells. J. Biol. Chem. *269*, 31310-31314.

Opresko,L.K., Chang,C.P., Will,B.H., Burke,P.M., Gill,G.N., and Wiley,H.S. (1995). Endocytosis and lysosomal targeting of epidermal growth factor receptors are mediated by distinct sequences independent of the tyrosine kinase domain. J. Biol. Chem. *270*, 4325-4333.

Ota,Y. and Samelson,L.E. (1997). The product of the proto-oncogene c-cbl: a negative regulator of the Syk tyrosine kinase. Science. *276*, 418-420.

Ozcan,F., Klein,P., Lemmon,M.A., Lax,I., and Schlessinger,J. (2006). On the nature of low- and high-affinity EGF receptors on living cells. Proc. Natl. Acad. Sci. U. S. A. *103*, 5735-5740.

Pardee,A.B. (1974). A restriction point for control of normal animal cell proliferation. Proc. Natl. Acad. Sci. U. S. A. *71*, 1286-1290.

Pardee,A.B. (1989). G1 events and regulation of cell proliferation. Science. *246*, 603-608.

Pawson,T. (1995). Protein modules and signalling networks. Nature. *373*, 573-580.

Pawson,T., Raina,M., and Nash,P. (2002). Interaction domains: from simple binding events to complex cellular behavior. FEBS Lett. *20;513*, 2-10.

Peeper,D.S., Upton,T.M., Ladha,M.H., Neuman,E., Zalvide,J., Bernards,R., DeCaprio,J.A., and Ewen,M.E. (1997). Ras signalling linked to the cell-cycle machinery by the retinoblastoma protein. Nature. *386*, 177-181.

Peles,E. and Yarden,Y. (1993). Neu and its ligands: from an oncogene to neural factors. Bioessays. *15*, 815-824.

Pennock,S. and Wang,Z. (2003). Stimulation of cell proliferation by endosomal epidermal growth factor receptor as revealed through two distinct phases of signaling. Mol. Cell Biol. *23*, 5803-5815.

Petrelli,A., Gilestro,G.F., Lanzardo,S., Comoglio,P.M., Migone,N., and Giordano,S. (2002). The endophilin-CIN85-Cbl complex mediates ligand-dependent downregulation of c-Met. Nature. *416*, 187-190.

Peus,D., Meves,A., Vasa,R.A., Beyerle,A., O'Brien,T., and Pittelkow,M.R. (1999). H2O2 is required for UVB-induced EGF receptor and downstream signaling pathway activation. Free Radic. Biol. Med. *27*, 1197-1202.

Pippig,S., Andexinger,S., and Lohse,M.J. (1995). Sequestration and recycling of beta 2-adrenergic receptors permit receptor resensitization. Mol. Pharmacol. *47*, 666-676.

Planas-Silva,M.D. and Weinberg,R.A. (1997). The restriction point and control of cell proliferation. Curr. Opin. Cell Biol. *9*, 768-772.

Pledger,W.J., Stiles,C.D., Antoniades,H.N., and Scher,C.D. (1977). Induction of DNA synthesis in BALB/c 3T3 cells by serum components: reevaluation of the commitment process. Proc. Natl. Acad. Sci. U. S. A. *74*, 4481-4485.

Pledger,W.J., Stiles,C.D., Antoniades,H.N., and Scher,C.D. (1978). An ordered sequence of events is required before BALB/c-3T3 cells become committed to DNA synthesis. Proc. Natl. Acad. Sci. U. S. A. *75*, 2839-2843.

Ravid,T., Heidinger,J.M., Gee,P., Khan,E.M., and Goldkorn,T. (2004). c-Cbl-mediated ubiquitinylation is required for epidermal growth factor receptor exit from the early endosomes. J. Biol. Chem. *279*, 37153-37162.

Rimerman,R.A., Gellert-Randleman,A., and Diehl,J.A. (2000). Wnt1 and MEK1 cooperate to promote cyclin D1 accumulation and cellular transformation. J. Biol. Chem. *275*, 14736-14742.

Robinson,M.S. (1994). The role of clathrin, adaptors and dynamin in endocytosis. Curr. Opin. Cell Biol. *6*, 538-544.

Roche,S., Koegl,M., and Courtneidge,S.A. (1994). The phosphatidylinositol 3-kinase alpha is required for DNA synthesis induced by some, but not all, growth factors. Proc. Natl. Acad. Sci. U. S. A. *91*, 9185-9189.

Roche,S., McGlade,J., Jones,M., Gish,G.D., Pawson,T., and Courtneidge,S.A. (1996). Requirement of phospholipase C gamma, the tyrosine phosphatase Syp and the adaptor proteins Shc and Nck for PDGF-induced DNA synthesis: evidence for the existence of Ras-dependent and Ras-independent pathways. EMBO J. *15*, 4940-4948.

Rose,D.W., Xiao,S., Pillay,T.S., Kolch,W., and Olefsky,J.M. (1998). Prolonged vs transient roles for early cell cycle signaling components. Oncogene. *20;17*, 889-899.

Ross,R., Glomset,J., Kariya,B., and Harker,L. (1974). A platelet-dependent serum factor that stimulates the proliferation of arterial smooth muscle cells in vitro. Proc. Natl. Acad. Sci. U. S. A. *71*, 1207-1210.

Rozakis-Adcock,M., McGlade,J., Mbamalu,G., Pelicci,G., Daly,R., Li,W., Batzer,A., Thomas,S., Brugge,J., Pelicci,P.G., and . (1992). Association of the Shc and Grb2/Sem5 SH2-containing proteins is implicated in activation of the Ras pathway by tyrosine kinases. Nature. *360*, 689-692.

Rush,J., Moritz,A., Lee,K.A., Guo,A., Goss,V.L., Spek,E.J., Zhang,H., Zha,X.M., Polakiewicz,R.D., and Comb,M.J. (2005). Immunoaffinity profiling of tyrosine phosphorylation in cancer cells. Nat. Biotechnol. *23*, 94-101.

Sako,Y., Minoghchi,S., and Yanagida,T. (2000). Single-molecule imaging of EGFR signalling on the surface of living cells. Nat. Cell Biol. *2*, 168-172.

Schlessinger,J. (1986). Allosteric regulation of the epidermal growth factor receptor kinase. J. Cell Biol. *103*, 2067-2072.

Schlessinger,J. (1988). Signal transduction by allosteric receptor oligomerization. Trends Biochem. Sci. *13*, 443-447.

Schlessinger,J. (1994). SH2/SH3 signaling proteins. Curr. Opin. Genet. Dev. *4*, 25-30.

Schlessinger,J. (2000). Cell signaling by receptor tyrosine kinases. Cell. *103*, 211-225.

Schlessinger,J. and Lemmon,M.A. (2003). SH2 and PTB domains in tyrosine kinase signaling. Sci. STKE. *2003*, RE12.

Schlessinger,J. and Ullrich,A. (1992). Growth factor signaling by receptor tyrosine kinases. Neuron. *9*, 383-391.

Serth,J., Weber,W., Frech,M., Wittinghofer,A., and Pingoud,A. (1992). Binding of the H-ras p21 GTPase activating protein by the activated epidermal growth factor receptor leads to inhibition of the p21 GTPase activity in vitro. Biochemistry. *31*, 6361-6365.

Shen,Y., Xu,L., and Foster,D.A. (2001). Role for phospholipase D in receptor-mediated endocytosis. Mol. Cell Biol. *21*, 595-602.

Sherr,C.J. (1994). G1 phase progression: cycling on cue. Cell. *79*, 551-555.

Sherr,C.J. (1996). Cancer cell cycles. Science. *274*, 1672-1677.

Sorkin,A. and Waters,C.M. (1993). Endocytosis of growth factor receptors. Bioessays. *15*, 375-382.

Soubeyran,P., Kowanetz,K., Szymkiewicz,I., Langdon,W.Y., and Dikic,I. (2002). Cbl-CIN85-endophilin complex mediates ligand-induced downregulation of EGF receptors. Nature. *416*, 183-187.

Stamos,J., Sliwkowski,M.X., and Eigenbrot,C. (2002). Structure of the epidermal growth factor receptor kinase domain alone and in complex with a 4-anilinoquinazoline inhibitor. J. Biol. Chem. *277*, 46265-46272.

Stang,E., Blystad,F.D., Kazazic,M., Bertelsen,V., Brodahl,T., Raiborg,C., Stenmark,H., and Madshus,I.H. (2004). Cbl-dependent ubiquitination is required for progression of EGF receptors into clathrin-coated pits. Mol. Biol. Cell. *15*, 3591-3604.

Stang,E., Johannessen,L.E., Knardal,S.L., and Madshus,I.H. (2000). Polyubiquitination of the epidermal growth factor receptor occurs at the plasma membrane upon ligand-induced activation. J. Biol. Chem. *275*, 13940-13947.

Stein,B.S., Bensch,K.G., and Sussman,H.H. (1984). Complete inhibition of transferrin recycling by monensin in K562 cells. J. Biol. Chem. *259*, 14762-14772.

Stiles,C.D., Capone,G.T., Scher,C.D., Antoniades,H.N., Van Wyk,J.J., and Pledger,W.J. (1979a). Dual control of cell growth by somatomedins and platelet-derived growth factor. Proc. Natl. Acad. Sci. U. S. A. *76*, 1279-1283.

Stiles,C.D., Isberg,R.R., Pledger,W.J., Antoniades,H.N., and Scher,C.D. (1979b). Control of the Balb/c-3T3 cell cycle by nutrients and serum factors: analysis using platelet-derived growth factor and platelet-poor plasma. J. Cell Physiol. *99*, 395-405.

Sun,X.J., Crimmins,D.L., Myers,M.G., Jr., Miralpeix,M., and White,M.F. (1993). Pleiotropic insulin signals are engaged by multisite phosphorylation of IRS-1. Mol. Cell Biol. *13*, 7418-7428.

Szymkiewicz,I., Kowanetz,K., Soubeyran,P., Dinarina,A., Lipkowitz,S., and Dikic,I. (2002). CIN85 participates in Cbl-b-mediated down-regulation of receptor tyrosine kinases. J. Biol. Chem. *277*, 39666-39672.

Takuwa,N. and Takuwa,Y. (1997). Ras activity late in G1 phase required for p27kip1 downregulation, passage through the restriction point, and entry into S phase in growth factor-stimulated NIH 3T3 fibroblasts. Mol. Cell Biol. *17*, 5348-5358.

Tanaka,S., Neff,L., Baron,R., and Levy,J.B. (1995). Tyrosine phosphorylation and translocation of the c-cbl protein after activation of tyrosine kinase signaling pathways. J. Biol. Chem. *270*, 14347-14351.

Tartakoff,A.M. (1983). Perturbation of vesicular traffic with the carboxylic ionophore monensin. Cell. *32*, 1026-1028.

Taylor,S.J. and Shalloway,D. (1996). Cell cycle-dependent activation of Ras. Curr. Biol. *6*, 1621-1627.

Thien,C.B. and Langdon,W.Y. (2001). Cbl: many adaptations to regulate protein tyrosine kinases. Nat. Rev. Mol. Cell Biol. *2*, 294-307.

Thien,C.B., Walker,F., and Langdon,W.Y. (2001). RING finger mutations that abolish c-Cbl-directed polyubiquitination and downregulation of the EGF receptor are insufficient for cell transformation. Mol. Cell. *7*, 355-365.

Toker,A. and Newton,A.C. (2000a). Akt/protein kinase B is regulated by autophosphorylation at the hypothetical PDK-2 site. J. Biol. Chem. *275*, 8271-8274.

Toker,A. and Newton,A.C. (2000b). Cellular signaling: pivoting around PDK-1. Cell. *103*, 185-188.

Ullrich,A. and Schlessinger,J. (1990). Signal transduction by receptors with tyrosine kinase activity. Cell. *20;61*, 203-212.

Valencia,A., Chardin,P., Wittinghofer,A., and Sander,C. (1991). The ras protein family: evolutionary tree and role of conserved amino acids. Biochemistry. *30*, 4637-4648.

van der Geer,P., Hunter,T., and Lindberg,R.A. (1994). Receptor protein-tyrosine kinases and their signal transduction pathways. Annu. Rev. Cell Biol. *10:251-337.*, 251-337.

Vieira,A.V., Lamaze,C., and Schmid,S.L. (1996). Control of EGF receptor signaling by clathrin-mediated endocytosis. Science. *20;274*, 2086-2089.

von Montfort,C., Fernau,N.S., Beier,J.I., Sies,H., and Klotz,L.O. (2006). Extracellular generation of hydrogen peroxide is responsible for activation of EGF receptor by ultraviolet A radiation. Free Radic. Biol. Med. *41*, 1478-1487.

Wada,T., Qian,X.L., and Greene,M.I. (1990). Intermolecular association of the p185neu protein and EGF receptor modulates EGF receptor function. Cell. *61*, 1339-1347.

Wahl,M.I., Nishibe,S., Kim,J.W., Kim,H., Rhee,S.G., and Carpenter,G. (1990). Identification of two epidermal growth factor-sensitive tyrosine phosphorylation sites of phospholipase C-gamma in intact HSC-1 cells. J. Biol. Chem. *265*, 3944-3948.

Wakshull,E.M. and Wharton,W. (1985). Stabilized complexes of epidermal growth factor and its receptor on the cell surface stimulate RNA synthesis but not mitogenesis. Proceedings of the National Academy of Sciences of the United States of America *82*, 8513-8517.

Wang,Q., Villeneuve,G., and Wang,Z. (2005). Control of epidermal growth factor receptor endocytosis by receptor dimerization, rather than receptor kinase activation. EMBO Rep. *6*, 942-948.

Wang,Q., Zhu,F., and Wang,Z. (2007). Identification of EGF receptor C-terminal sequences 1005-1017 and di-leucine motif 1010LL1011 as essential in EGF receptor endocytosis. Exp. Cell Res. *313*, 3349-3363.

Wang,Y., Pennock,S., Chen,X., and Wang,Z. (2002a). Endosomal signaling of epidermal growth factor receptor stimulates signal transduction pathways leading to cell survival. Mol. Cell Biol. *22*, 7279-7290.

Wang,Y., Pennock,S., Chen,X., and Wang,Z. (2002b). Internalization of inactive EGF receptor into endosomes and the subsequent activation of endosome-associated EGF receptors. Epidermal growth factor. Sci. STKE. *2002*, L17.

Wang,Y., Pennock,S.D., Chen,X., Kazlauskas,A., and Wang,Z. (2004). Platelet-derived growth factor receptor-mediated signal transduction from endosomes. J. Biol. Chem. *279*, 8038-8046.

Wang,Y., Yeung,Y.G., Langdon,W.Y., and Stanley,E.R. (1996a). c-Cbl is transiently tyrosine-phosphorylated, ubiquitinated, and membrane-targeted following CSF-1 stimulation of macrophages. J. Biol. Chem. *271*, 17-20.

Wang,Z., Tung,P.S., and Moran,M.F. (1996b). Association of p120 ras GAP with endocytic components and colocalization with epidermal growth factor (EGF) receptor in response to EGF stimulation. Cell Growth Differ. *7*, 123-133.

Wang,Z., Zhang,L., Yeung,T.K., and Chen,X. (1999). Endocytosis deficiency of epidermal growth factor (EGF) receptor-ErbB2 heterodimers in response to EGF stimulation. Mol. Biol. Cell. *10*, 1621-1636.

Waskiewicz,A.J. and Cooper,J.A. (1995). Mitogen and stress response pathways: MAP kinase cascades and phosphatase regulation in mammals and yeast. Curr. Opin. Cell Biol. *7*, 798-805.

Waterman,H., Alroy,I., Strano,S., Seger,R., and Yarden,Y. (1999a). The C-terminus of the kinase-defective neuregulin receptor ErbB-3 confers mitogenic superiority and dictates endocytic routing. EMBO J. *18*, 3348-3358.

Waterman,H., Levkowitz,G., Alroy,I., and Yarden,Y. (1999b). The RING finger of c-Cbl mediates desensitization of the epidermal growth factor receptor. J. Biol. Chem. *274*, 22151-22154.

Waterman,H., Sabanai,I., Geiger,B., and Yarden,Y. (1998). Alternative intracellular routing of ErbB receptors may determine signaling potency. J. Biol. Chem. *273*, 13819-13827.

Wells,A. (1999). EGF receptor. Int. J. Biochem. Cell Biol. *31*, 637-643.

Wells,A., Welsh,J.B., Lazar,C.S., Wiley,H.S., Gill,G.N., and Rosenfeld,M.G. (1990). Ligand-induced transformation by a noninternalizing epidermal growth factor receptor. Science. *247*, 962-964.

Wileman,T., Boshans,R.L., Schlesinger,P., and Stahl,P. (1984). Monensin inhibits recycling of macrophage mannose-glycoprotein receptors and ligand delivery to lysosomes. Biochem. J. *220*, 665-675.

Wiley,H.S. and Burke,P.M. (2001). Regulation of receptor tyrosine kinase signaling by endocytic trafficking. Traffic. *2*, 12-18.

Winston,J.T., Coats,S.R., Wang,Y.Z., and Pledger,W.J. (1996). Regulation of the cell cycle machinery by oncogenic ras. Oncogene. *12*, 127-134.

Wood,E.R., Truesdale,A.T., McDonald,O.B., Yuan,D., Hassell,A., Dickerson,S.H., Ellis,B., Pennisi,C., Horne,E., Lackey,K., Alligood,K.J., Rusnak,D.W., Gilmer,T.M., and Shewchuk,L. (2004). A unique structure for epidermal growth factor receptor bound to GW572016 (Lapatinib): relationships among protein conformation, inhibitor off-rate, and receptor activity in tumor cells. Cancer Res. *64*, 6652-6659.

Worthylake,R., Opresko,L.K., and Wiley,H.S. (1999). ErbB-2 amplification inhibits down-regulation and induces constitutive activation of both ErbB-2 and epidermal growth factor receptors. J. Biol. Chem. *274*, 8865-8874.

Wu,W.J., Tu,S., and Cerione,R.A. (2003). Activated Cdc42 sequesters c-Cbl and prevents EGF receptor degradation. Cell. *19;114*, 715-725.

Wymann,M.P., Pirola,L., Katanaev,V.L., and Bulgarelli-Leva,G. (1999). Phosphoinositide 3-kinase signalling: no lipids. Biochem. Soc. Trans. *27*, 629-634.

Yarden,Y. (2001). The EGFR family and its ligands in human cancer. signalling mechanisms and therapeutic opportunities. Eur. J. Cancer. *37 Suppl 4:S3-8.*, S3-S8.

Yarden,Y. and Sliwkowski,M.X. (2001). Untangling the ErbB signalling network. Nat. Rev. Mol. Cell Biol. *2*, 127-137.

Yoeli-Lerner,M. and Toker,A. (2006). Akt/PKB signaling in cancer: a function in cell motility and invasion. Cell Cycle. *5*, 603-605.

Yokouchi,M., Kondo,T., Houghton,A., Bartkiewicz,M., Horne,W.C., Zhang,H., Yoshimura,A., and Baron,R. (1999). Ligand-induced ubiquitination of the epidermal growth factor receptor involves the interaction of the c-Cbl RING finger and UbcH7. J. Biol. Chem. *274*, 31707-31712.

Yoon,C.H., Lee,J., Jongeward,G.D., and Sternberg,P.W. (1995). Similarity of sli-1, a regulator of vulval development in C. elegans, to the mammalian proto-oncogene c-cbl. Science. *269*, 1102-1105.

Zaremba,S. and Keen,J.H. (1983). Assembly polypeptides from coated vesicles mediate reassembly of unique clathrin coats. J. Cell Biol. *97*, 1339-1347.

Zhu,G., Decker,S.J., MacLean,D., McNamara,D.J., Singh,J., Sawyer,T.K., and Saltiel,A.R. (1994). Sequence specificity in the recognition of the epidermal growth factor receptor by the abl Src homology 2 domain. Oncogene. *9*, 1379-1385.